université PARIS-SACLAY

TELECOM ParisTech

NNT : 2019SACLT028

Thèse de doctorat

On the Capacity of Free-Space Optical Intensity Channels

Thèse de doctorat de l'Université Paris-Saclay
préparée à Télécom ParisTech

Ecole doctorale n°528: sciences et technologies de l'information et de la communication (STIC)
Spécialité de doctorat : réseaux, information et communications

Thèse présentée et soutenue à Paris, le 13 Juillet 2019, par

LONGGUANG LI

Composition du Jury :

M. Philippe Ciblat Professeur, Télécom ParisTech	Président
M. Amos Lapidoth Professeur, ETH Zurich	Rapporteur
M. Andrew Eckford Professeur, York University	Rapporteur
M. Ligong Wang Chargé de recherche, CNRS	Examinateur
Mme Lina Mroueh Maître de Conférences, Institut Supérieur d'Electronique de Paris	Examinateur
Mme Michèle Wigger Professeur, Télécom ParisTech	Directeur de thèse
M. Stefan Moser Professeur, NCTU and ETH Zurich	Co-directeur de thèse

université PARIS-SACLAY

ÉCOLE DOCTORALE
Sciences et technologies de l'information et de la communication (STIC)

Titre : Sur la Capacité des Canaux d'Intensité Optique en Espace Libre

Mots clés : Capacité des Canaux, Communication d'Intensité Optique, Entrées Multiples et Sorties Multiples (MIMO)

Résumé : Les systèmes de communication à intensité optique en espace libre (FSOI) sont largement utilisés dans les communications à courte portée, telles que les communications infrarouges entre des dispositifs électroniques portables. L'émetteur de ces systèmes module sur l'intensité des signaux optiques émis par des diodes électroluminescentes (LEDs) ou des diodes laser (LDs), et le récepteur mesure les intensités optiques entrantes au moyen de photodétecteurs. Les entrées ne sont pas négatives car elles représentent des intensités. En outre, ils sont généralement soumis à des contraintes de puissance de pointe et moyenne, la contrainte de puissance de pointe étant principalement dû aux limitations techniques des composants utilisés, alors que la contrainte de puissance moyenne est imposée par des limitations de batterie et des considérations de sécurité. En première approximation, le bruit dans de tels systèmes peut être supposé être gaussien et indépendant du signal transmis.

Cette thèse porte sur les limites fondamentales des systèmes de communication FSOI, plus précisément sur leur capacité. L'objectif principal de notre travail est d'étudier la capacité d'un canal FSOI général à entrées multiples et sorties multiples (MIMO) avec une contrainte de puissance de crête par entrée et une contrainte de puissance moyenne totale sur toutes les antennes d'entrée. Nous présentons plusieurs résultats de capacité sur le scénario quand il y a plus d'antennes d'émission que d'antennes de réception, c'est-à-dire, $n_{\mathsf{T}} > n_{\mathsf{R}} > 1$. Dans ce scénario, différents vecteurs d'entrée peuvent donner des distributions identiques à la sortie, lorsqu'ils aboutissent au même vecteur d'image multiplié par la matrice de canal. Nous déterminons d'abord les vecteurs d'entrée d'énergie minimale permettant d'atteindre chacun de ces vecteurs d'image. Il définit à chaque instant dans le temps un sous-ensemble de $n_{\mathsf{T}} - n_{\mathsf{R}}$ antennes à zéro ou à pleine puissance et utilise uniquement les n_{R} antennes restantes pour la signalisation. Sur cette base, nous obtenons une expression de capacité équivalente en termes de vecteur d'image, ce qui permet de décomposer le canal d'origine en un ensemble de canaux presque parallèles. Chacun des canaux parallèles est un canal MIMO $n_{\mathsf{R}} \times n_{\mathsf{R}}$ à contrainte d'amplitude, avec une contrainte de puissance linéaire, pour laquelle des limites de capacité sont connues. Avec cette décomposition, nous établissons de nouvelles limites supérieures en utilisant une technique de limite supérieure basée sur la dualité, et des limites inférieures en utilisant l'inégalité de puissance d'entropie (EPI). Les limites supérieure et inférieure dérivées correspondent lorsque le rapport signal sur bruit (SNR) tend vers l'infini, établissant la capacité asymptotique à haut SNR. À faible SNR, il est connu que la pente de capacité est déterminée par la trace maximale de la matrice de covariance du vecteur image. Nous avons trouvé une caractérisation de cette trace maximale qui est plus facile à évaluer en calcul que les formes précédentes.

Title : On the Capacity of Free-Space Optical Intensity Channels

Keywords : Channel Capacity, Optical Intensity Communications, Multiple-Input Multiple-Output (MIMO)

Abstract : Free-space optical intensity (FSOI) communication systems are widely used in short-range communication such as the infrared communication between electronic handheld devices. The transmitter in these systems modulates on the intensity of optical signals emitted by light emitting diodes (LEDs) or laser diodes (LDs), and the receiver measures incoming optical intensities by means of photodetectors. Inputs are nonnegative because they represent intensities. Moreover, they are typically subject to both peak- and average-power constraints, where the peak-power constraint is mainly due to technical limitations of the used components, whereas the average-power constraint is imposed by battery limitations and safety considerations. As a first approximation, the noise in such systems can be assumed to be Gaussian and independent of the transmitted signal.

This thesis focuses on the fundamental limits of FSOI communication systems, more precisely on their capacity. The major aim of our work is to study the capacity of a general multiple-input multiple-output (MIMO) FSOI channel under a per-input-antenna peak-power constraint and a total average-power constraint over all input antennas. We present several capacity results on the scenario when there are more transmit than receive antennas, i.e., $n_{\mathsf{T}} > n_{\mathsf{R}} > 1$. In this scenario, different input vectors can yield identical distributions at the output, when they result in the same image vector under multiplication by the channel matrix. We first determine the minimum-energy input vectors that attain each of these image vectors. It sets at each instant in time a subset of $n_{\mathsf{T}} - n_{\mathsf{R}}$ antennas to zero or to full power, and uses only the remaining n_{R} antennas for signaling. Based on this, we derive an equivalent capacity expression in terms of the image vector, which helps to decompose the original channel into a set of almost parallel channels. Each of the parallel channels is an amplitude-constrained $n_{\mathsf{R}} \times n_{\mathsf{R}}$ MIMO channel, with a linear power constraint, for which bounds on the capacity are known. With this decomposition, we establish new upper bounds by using a duality-based upper-bounding technique, and lower bounds by using the Entropy Power Inequality (EPI). The derived upper and lower bounds match when the signal-to-noise ratio (SNR) tends to infinity, establishing the high-SNR asymptotic capacity. At low SNR, it is known that the capacity slope is determined by the maximum trace of of the covariance matrix of the image vector. We found a characterization to this maximum trace that is computationally easier to evaluate than previous forms.

Université Paris-Saclay
Espace Technologique / Immeuble Discovery
Route de l'Orme aux Merisiers RD 128 / 91190 Saint-Aubin, France

Contents

List of Figures

Acknowledgement

I would like to take this opportunity to thank all those who supported me during my thesis. First and foremost, I would like to express my sincere gratitude to my advisors Prof. Michèle WIGGER and Prof. Stefan MOSER for the continuous support of my Ph.D study and research, for their patience, motivation, enthusiasm, and immense knowledge. I have learned so much from them, and it is a wonderful experience to work with them. Thanks so much!

My sincere thanks also goes to Prof. Ligong WANG for his endless support, appreciable help and technical discussions. It's my great pleasure to working with him, and I learned a lot from him.

Then I would want to thank Prof. Aslan TCHAMKERTEN for his support and guidance when I first touch into Information Theory. Although I do not include our joint works on bursty communication into this thesis, those research results are very valuable to me. I'm very grateful to his help.

Next, I would like to mention my colleagues in our group: Dr. Sarah KAMEL, Pierre ESCAMILLA, Homa NIKBAKHT, Dr. K. G. NAGANANDA, Samet GELINCIK, Mehrasa AHMADIPOUR, and Haoyue TANG. I have enjoyed talking with them very much.

I am also deeply thankful to my schoolmates and friends at TELECOM ParisTech: Dr. Jinxin DU, Jianan DUAN, Dr. Heming HUANG, Dr. Pengwenlong GU, Dr. Qifa YAN, Dr. Mengdi SONG for all the fun we have had in the last three years.

Last but not the least, I would like to thank my family: my mother Cuiduo YANG, my three siblings Fei LI, Xiaohong LI, and Yan LI, and my girlfriend Yumei Zhang for their spiritual support throughout my life.

List of abbreviations

- **CSI**: Channel State Information.
- **EPI**: Entropy-Power Inequality.
- **FSOI**: Free-Space Optical Intensity.
- **LD**: Laser Diode.
- **LED**: Light Emitting Diode.
- **MIMO**: Multiple-Input Multiple-Output.
- **MISO**: Multiple-Input Single-Output.
- **PMF**: Probability Mass Function.
- **RF**: Radio Frequency.
- **SISO**: Single-Input Single-Output.
- **SNR**: Signal-to-Noise Ratio.
- **OWC**: Optical Wireless Communication.
- **UV**: Ultraviolet.

Abstract

Free-space optical intensity (FSOI) communication systems are widely used in short-range communication such as the infrared communication between electronic hand-held devices. The transmitter in these systems modulates on the intensity of optical signals emitted by light emitting diodes (LEDs) or laser diodes (LDs), and the receiver measures incoming optical intensities by means of photodetectors. Inputs are nonnegative because they represent intensities. Moreover, they are typically subject to both peak- and average-power constraints, where the peak-power constraint is mainly due to technical limitations of the used components, whereas the average-power constraint is imposed by battery limitations and safety considerations. As a first approximation, the noise in such systems can be assumed to be Gaussian and independent of the transmitted signal.

This thesis focuses on the fundamental limits of FSOI communication systems, more precisely on their *capacity*. The major aim of our work is to study the capacity of a general multiple-input multiple-output (MIMO) FSOI channel under a per-input-antenna peak-power constraint and a total average-power constraint over all input antennas. We present several capacity results on the scenario when there are more transmit than receive antennas, i.e., $n_{\mathrm{T}} > n_{\mathrm{R}} > 1$. In this scenario, different input vectors can yield identical distributions at the output, when they result in the same image vector under multiplication by the channel matrix. We first determine the minimum-energy input vectors that attain each of these image vectors. It sets at each instant in time a subset of $n_{\mathrm{T}} - n_{\mathrm{R}}$ antennas to zero or to full power, and uses only the remaining n_{R} antennas for signaling. Based on this, we derive an equivalent capacity expression in terms of the image vector, which helps to decompose the original channel into a set of almost parallel channels. Each of the parallel channels is an amplitude-constrained $n_{\mathrm{R}} \times n_{\mathrm{R}}$ MIMO channel, with a linear power constraint, for which bounds on the capacity are known. With this decomposition, we establish new upper bounds by using a duality-based upper-bounding technique, and lower bounds by using the Entropy Power Inequality (EPI). The derived upper and lower bounds match when the signal-to-noise ratio (SNR) tends to infinity, establishing the high-SNR asymptotic capacity. At low SNR, it is known that the capacity slope is determined by the maximum trace of of the covariance matrix of the image vector. We found a characterization to this maximum trace that is computationally easier to evaluate than previous forms.

We also consider the two special cases when $n_{\mathrm{T}} = n_{\mathrm{R}} = 1$ and $n_{\mathrm{T}} > n_{\mathrm{R}} = 1$. In the former single-input single-output (SISO) setup, we propose a new duality-

based upper bound that improves over all previous bounds in the moderate-SNR regime. This upper bound is also asymptotically tight at high SNR. For the latter multiple-input single-output (MISO) setup, we characterize the low-SNR slope of the capacity, and it can be achieved by an input vector that has at most three probability mass points. Furthermore, we present a new duality-based upper bound that beats other previous bounds at moderate SNR and also asymptotically tight at high SNR.

The last technical chapter considers the FSOI channel with block fading under different assumptions on the transmitter's channel state information (CSI) (The receiver is assumed to have perfect CSI throughout). Lower and upper bounds on the capacities are derived using the EPI and the duality-based upper-bounding technique, respectively. The lower-bounds for perfect and partial CSI utilize a transmit-antenna cooperation strategy based on the proposed minimum-energy signaling. For perfect CSI, this lower bound matches the upper bound asymptotically in the high SNR regime. For imperfect CSI, the lower bound is close to its perfect-CSI counterpart, showing that with only $(n_{\mathrm{T}} - n_{\mathrm{R}}) \log_2 \binom{n_{\mathrm{T}}}{n_{\mathrm{R}}}$ bits of channel state feedback, one can well approximate the perfect CSI capacity.

Chapter 1

Introduction

1.1 Background and Motivation

The spread of wireless communications emerges as one of the most prominent phenomena in the history of technology. The wide applications of wireless equipments have fundamentally influenced the development of the human society, and it will continue to play an essential role in the modern society for the future. Nowadays, because of the wide-scale deployment and utilization of wireless radio-frequency (RF) devices and systems, wireless communications usually refer to the RF communications. In recent years, there has been a tremendous growth in data traffic and the licensed RF bands face severe congestions. To accommodate the ever-growing data traffic in wireless communications, merely demanding for RF spectrum is not sufficient, and we have to seriously consider other feasible choices by using new parts of the electromagnetic spectrum.

As an excellent supplement to the existing RF communications, optical wireless communication (OWC) has attracted much attention in recent years. It operates in 350–1550nm band, and usually refers to the transmission in unguided propagation media by using optical carriers on the visible, infrared (IR) and ultraviolet (UV) band. When the OWC operates in near IR band, it is also widely referred to as Free-Space Optical (FSO) communication in the literature. Although its widespread use has been limited by its low link reliability particularly in long ranges due to atmospheric turbulence-induced fading and sensitivity to weather conditions, FSO link has a very high optical bandwidth available, allowing much higher data rates in short-range communication [1], [2]. Recently, many innovative physical layer concepts, originally introduced in the context of RF systems have been successfully applied in the FSO systems. The FSO communication has been regaining popularity, and it has been increasingly used to enhance the coverage area and improve the communication rate in existing RF networks. It has become an important supplement and substitute for the RF communications.

FSO systems can be broadly classified into two classes based on the type of detection: noncoherent and coherent. In coherent systems, amplitude, frequency, or phase

modulation can be used, while in noncoherent systems, the intensity of the emitted light is employed to convey the information. At the receiver side, the photodetector directly detects changes in the light intensity. The non-coherent systems are also known as free-space optical intensity-modulation direct-detection (IM/DD) systems or free-space optical intensity (FSOI) systems. Although coherent systems offer superior performance in terms of background noise rejection, mitigating turbulence-induced fading, and higher receiver sensitivity [3], FSOI systems are commonly used in the FSO links due to their simplicity and low costs.

Since in a FSOI system the input signal modulates the optical intensity of the emitted light, it is proportional to the light intensity and nonnegative. The receiver equipped with a front-end photodetector measures the incident optical intensity of the incoming light and produces an output signal which is proportional to the detected intensity, corrupted by white Gaussian noise. To preserve the battery and for safety reasons, the input signal is subject to a peak- and an average- intensity (power) constraints.

The noise sources at the receiver consist of the photo detector (PD) dark current, the transmitter noise, thermal noise, and the photo-current shot-noise (which is caused by input signal and background radiations). The PD dark current can be neglected for most practical purposes. The transmitter noise arises from the instability of the laser intensity and the resulting fluctuations of the photo-current at the receiver, which has usually a negligible effect on the receiver performance [3]. The two main noise sources affecting the receiver are thermal and shot noises. Thermal noise originates from the receiver electronic circuitry, and can be modeled as a Gaussian random process. On the other hand, shot noise, arises from random fluctuations of the current flowing through the PD and is modeled by a Poisson process. If the mean number of absorbed photons is relatively large, the shot noise can also be approximately modeled by a Gaussian process. In most FSOI applications, the received photon flux is high enough to allow this approximation. Hence, in practice, the noise in the receiver can always be modeled as a Gaussian process.

1.2 State of the Art of FSOI Communications

The FSOI channel has been extensively studied in the literature. There are many existing channel models for FSOI channels [7], and the most often studied model is the channel with input-independent Gaussian noise [4]. The input signal in this model is a positive random variable representing the intensity, and the noise is input-independent Gaussian. Besides its nonnegativity, the input signal is typically restricted by a peak- and an average- constraint. We also adopt this channel model in this thesis. A related channel model for optical communication is the Poisson channel for the discrete-time channel [5]–[7] and for the continuous-time channel [8]–[12]. A variation of the channel model, where the noise depends on the input, is also investigated in [13].

Although the capacity-achieving input distribution in our model is known to be discrete [4], [14], the closed-form expression of capacity is still an open problem. Despite the difficulty of the exact capacity characterization, many bounds have

been proposed to evaluate the capacity under different transmit and receive antenna settings. In the case of single-input single-output (SISO), i.e., $n_{\mathrm{T}} = n_{\mathrm{R}} = 1$, several upper and lower bounds on the capacity were presented in [14]–[17]. They show the differences between the derived upper and the lower bounds tend to zero as the SNR tends to infinity, and their ratios tend to one as the SNR tends to zero [16]. Improved bounds at finite SNR have subsequently been presented in [18]–[21] by choosing different auxiliary measures. The MISO scenario, i.e., $n_{\mathrm{T}} > n_{\mathrm{R}} = 1$, was treated in [22], [23]. By proposing an antenna-cooperation strategy, which relies as much as possible on antennas with larger channel gains, several asymptotically tight lower and upper bounds at high and low SNR were derived.

Many works also extended some of the above results to the MIMO case. In the current literature, the capacity of MIMO channels was mostly studied in special cases: 1) the channel matrix has full column rank, i.e., there are fewer transmit than receive antennas: $n_{\mathrm{T}} \leq n_{\mathrm{R}}$, and the channel matrix is of rank n_{T} [24]; 2) the multiple-input single-output (MISO) case where the receiver is equipped with only a single antenna: $n_{\mathrm{R}} = 1$; and 3) the general MIMO case but with only a peak-power constraint [25] or only an average-power constraint [26], [27]. More specifically, [24] determined the asymptotic capacity at high signal-to-noise ratio (SNR) when the channel matrix is of full column-rank. For general MIMO channels with average-power constraints only, the asymptotic high-SNR capacity was determined in [26], [27]. The coding schemes of [26], [27] were extended to channels with both peak- and average-power constraints, but they were only shown to achieve the high-SNR pre-log (degrees of freedom), and not necessarily the exact asymptotic capacity.

In [28], the asymptotic capacity slope in the low-SNR regime is considered for general MIMO channels under both a peak- and an average-power constraint. It is shown that the asymptotically optimal input distribution in the low-SNR regime puts the antennas in a certain order, and assigns positive mass points only to input vectors in such a way that if a given input antenna is set to full power, then also all preceding antennas in the specified order are set to full power. This strategy can be considered in some degree as a generalization of the optimal signaling strategy for MISO channels [22], [23]. However, whereas the optimal order in [28] needs to be determined numerically, in the MISO case the optimal order naturally follows the channel strengths of the input antennas.

Besides above bounds on capacity, many practical transmission schemes with different modulation methods, such as pulse-position modulation or LED index modulation based on orthogonal frequency-division multiplexing, were presented in [29]–[31]. Code constructions were described in [21], [32]–[34].

When the FSOI channel suffers from fading, many capacity results were presented in the so called atmospheric turbulence channels [35]–[37]. However, these results mainly focus on the analysis of the ergodic (average) capacity with different turbulence distribution modelings, and without taking a peak-power constraint into consideration. In this thesis we first attempt a theoretical analysis of the capacity in our adopted model when the channel suffers from block fading.

The capacity of block fading channels heavily depends on the channel modeling (such as the models for turbulence, fading, and antenna correlation) and the availability of channel state information (CSI) at the transmitter and receiver. In the

classic block fading Gaussian channel model for RF communication, where there exists an expected second moment constraint on its input, when both the transmitter and receiver have perfect CSI, capacity can be achieved by a waterfilling power allocation strategy [38], [39]. When the transmitter has no CSI, while the receiver has perfect CSI, capacity is achieved by allocating equal power over all transmit antennas [38], [40], [41]. When the transmitter has rate-limited CSI, which can be obtained from a channel state feedback link, and the receiver has perfect CSI, capacity then can be estimated by using feedback adaptation techniques, which include beamforming transmission [42]–[44], and space-time precoding [45], [46]. Inspired by above works, we assume that in our model, where the power is proportional to the first moment of its input, the receiver has perfect CSI, and study three different versions of transmitter CSI: no CSI, perfect CSI, and limited CSI.

1.3 Contributions

The main contributions of this thesis are as listed as below:

- MIMO FSOI Channel
  - We propose a minimum-energy signaling for MIMO channels with $n_{\mathrm{T}} > n_{\mathrm{R}} > 1$. It partitions the image space of vectors $\bar{\mathbf{x}} = \mathsf{H}\mathbf{x}$— an n_{R}-dimensional vector produced by multiplying an input vector $\mathbf{x}$ by the channel matrix H— into $\binom{n_{\mathrm{T}}}{n_{\mathrm{R}}}$ parallelepipeds, each one spanned by a different subset of n_{R} columns of the channel matrix (see Figures 3.1 and 3.2). In each parallelepiped, the minimum-energy signaling sets the $n_{\mathrm{T}} - n_{\mathrm{R}}$ inputs corresponding to the columns that were not chosen either to 0 or to the full power according to a predescribed rule and uses the n_{R} inputs corresponding to the chosen columns for signaling within the parallelepiped.
  - We can restrict to minimum-energy singaling to achieve capacity. This observation allows us to derive an equivalent capacity expression of the MIMO channel in terms of the random image vector $\bar{\mathbf{X}}$, where the power constraints on the input vector are translated into a set of constraints on $\bar{\mathbf{X}}$. The equivalent capacity expression shows that the original channel can be decomposed into a set of almost parallel $n_{\mathrm{R}} \times n_{\mathrm{R}}$ MIMO channels. This decomposition helps us to obtain new upper and lower bounds on channel capacity.
  - Lower bounds on the capacity of the channel of interest are obtained by applying the Entropy Power Inequality (EPI) and choosing input vectors that maximize the differential entropy of $\bar{\mathbf{X}}$ under the imposed power constraints.
  - Upper bounds are derived by applying the duality-based upper-bounding technique or maximum-entropy arguments to the equivalent capacity expression.

  - We restate the result that the low-SNR slope of the capacity of the MIMO channel is determined by the trace of the covariance matrix of $\bar{\mathbf{X}}$, and establish several properties for the optimal input distribution that maximizes this trace. We show that the covariance-trace maximizing input distribution puts positive mass points in a way that if an antenna is set to full power, then all preceding antennas in a specified order are also set to full power. Further, the optimal probability mass function puts nonzero probability to the origin and to at most $n_{\mathrm{R}} + 1$ other input vectors.
  - We present the asymptotic capacity when the SNR tends to infinity, and also give the slope of capacity when the SNR tends to zero. (This later result was already proven in [28], but as described above, our results simplify the computation of the slope.)

- SISO and MISO FSOI Channel

  - We present a new duality-based upper bound for the SISO channel. It beats all existing bounds in the moderate-SNR regime, and also asymptotically tight at high SNR.
  - The asymptotic low-SNR capacity slope of the MISO channel is derived, and it is achieved by an input vector that has two or three probability mass points, irrespective of the number of antennas.
  - We also derive a new duality-based upper bound for the MISO channel. The upper bound is an extension of the derived upper bound in the SISO case and also improves over all previous bounds in the moderate-SNR regime.

- Block Fading FSOI Channel

  We always assume that the receiver has perfect CSI. Then,

  - Lower bounds are presented for the capacities without CSI, with perfect CSI, and with limited CSI.
  - The lower bounds for perfect and limited CSI are obtained based on the proposed minimum-energy signaling strategy.
  - For perfect CSI, the lower bound matches a new duality-based upper bound in the high signal-to-noise ratio (SNR) regime.
  - For limited CSI, the lower bound is close to the one with perfect CSI, but requires only $(n_{\mathrm{T}} - n_{\mathrm{R}}) \log_2 \binom{n_{\mathrm{T}}}{n_{\mathrm{R}}}$ bits of feedback in each block.

1.4 Organization of the Thesis

This remainder of thesis is organized as follows:

Chapter 2 gives a precise description of the FSOI channel model. The capacity expression on this channel is derived, and a useful bounding technique is also introduced.

In Chapters 3 and 4, we present two important auxiliary results which are useful to the capacity analysis. In Chapter 3, the minimum-energy signaling is described in detail. Chapter 4 characterizes the properties of channel input distribution that maximizes the trace of the input covariance matrix.

Chapters 5 and 6 present our capacity results. In Chapter 5, the MISO channel is investigated. The asymptotic slope at low SNR is characterized, and an asymptotically tight upper bound at high SNR is also presented. Chapter 6 considers the general MIMO channel. Several upper and lower bounds are presented, and the asymptotic capacities at high and low SNR are also derived.

Chapter 7 investigates the capacity when the channel suffers from block fading. Upper and lower bounds on capacity are derived under three different assumptions on the availability of CSI at the transmitter side: no CSI, perfect CSI, and limited CSI.

1.5 Notation

We distinguish between random and deterministic quantities. A random variable is denoted by a capital Roman letter, e.g., Z, while its realization is denoted by the corresponding small Roman letter, e.g., z. Vectors are boldfaced, e.g., $\mathbf{X}$ denotes a random vector and $\mathbf{x}$ its realization. The matrices in the thesis are denoted in capital letters. The deterministic matrices are typeset in a special font, e.g., H, while the random ones are typeset in another font, e.g., $\mathbb{H}$. Constants are typeset either in small Romans, in Greek letters, or in a special font, e.g., E or A. Entropy is typeset as $\mathsf{H}(\cdot)$, differential entropy as $\mathsf{h}(\cdot)$, and mutual information as $\mathsf{I}(\cdot;\cdot)$. The relative entropy (Kullback-Leibler divergence) between probability vectors $\mathbf{p}$ and $\mathbf{q}$ is denoted by $\mathsf{D}(\mathbf{p}\|\mathbf{q})$. The $\mathcal{L}_1$-norm is indicate by $\|\cdot\|_1$, while $\|\cdot\|_2$ denotes the $\mathcal{L}_2$-norm. The logarithmic function $\log(\cdot)$ and $\log_2(\cdot)$ denote the natural and base-2 logarithm, respectively.

Chapter 2

Free-Space Optical Intensity Channel

In this chapter, we discuss a specific free-space optical intensity (FSOI) channel model used for modeling one type of optical wireless communications. The channel input corresponds to the optical intensity, therefore nonnegative, and is also constrained by an average- and a peak-power constraint. We consider the scenario when the noise at the receiver is mainly due to the thermal noise, and other noise sources can be neglected. Hence the noise can be assumed to be independent of the channel input.

2.1 Channel Model

2.1.1 Physical Description

In the FSOI channel, the input signal is transmitted by the light emitting diodes (LED) or laser diodes (LD). Conventional diodes emit light of wavelength between 850 and 950 nm, i.e., in the infrared spectrum. The modulation of the signals onto this infrared light is technically very difficult using amplitude or frequency modulation, as used for example in radio communication. Instead the simplest way is to modulate the signal onto the optical intensity of the emitted light, which is proportional to the optical intensity. Using intensity modulation, the intensity of the emitted light is proportional to the electrical input current. Therefore, the instantaneous optical power is proportional to the electrical input current and not to its square as is usually the case for radio communication.

At the receiver, direct detection of the incident optical intensity is performed. This means that the photo-detector produces an electrical current at the output which is proportional to the detected intensity.

For our model we will neglect the impact of inter-symbol interference due to multi-path propagation and assume that the direct line-of-sight path is dominant. However, we do take into account that the signal is corrupted by additive noise. Since the signal is transmitted through air and not any special optical medium like, e.g., a fiber cable, the dominant noise source for the optical intensity is strong

ambient light. Even if optical filters are used to filter the ambient light, some part of it always arrives at the photo-detector and has typically much larger power than the actual signal. This effect causes high intensity shot noise in the received electrical signal that is independent of the signal itself. Due to eye safety and the danger of potential thermal skin damage the optical peak-power and the optical average-power have to be constrained.

2.1.2 Mathematical Model

We abstract the above physical description into the following $n_{\mathrm{R}} \times n_{\mathrm{T}}$ channel model:

$$\mathbf{Y} = \mathsf{H}\mathbf{x} + \mathbf{Z}. \tag{2.1}$$

Here $\mathbf{x} = (x_1, \ldots, x_{n_{\mathrm{T}}})^{\mathsf{T}}$ denotes the n_{T}-dimensional channel input vector, where $\mathbf{Z}$ denotes the n_{R}-dimensional noise vector with independent standard Gaussian entries,

$$\mathbf{Z} \sim \mathcal{N}(\mathbf{0}, \mathsf{I}), \tag{2.2}$$

and where

$$\mathsf{H} = [\mathbf{h}_1, \mathbf{h}_2, \ldots, \mathbf{h}_{n_{\mathrm{T}}}] \tag{2.3}$$

is the deterministic $n_{\mathrm{R}} \times n_{\mathrm{T}}$ channel matrix with nonnegative entries (hence $\mathbf{h}_1, \ldots, \mathbf{h}_{n_{\mathrm{T}}}$ are n_{R}-dimensional column vectors).

Since the channel inputs correspond to optical intensities sent by the LEDs, they are nonnegative:

$$x_k \in \mathbb{R}_0^+, \quad k = 1, \ldots, n_{\mathrm{T}}. \tag{2.4}$$

We assume the inputs are subject to a peak-power (peak-intensity) and an average-power (average-intensity) constraint:

$$\Pr\big[X_k > \mathsf{A}\big] = 0, \quad \forall\, k \in \{1, \ldots, n_{\mathrm{T}}\}, \tag{2.5a}$$

$$\mathsf{E}\big[\|\mathbf{X}\|_1\big] \leq \mathsf{E}, \tag{2.5b}$$

for some fixed parameters $\mathsf{A}, \mathsf{E} > 0$. It should be noted that the average-power constraint is on the expectation of the channel input and not on its square. Also note that A describes the maximum power of each single LED, while E describes the allowed total average power of all LEDs together. We denote the ratio between the allowed average power and the allowed peak power by α:

$$\alpha \triangleq \frac{\mathsf{E}}{\mathsf{A}}. \tag{2.6}$$

Throughout this thesis, we assume that

$$\operatorname{rank}(\mathsf{H}) = n_{\mathrm{R}}. \tag{2.7}$$

In fact, if $r \triangleq \operatorname{rank}(\mathsf{H})$ is less than n_{R}, then the receiver can first compute $\mathsf{U}^{\mathsf{T}}\mathbf{Y}$, where $\mathsf{U}\mathsf{\Sigma}\mathsf{V}^{\mathsf{T}}$ denotes the singular value decomposition of H, and then discard the $n_{\mathrm{R}} - r$ entries in $\mathsf{U}^{\mathsf{T}}\mathbf{Y}$ that correspond to zero singular values. The problem is then reduced to one for which (2.7) holds.[1]

[1] A similar approach can be used to handle the case where the components of the noise vector $\mathbf{Z}$ are correlated.

2.2 Channel Capacity

Shannon [47] showed that for memoryless channels with finite discrete input alphabet $\mathcal{X}$, finite discrete output alphabet $\mathcal{Y}$, and input constraint function $g(\cdot)$, the channel capacity C is given by

$$\mathsf{C} = \max_{Q} \mathrm{I}(X;Y) \tag{2.8}$$

where the maximum is taken over all input probability distributions Q on X that satisfy the constraint:

$$\mathsf{E}_Q[g(X)] \leq \mathcal{E}, \tag{2.9}$$

where $\mathcal{E}$ is the average-cost constraint on the channel input X. This result for memoryless channels with finite alphabets was generalized to the continuous alphabet in [48], [49].

Hence the capacity for this channel has the following formula:

$$\mathsf{C}_{\mathsf{H}}(\mathsf{A}, \alpha\mathsf{A}) = \max_{P_{\mathbf{X}} \text{ satisfying (2.5)}} \mathrm{I}(\mathbf{X};\mathbf{Y}). \tag{2.10}$$

The next proposition shows that, when $\alpha > \frac{n_{\mathrm{T}}}{2}$, the channel essentially reduces to one with only a peak-power constraint. The other case where $\alpha \leq \frac{n_{\mathrm{T}}}{2}$ will be the main focus of this thesis.

Proposition 1. *If $\alpha > \frac{n_{\mathrm{T}}}{2}$, then the average-power constraint* (2.5b) *is inactive, i.e.,*

$$\mathsf{C}_{\mathsf{H}}(\mathsf{A}, \alpha\mathsf{A}) = \mathsf{C}_{\mathsf{H}}\Big(\mathsf{A}, \frac{n_{\mathrm{T}}}{2}\mathsf{A}\Big), \quad \alpha > \frac{n_{\mathrm{T}}}{2}. \tag{2.11}$$

If $\alpha \leq \frac{n_{\mathrm{T}}}{2}$, then there exists a capacity-achieving input distribution $P_{\mathbf{X}}$ in (2.10) *that satisfies the average-power constraint* (2.5b) *with equality.*

Proof: See Appendix A.1.1. □

2.3 Duality Capacity Expression

Since in this thesis we are interested in deriving capacity bounds, we introduce a dual capacity expression for the channel capacity which will prove useful to get upper bounds in Chapters 5, 6, and 7.

In the case of a channel with finite input and output alphabets $\mathcal{X}$ and $\mathcal{Y}$, respectively, a dual expression for channel capacity is

$$\mathsf{C} = \min_{R(\cdot)} \max_{x \in \mathcal{X}} \mathrm{D}\big(W(\cdot|x) \big\| R(\cdot)\big). \tag{2.12}$$

Every choice of a probability measure $R(\cdot)$ on the output Y thus leads to an upper bound on channel capacity

$$\mathsf{C} \leq \max_{x \in \mathcal{X}} \mathrm{D}\big(W(\cdot|x) \big\| R(\cdot)\big), \quad R(\cdot) \in \mathcal{P}(Y). \tag{2.13}$$

In fact, by using the following identity [50],

$$\sum_{x\in\mathcal{X}} P(x)\mathsf{D}\big(W(\cdot|x)\big\|R(\cdot)\big) = \mathrm{I}(X,Y) + \sum_{x\in\mathcal{X}} P(x)\mathsf{D}\big(PW(\cdot)\big\|R(\cdot)\big), \tag{2.14}$$

and because of the nonnegativity of the relative entropy, we get

$$\mathrm{I}(X,Y) \leq \sum_{x\in\mathcal{X}} P(x)\mathsf{D}\big(W(\cdot|x)\big\|R(\cdot)\big). \tag{2.15}$$

Above results are useful in this thesis, and they can be extended to channels over infinite alphabets [51, Theorem 2.1].

Chapter 3

Minimum-Energy Signaling

In this chapter we describe the minimum-energy signaling method for the FSOI channel. This result is useful to get an alternative capacity expression in terms of this random image vector, which we will specify in Chapter 5.

3.1 Problem Formulation

We first alternatively write the input-output relation as

$$\mathbf{Y} = \bar{\mathbf{x}} + \mathbf{Z}, \tag{3.1}$$

where we set

$$\bar{\mathbf{x}} \triangleq \mathsf{H}\mathbf{x}. \tag{3.2}$$

Define now the set

$$\mathcal{R}(\mathsf{H}) \triangleq \left\{ \sum_{i=1}^{k} \lambda_i \mathbf{h}_i \colon \lambda_1, \ldots, \lambda_k \in [0, \mathsf{A}] \right\}. \tag{3.3}$$

Note that this set is a *zonotope*. Since the n_{T}-dimensional input vector $\mathbf{x}$ is constrained to the n_{T}-dimensional hypercube $[0, \mathsf{A}]^{n_{\mathrm{T}}}$, the n_{R}-dimensional image vector $\bar{\mathbf{x}}$ takes value in the zonotope $\mathcal{R}(\mathsf{H})$.

For each $\bar{\mathbf{x}} \in \mathcal{R}(\mathsf{H})$, let

$$\mathcal{S}(\bar{\mathbf{x}}) \triangleq \left\{ \mathbf{x} \in [0, \mathsf{A}]^{n_{\mathrm{T}}} : \mathsf{H}\mathbf{x} = \bar{\mathbf{x}} \right\} \tag{3.4}$$

be the set of input vectors inducing $\bar{\mathbf{x}}$. In the following section we derive the most energy-efficient signaling method to attain a given $\bar{\mathbf{x}}$. This will allow us to express the capacity in terms of $\bar{\mathbf{X}} = \mathsf{H}\mathbf{X}$ instead of $\mathbf{X}$, which will prove useful in the next chapters.

Since the energy of an input vector $\mathbf{x}$ is $\|\mathbf{x}\|_1$, we are interested in finding an $\mathbf{x}_{\min}$ that satisfies

$$\|\mathbf{x}_{\min}\|_1 = \min_{\mathbf{x} \in \mathcal{S}(\bar{\mathbf{x}})} \|\mathbf{x}\|_1. \tag{3.5}$$

3.2 MISO Minimum-Energy Signaling

In this section we consider the minimum-energy signaling in the MISO channel, i.e., $n_{\mathrm{R}} = 1$. In this case it can be described in a much simpler way. To see this, we first permuate the entries in the channel vector $\mathbf{h}^{\mathsf{T}} = (h_1, \ldots, h_{n_{\mathrm{T}}})$ such that they are ordered decreasingly:

$$h_1 \geq h_2 \geq \cdots \geq h_{n_{\mathrm{T}}} > 0. \tag{3.6}$$

Then, let

$$s_0 \triangleq 0 \tag{3.7a}$$

$$s_k \triangleq \sum_{k'=1}^{k} h_{k'}, \qquad k \in \{1, \ldots, n_{\mathrm{T}}\}. \tag{3.7b}$$

Also, notice that $\bar{X}$ in this scenario is just a scalar:

$$\bar{X} = \mathbf{h}^{\mathsf{T}}\mathbf{X} = \sum_{k=1}^{n_{\mathrm{T}}} h_k X_k. \tag{3.8}$$

Then, the minimum-energy signaling is given by the following lemma, whose proof can be found in [23].

Lemma 2. *Fix some $k \in \{1, 2, \cdots, n_{\mathrm{T}}\}$ and some $\bar{x} \in [\mathsf{A}s_{k-1}, \mathsf{A}s_k)$. The vector that induces $\bar{x}$ with minimum energy is given by $\mathbf{x} = (x_1, \ldots, x_{n_{\mathrm{T}}})^{\mathsf{T}}$, where*

$$x_i = \begin{cases} \mathsf{A} & \text{if } i < k, \\ \frac{\bar{x} - \mathsf{A}s_{k-1}}{h_k} & \text{if } i = k, \\ 0 & \text{if } i > k. \end{cases} \tag{3.9}$$

The above results just show that the optimal signaling strategy in the MISO channel is to rely as much as possible on antennas with larger channel gains. Specifically, if an antenna is used for active signaling in a channel use, then all antennas with larger channel gains should transmit at maximum allowed peak power A, and all antennas with smaller channel gains should be silenced, i.e., send 0.

3.3 An Example of MIMO Minimum-Energy Signaling

Before describing the minimum-energy signaling strategy on a general MIMO channel, we present a simple example.

Example 3. Consider the 2×3 MIMO channel matrix

$$\mathsf{H} = \begin{pmatrix} 2.5 & 2 & 1 \\ 1 & 2 & 2 \end{pmatrix} \tag{3.10}$$

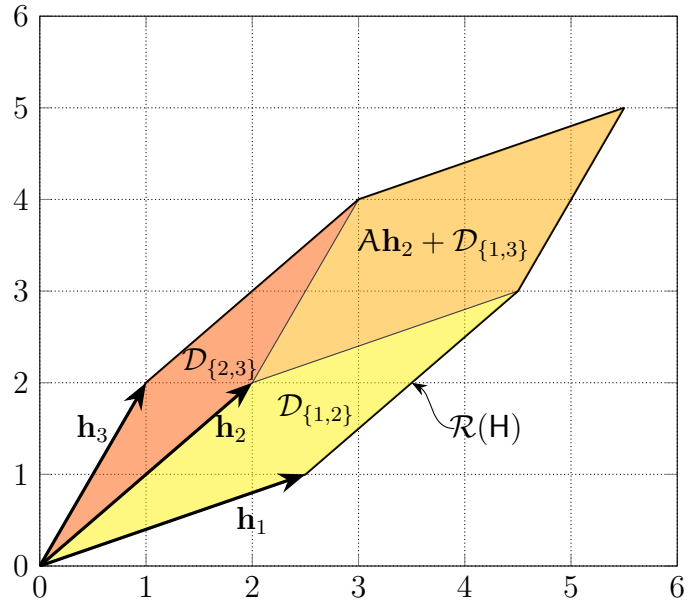

Figure 3.1: The zonotope $\mathcal{R}(\mathsf{H})$ for the 2×3 MIMO channel matrix $\mathsf{H} = [2.5, 2, 1; 1, 2, 2]$ and its minimum-energy decomposition into three parallelograms.

composed of the three column vectors $\mathbf{h}_1 = (2.5, 1)^\mathsf{T}$, $\mathbf{h}_2 = (2, 2)^\mathsf{T}$, and $\mathbf{h}_3 = (1, 2)^\mathsf{T}$. Figure 3.1 depicts the zonotope $\mathcal{R}(\mathsf{H})$ and partitions it into three parallelograms. For any $\bar{\mathbf{x}}$ in the parallelogram $\mathcal{D}_{\{1,2\}} \triangleq \mathcal{R}\big(\mathsf{H}_{\{1,2\}}\big)$, where $\mathsf{H}_{\{1,2\}} \triangleq [\mathbf{h}_1,\ \mathbf{h}_2]$, the minimum-energy input $\mathbf{x}_{\min}$ inducing $\bar{\mathbf{x}}$ has 0 as its third component. Since $\mathsf{H}_{\{1,2\}}$ has full rank, there is only one such input inducing $\bar{\mathbf{x}}$:

$$\mathbf{x}_{\min} = \begin{pmatrix} \mathsf{H}_{\{1,2\}}^{-1}\bar{\mathbf{x}} \\ 0 \end{pmatrix}, \qquad \text{if } \ \bar{\mathbf{x}} \in \mathcal{D}_{\{1,2\}}. \tag{3.11}$$

Similarly, for any $\bar{\mathbf{x}}$ in the parallelogram $\mathcal{D}_{\{2,3\}} \triangleq \mathcal{R}\big(\mathsf{H}_{\{2,3\}}\big)$, where $\mathsf{H}_{\{2,3\}} \triangleq [\mathbf{h}_2,\ \mathbf{h}_3]$, the minimum-energy input $\mathbf{x}_{\min}$ inducing $\bar{\mathbf{x}}$ has 0 as its first component. Therefore,

$$\mathbf{x}_{\min} = \begin{pmatrix} 0 \\ \mathsf{H}_{\{2,3\}}^{-1}\bar{\mathbf{x}} \end{pmatrix}, \qquad \text{if } \ \bar{\mathbf{x}} \in \mathcal{D}_{\{2,3\}}. \tag{3.12}$$

Finally, for any $\bar{\mathbf{x}}$ in the parallelogram $\mathsf{A}\mathbf{h}_2 + \mathcal{D}_{\{1,3\}}$, where $\mathcal{D}_{\{1,3\}} \triangleq \mathcal{R}\big(\mathsf{H}_{\{1,3\}}\big)$ and $\mathsf{H}_{\{1,3\}} \triangleq [\mathbf{h}_1,\ \mathbf{h}_3]$, the minimum-energy input $\mathbf{x}_{\min}$ inducing $\bar{\mathbf{x}}$ has A as its second component, and hence

$$\mathbf{x}_{\min} = \begin{pmatrix} x_{\min,1} \\ \mathsf{A} \\ x_{\min,3} \end{pmatrix}, \qquad \text{if } \ \bar{\mathbf{x}} \in \mathsf{A}\mathbf{h}_2 + \mathcal{D}_{\{1,3\}}, \tag{3.13}$$

where

$$\begin{pmatrix} x_{\min,1} \\ x_{\min,3} \end{pmatrix} = \mathsf{H}_{\{1,3\}}^{-1}(\bar{\mathbf{x}} - \mathsf{A}\mathbf{h}_2). \tag{3.14}$$

$\Diamond$

3.4 MIMO Minimum-Energy Signaling

In this section we now formally solve the optimization problem in (3.5) for an arbitrary $n_{\mathrm{T}} \times n_{\mathrm{R}}$ channel matrix H. To this end, we need some further definitions. Denote by $\mathcal{U}$ the set of all choices of n_{R} columns of H that are linearly independent:

$$\mathcal{U} \triangleq \Big\{\mathcal{I} = \{i_1, \ldots, i_{n_{\mathrm{R}}}\} \subseteq \{1, \ldots, n_{\mathrm{T}}\} \colon \mathbf{h}_{i_1}, \ldots, \mathbf{h}_{i_{n_{\mathrm{R}}}} \text{are linearly independent}\Big\}. \tag{3.15}$$

For every one of these index sets $\mathcal{I} \in \mathcal{U}$, we denote its complement by

$$\mathcal{I}^{\mathrm{c}} \triangleq \{1, \ldots, n_{\mathrm{T}}\} \setminus \mathcal{I}; \tag{3.16}$$

we define the $n_{\mathrm{R}} \times n_{\mathrm{R}}$ matrix $\mathsf{H}_{\mathcal{I}}$ containing the columns of H indicated by $\mathcal{I}$:

$$\mathsf{H}_{\mathcal{I}} \triangleq [\mathbf{h}_i \colon i \in \mathcal{I}]; \tag{3.17}$$

and we define the n_{R}-dimensional parallelepiped

$$\mathcal{D}_{\mathcal{I}} \triangleq \mathcal{R}(\mathsf{H}_{\mathcal{I}}). \tag{3.18}$$

We shall see (Lemma 6 ahead) that $\mathcal{R}(\mathsf{H})$ can be partitioned into parallelepipeds that are shifted versions of $\{\mathcal{D}_{\mathcal{I}}\}$ in such a way that, within each parallelepiped, $\mathbf{x}_{\min}$ has the same form, in a sense similar to (3.11)–(3.13) in Example 3.

We now specify the shifts of the parallelepipeds, which determine the partition of $\mathcal{R}(\mathsf{H})$. Define the n_{R}-dimensional vector

$$\boldsymbol{\gamma}_{\mathcal{I},j} \triangleq \mathsf{H}_{\mathcal{I}}^{-1}\mathbf{h}_j, \quad \mathcal{I} \in \mathcal{U},\ j \in \mathcal{I}^{\mathrm{c}}, \tag{3.19}$$

and the sum of its components

$$a_{\mathcal{I},j} \triangleq \mathbf{1}_{n_{\mathrm{R}}}^{\mathsf{T}} \boldsymbol{\gamma}_{\mathcal{I},j}, \quad \mathcal{I} \in \mathcal{U},\ j \in \mathcal{I}^{\mathrm{c}}. \tag{3.20}$$

The shifts $\mathbf{v}_{\mathcal{I}}$ are then chosen as (3.21) where the binary coefficients $\{g_{\mathcal{I},j}\}_{\mathcal{I}\in\mathcal{U}}$ are obtained through the following rule.

$$\mathbf{v}_{\mathcal{I}} \triangleq \mathsf{A} \sum_{j \in \mathcal{I}^{\mathrm{c}}} g_{\mathcal{I},j}\mathbf{h}_j, \quad \mathcal{I} \in \mathcal{U}. \tag{3.21}$$

- If

$$a_{\mathcal{I},j} \neq 1, \quad \forall\, \mathcal{I} \in \mathcal{U},\ \forall\, j \in \mathcal{I}^{\mathrm{c}}, \tag{3.22}$$

  then let

$$g_{\mathcal{I},j} \triangleq \begin{cases} 1 & \text{if } a_{\mathcal{I},j} > 1, \\ 0 & \text{otherwise,} \end{cases} \quad \mathcal{I} \in \mathcal{U},\ j \in \mathcal{I}^{\mathrm{c}}. \tag{3.23}$$

- If (3.22) is violated, then run Algorithm 4 below to determine $\{g_{\mathcal{I},j}\}$.

Algorithm 4.

for $j \in \{1, \dots, n_{\mathrm{T}}\}$ **do**
  for $\mathcal{I} \in \mathcal{U}$ such that $\mathcal{I} \subseteq \{j, \dots, n_{\mathrm{T}}\}$ **do**
    if $j \in \mathcal{I}^{\mathrm{c}}$ **then**

$$g_{\mathcal{I},j} \triangleq \begin{cases} 1 & \text{if } a_{\mathcal{I},j} \geq 1, \\ 0 & \text{otherwise} \end{cases} \tag{3.24}$$

    else
      for $k \in \mathcal{I}^{\mathrm{c}} \cap \{j+1, \dots, n_{\mathrm{T}}\}$ **do**

$$g_{\mathcal{I},k} \triangleq \begin{cases} 1 & \text{if } a_{\mathcal{I},k} > 1 \text{ or } \big(a_{\mathcal{I},k} = 1 \text{ and the first component} \\ & \qquad\qquad \text{of } \boldsymbol{\gamma}_{\mathcal{I},j} \text{ is negative}\big), \\ 0 & \text{otherwise} \end{cases} \tag{3.25}$$

      end for
    end if
  end for
end for

Remark 5. The purpose of Algorithm 4 is to break ties when the minimum in (3.5) is not unique. Concretely, if (3.22) is satisfied, then for all $\bar{\mathbf{x}} \in \mathcal{R}(\mathsf{H})$ the input vector that achieves the minimum in (3.5) is unique. If there exists some $a_{\mathcal{I},j} = 1$, then there may exist multiple equivalent choices. The algorithm simply picks the first one according to a certain order. △

We are now ready to describe our partition of $\mathcal{R}(\mathsf{H})$.

Lemma 6. *Let $\mathcal{D}_{\mathcal{I}}$, $g_{\mathcal{I},j}$, and $\mathbf{v}_{\mathcal{I}}$ be as given in* (3.18), (3.23) *or Algorithm 4, and* (3.21)*, respectively.*

1. *The zonotope $\mathcal{R}(\mathsf{H})$ is covered by the parallelepipeds $\{\mathbf{v}_{\mathcal{I}} + \mathcal{D}_{\mathcal{I}}\}_{\mathcal{I} \in \mathcal{U}}$, which overlap only on sets of measure zero:*

$$\bigcup_{\mathcal{I} \in \mathcal{U}} \big(\mathbf{v}_{\mathcal{I}} + \mathcal{D}_{\mathcal{I}}\big) = \mathcal{R}(\mathsf{H}) \tag{3.26}$$

   and

$$\mathrm{vol}\Big(\big(\mathbf{v}_{\mathcal{I}} + \mathcal{D}_{\mathcal{I}}\big) \cap \big(\mathbf{v}_{\mathcal{J}} + \mathcal{D}_{\mathcal{J}}\big)\Big) = 0, \qquad \mathcal{I} \neq \mathcal{J}, \tag{3.27}$$

   where $\mathrm{vol}(\cdot)$ *denotes the (n_{R}-dimensional) Lebesgue measure.*

2. *Fix some $\mathcal{I} \in \mathcal{U}$ and some $\bar{\mathbf{x}} \in \mathbf{v}_{\mathcal{I}} + \mathcal{D}_{\mathcal{I}}$. The vector that induces $\bar{\mathbf{x}}$ with minimum energy, i.e., $\mathbf{x}_{\min}$ in* (3.5)*, is given by $\mathbf{x} = (x_1, \dots, x_{n_{\mathrm{T}}})^{\mathsf{T}}$, where*

$$x_i = \begin{cases} \mathsf{A} \cdot g_{\mathcal{I},i} & \text{if } i \in \mathcal{I}^{\mathrm{c}}, \\ \beta_i & \text{if } i \in \mathcal{I}, \end{cases} \tag{3.28}$$

   where the vector $\boldsymbol{\beta} = (\beta_i \colon i \in \mathcal{I})^{\mathsf{T}}$ is given by

$$\boldsymbol{\beta} \triangleq \mathsf{H}_{\mathcal{I}}^{-1}(\bar{\mathbf{x}} - \mathbf{v}_{\mathcal{I}}). \tag{3.29}$$

Proof: The proof is deferred to Appendix A.2.1. □

Figure 3.2 shows the partition of $\mathcal{R}(\mathsf{H})$ into the union (3.26) for two 2×4 examples. Figure 3.3 shows the union for a 2×3 example when there exist 2 column vectors in the channel matrix that are linearly dependent.

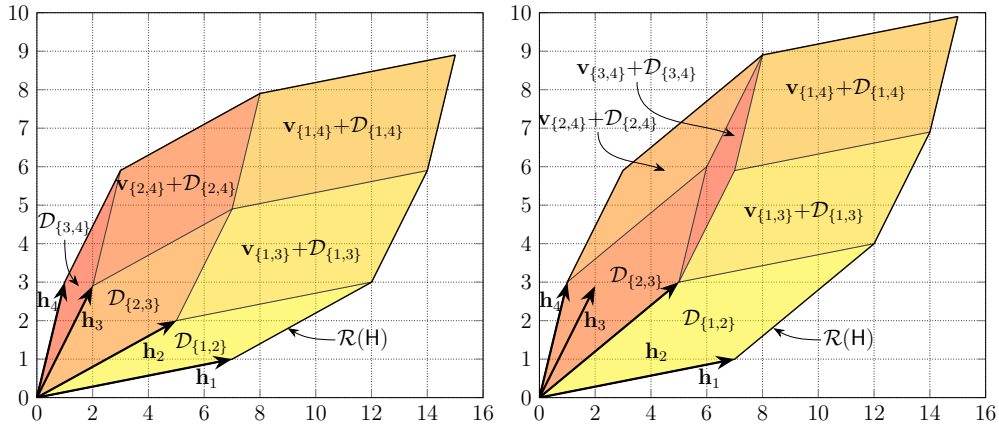

Figure 3.2: Partition of $\mathcal{R}(\mathsf{H})$ into the union (3.26) for two 2×4 MIMO examples. The example on the left is for $\mathsf{H} = [7, 5, 2, 1; 1, 2, 2.9, 3]$ and the example on the right for $\mathsf{H} = [7, 5, 2, 1; 1, 3, 2.9, 3]$.

Remark 7. If Condition (3.22) holds, then the vector $\mathbf{x}$ that solves the minimization problem in (3.5) is unique. △

Hence the minimum-energy signaling strategy partitions the image space of vectors $\bar{\mathbf{x}}$ into $\binom{n_\mathrm{T}}{n_\mathrm{R}}$ parallelepipeds, each one spanned by a different subset of n_R columns of the channel matrix. In each parallelepiped, the minimum-energy signaling sets the $n_\mathrm{T} - n_\mathrm{R}$ inputs corresponding to the columns that were not chosen either to 0 or to A according to a the rule specified in (3.21) and uses the n_R inputs corresponding to the chosen columns for signaling within the parallelepiped.

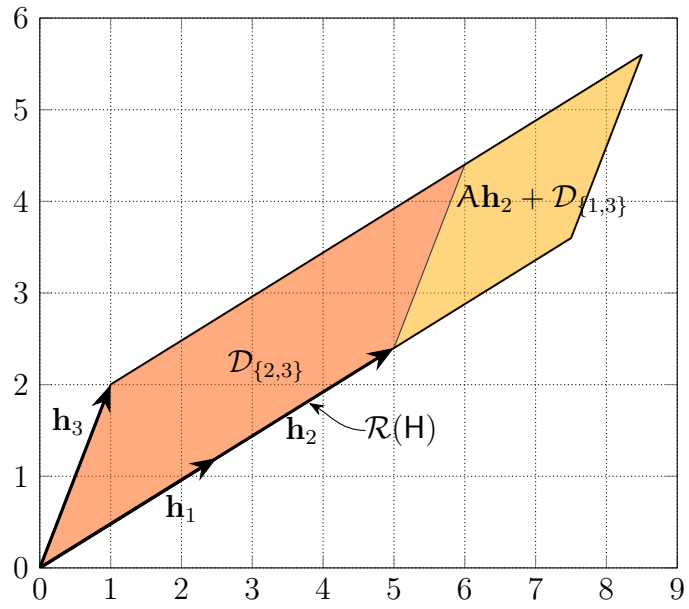

Figure 3.3: The zonotope $\mathcal{R}(\mathsf{H})$ for the 2×3 MIMO channel matrix $\mathsf{H} = [2.5, 5, 1; 1.2, 2.4, 2]$ and its minimum-energy decomposition into two parallelograms.

Chapter 4

Maximum-Variance Signaling

This chapter describes a maximum-variance signaling that maximizes the trace of the covariance matrix of the random image vector $\bar{\mathbf{X}}$. We characterize several properties of the corresponding optimal input distribution that are useful to obtain the low-SNR capacity slope in Chapters 5 and 6.

4.1 Problem Formulation

As we shall see in Chapters 5 and 6 ahead and in [28], at low SNR the asymptotic capacity is characterized by the maximum trace of the covariance matrix of $\bar{\mathbf{X}} = \mathsf{H}\mathbf{X}$, which we denote

$$\mathsf{K}_{\bar{\mathbf{X}}\bar{\mathbf{X}}} \triangleq \mathsf{E}\big[(\bar{\mathbf{X}} - \mathsf{E}[\bar{\mathbf{X}}])(\bar{\mathbf{X}} - \mathsf{E}[\bar{\mathbf{X}}])^{\mathsf{T}}\big]. \tag{4.1}$$

In this chapter we discuss properties of an optimal input distribution for $\mathbf{X}$ that maximizes this trace. Thus, we are interested in the following maximization problem:

$$\max_{P_{\mathbf{X}} \text{ satisfying (2.5)}} \operatorname{tr}\big(\mathsf{K}_{\bar{\mathbf{X}}\bar{\mathbf{X}}}\big) \tag{4.2}$$

where the maximization is over all input distributions $P_{\mathbf{X}}$ satisfying the peak- and average-power constraints given in (2.5).

4.2 MIMO Maximum-Variance Signaling

The following three lemmas show that the optimal input to the optimization problem in (4.2) has certain structures: Lemma 8 shows that it is discrete with all entries taking values in $\{0, \mathsf{A}\}$; Lemma 9 shows that the possible values of the optimal $\mathbf{X}$ form a "path" in $[0, \mathsf{A}]^{n_{\mathrm{T}}}$ starting from the origin; and Lemma 10 shows that, under mild assumptions, this optimal $\mathbf{X}$ takes at most $n_{\mathrm{R}} + 2$ values.

The proofs to the lemmas in this section are given in Appendix A.3.

Lemma 8. *An optimal input to the maximization problem in* (4.2) *uses for each component of* $\mathbf{X}$ *only the values* 0 *and* A*:*

$$X_i \in \{0, \mathsf{A}\} \quad \text{with probability 1}, \quad i = 1, \ldots, n_{\mathrm{T}}. \tag{4.3}$$

Lemma 9. *An optimal input to the optimization problem in* (4.2) *is a PMF* $P^*_{\mathbf{X}}$ *over a set* $\{\mathbf{x}^*_1, \mathbf{x}^*_2, \ldots\}$ *satisfying*

$$x^*_{k,\ell} \leq x^*_{k',\ell} \quad \text{for all } k < k',\ \ell = 1, \ldots, n_{\mathrm{T}}. \tag{4.4}$$

Furthermore, the first point is $\mathbf{x}^*_1 = \mathbf{0}$*, and*

$$P^*_{\mathbf{X}}(\mathbf{0}) > 0. \tag{4.5}$$

Notice that Lemma 8 and the first part of Lemma 9 have already been proven in [28]. A proof is given in the appendix for completeness.

Lemma 10. *Define* $\mathcal{T}$ *to be the power set of* $\{1, \ldots, n_{\mathrm{T}}\}$ *without the empty set, and define for every* $\mathcal{J} \in \mathcal{T}$ *and every* $i \in \{1, \ldots, n_{\mathrm{R}}\}$

$$r_{\mathcal{J},i} \triangleq \sum_{k=1}^{n_{\mathrm{T}}} h_{i,k}\, \mathbb{1}\{k \in \mathcal{J}\}, \quad \forall\, \mathcal{J} \in \mathcal{T},\ \forall\, i \in \{1, \ldots, n_{\mathrm{R}}\}. \tag{4.6}$$

(Here $\mathcal{J}$ *describes a certain choice of input antennas that will be set to* A*, while the remaining antennas will be set to* 0*.) Number all possible* $\mathcal{J} \in \mathcal{T}$ *from* $\mathcal{J}_1$ *to* $\mathcal{J}_{2^{n_{\mathrm{T}}}-1}$ *and define the matrix*

$$\mathsf{R} \triangleq \begin{pmatrix} 2r_{\mathcal{J}_1,1} & \cdots & 2r_{\mathcal{J}_1,n_{\mathrm{R}}} & |\mathcal{J}_1| & \|\mathbf{r}_{\mathcal{J}_1}\|_2^2 \\ 2r_{\mathcal{J}_2,1} & \cdots & 2r_{\mathcal{J}_2,n_{\mathrm{R}}} & |\mathcal{J}_2| & \|\mathbf{r}_{\mathcal{J}_2}\|_2^2 \\ \vdots & \ddots & \vdots & \vdots & \vdots \\ 2r_{\mathcal{J}_{2^{n_{\mathrm{T}}}-1},1} & \cdots & 2r_{\mathcal{J}_{2^{n_{\mathrm{T}}}-1},n_{\mathrm{R}}} & |\mathcal{J}_{2^{n_{\mathrm{T}}}-1}| & \|\mathbf{r}_{\mathcal{J}_{2^{n_{\mathrm{T}}}-1}}\|_2^2 \end{pmatrix} \tag{4.7}$$

where

$$\mathbf{r}_{\mathcal{J}} \triangleq \left(r_{\mathcal{J},1}, r_{\mathcal{J},2}, \ldots, r_{\mathcal{J},n_{\mathrm{R}}}\right)^{\mathsf{T}}, \quad \forall\, \mathcal{J} \in \mathcal{T}. \tag{4.8}$$

If for every $(n_{\mathrm{R}}+2) \times (n_{\mathrm{R}}+2)$ *submatrix* $\mathsf{R}_{n_{\mathrm{R}}+2}$ *of matrix* R *is full-rank*

$$\operatorname{rank}(\mathsf{R}_{n_{\mathrm{R}}+2}) = n_{\mathrm{R}} + 2, \quad \forall\, \mathsf{R}_{n_{\mathrm{R}}+2}, \tag{4.9}$$

then the optimal input to the optimization problem in (4.2) *is a PMF* $P^*_{\mathbf{X}}$ *over a set* $\{\mathbf{0}, \mathbf{x}^*_1, \ldots, \mathbf{x}^*_{n_{\mathrm{R}}+1}\}$ *with* $n_{\mathrm{R}} + 2$ *points.*

Remark 11. Lemmas 6 and 8 together imply that the optimal $\bar{\mathbf{X}}$ in (4.2) takes value only in the set $\mathcal{F}_{\mathrm{CP}}$ of corner points of the parallelepipeds $\{\mathbf{v}_{\mathcal{I}} + \mathcal{D}_{\mathcal{I}}\}$:

$$\mathcal{F}_{\mathrm{CP}} \triangleq \bigcup_{\mathcal{I} \in \mathcal{U}} \left\{ \mathbf{v}_{\mathcal{I}} + \sum_{i \in \mathcal{I}} \lambda_i \mathbf{h}_i \colon \lambda_i \in \{0, \mathsf{A}\},\ \forall\, i \in \mathcal{I} \right\}. \tag{4.10}$$

Lemmas 9 and 10 further imply that the possible values of this optimal $\bar{\mathbf{X}}$ form a path in $\mathcal{F}_{\mathrm{CP}}$, starting from $\mathbf{0}$, and containing no more than $n_{\mathrm{R}} + 2$ points. △

Table 4.1 (see next page) illustrates four examples of distributions that maximize the trace of the covariance matrix in some MIMO channels.

Table 4.1: Maximum variance for different channel coefficients

channel gains	α	$\max_{P_{\mathbf{x}}} \mathrm{tr}\big(\mathsf{K}_{\bar{\mathbf{x}}\bar{\mathbf{x}}}\big)$	$P_{\mathbf{X}}\colon \max_{P_{\mathbf{x}}} \mathrm{tr}\big(\mathsf{K}_{\bar{\mathbf{x}}\bar{\mathbf{x}}}\big)$
$\mathsf{H} = \begin{pmatrix} 1.3 & 0.6 & 1 & 0.1 \\ 2.1 & 4.5 & 0.7 & 0.5 \end{pmatrix}$	1.5	$16.3687\mathsf{A}^2$	$P_{\mathbf{X}}(0,0,0,0) = 0.625,$ $P_{\mathbf{X}}(\mathsf{A},\mathsf{A},\mathsf{A},\mathsf{A}) = 0.375$
$\mathsf{H} = \begin{pmatrix} 1.3 & 0.6 & 1 & 0.1 \\ 2.1 & 4.5 & 0.7 & 0.5 \end{pmatrix}$	0.9	$12.957\mathsf{A}^2$	$P_{\mathbf{X}}(0,0,0,0) = 0.7,$ $P_{\mathbf{X}}(\mathsf{A},\mathsf{A},\mathsf{A},0) = 0.3$
$\mathsf{H} = \begin{pmatrix} 1.3 & 0.6 & 1 & 0.1 \\ 2.1 & 4.5 & 0.7 & 0.5 \end{pmatrix}$	0.6	$9.9575\mathsf{A}^2$	$P_{\mathbf{X}}(0,0,0,0) = 0.7438,$ $P_{\mathbf{X}}(\mathsf{A},\mathsf{A},0,0) = 0.1687,$ $P_{\mathbf{X}}(\mathsf{A},\mathsf{A},\mathsf{A},0) = 0.0875$
$\mathsf{H} = \begin{pmatrix} 1.3 & 0.6 & 1 & 0.1 \\ 2.1 & 4.5 & 0.7 & 0.5 \end{pmatrix}$	0.3	$6.0142\mathsf{A}^2$	$P_{\mathbf{X}}(0,0,0,0) = 0.85,$ $P_{\mathbf{X}}(\mathsf{A},\mathsf{A},0,0) = 0.15$
$\mathsf{H} = \begin{pmatrix} 0.9 & 3.2 & 1 & 2.1 \\ 0.5 & 3.5 & 1.7 & 2.5 \\ 0.7 & 1.1 & 1.1 & 1.3 \end{pmatrix}$	0.9	$23.8405\mathsf{A}^2$	$P_{\mathbf{X}}(0,0,0,0) = 0.7755,$ $P_{\mathbf{X}}(\mathsf{A},\mathsf{A},\mathsf{A},\mathsf{A}) = 0.2245$
$\mathsf{H} = \begin{pmatrix} 0.9 & 3.2 & 1 & 2.1 \\ 0.5 & 3.5 & 1.7 & 2.5 \\ 0.7 & 1.1 & 1.1 & 1.3 \end{pmatrix}$	0.75	$20.8950\mathsf{A}^2$	$P_{\mathbf{X}}(0,0,0,0) = 0.7772,$ $P_{\mathbf{X}}(\mathsf{A},\mathsf{A},\mathsf{A},0) = 0.1413,$ $P_{\mathbf{X}}(\mathsf{A},\mathsf{A},\mathsf{A},\mathsf{A}) = 0.0815$
$\mathsf{H} = \begin{pmatrix} 0.9 & 3.2 & 1 & 2.1 \\ 0.5 & 3.5 & 1.7 & 2.5 \\ 0.7 & 1.1 & 1.1 & 1.3 \end{pmatrix}$	0.6	$17.7968\mathsf{A}^2$	$P_{\mathbf{X}}(0,0,0,0) = 0.8,$ $P_{\mathbf{X}}(\mathsf{A},\mathsf{A},\mathsf{A},0) = 0.2$

4.3 MISO Maximum-Variance Signaling

When $n_{\mathrm{R}} = 1$, the channel reduces to the MISO channel. Since $\bar{X}$ in this case is just a scalar, then the maximum variance of $\bar{X}$ can be characterized by

$$\mathsf{V}_{\max}(\mathsf{A}, \alpha\mathsf{A}) \triangleq \max_{P_{\bar{X}}} \mathsf{E}\Big[\big(\bar{X} - \mathsf{E}[\bar{X}]\big)^2\Big], \tag{4.11}$$

where the maximization is over all distributions on $\bar{X} \in \mathbb{R}_0^+$ satisfying the power constraints.

The following Lemma 12 characterizes the optimal input to the optimization problem in (4.11) in the MISO channel.

Lemma 12 (Lemma 8, [23]). *1. The maximum variance $\mathsf{V}_{\max}(\mathsf{A}, \alpha\mathsf{A})$ can be achieved by restricting $P_{\bar{X}}$ to the support set*

$$\{0, s_1\mathsf{A}, s_2\mathsf{A}, \ldots, s_{n_{\mathrm{T}}}\mathsf{A}\}. \tag{4.12}$$

2. The maximum variance $\mathsf{V}_{\max}(\mathsf{A}, \alpha\mathsf{A})$ satisfies

$$\mathsf{V}_{\max}(\mathsf{A}, \alpha\mathsf{A}) = \mathsf{A}^2\gamma \tag{4.13}$$

where

$$\gamma \triangleq \max_{\substack{q_1,\ldots,\ q_{n_{\mathrm{T}}} \geq 0: \\ \sum_{k=1}^{n_{\mathrm{T}}} q_k \leq 1 \\ \sum_{k=1}^{n_{\mathrm{T}}} k \cdot q_k \leq \alpha}} \left\{ \sum_{k=1}^{n_{\mathrm{T}}} s_k^2 q_k - \left(\sum_{k=1}^{n_{\mathrm{T}}} s_k q_k \right)^2 \right\}. \tag{4.14}$$

3. The optimal solution $\mathbf{q}^* = (q_1^*, \ldots, q_{n_{\mathrm{T}}}^*)$ in (4.14) satisfies $\sum_{k=1}^{n_{\mathrm{T}}} q_k < 1$ with strict inequality and $\sum_{k=1}^{n_{\mathrm{T}}} k \cdot q_k = \alpha$ with equality. Furthermore, whenever

$$\operatorname{rank} \begin{pmatrix} 1 & \frac{1}{s_1} & s_1 \\ 1 & \frac{2}{s_2} & s_2 \\ \vdots & \vdots & \vdots \\ 1 & \frac{n_{\mathrm{T}}}{s_{n_{\mathrm{T}}}} & s_{n_{\mathrm{T}}} \end{pmatrix} = 3, \tag{4.15}$$

the solution $\mathbf{q}^*$ to (4.14) has at most two nonzero elements, i.e., under condition (4.15), the maximum variance $\mathsf{V}_{\max}$ is achieved by an $\bar{X}^*$ with positive probability masses at 0 and at most two points from the set $\{s_1\mathsf{A}, \ldots, s_{n_{\mathrm{T}}}\mathsf{A}\}$.

See Table 4.2 for a few examples on numerical solution to the maximization problem in (4.14).

For many examples, the optimizing $\mathbf{q}^*$ has only a single positive entry, and thus $\mathsf{V}_{\max}$ is achieved by an $\bar{X}^*$ that has only two point masses (one of them at 0). Table 4.1 presents some examples of maximum variances $\mathsf{V}_{\max}$ and the probability mass functions of $\bar{X}^*$ achieving $\mathsf{V}_{\max}$.

Table 4.2: Maximum Variance for Different Channel Coefficients

channel gains	α	$\mathsf{V}_{\max}$	$Q_{\bar{X}}$ achieving $\mathsf{V}_{\max}$
$\mathbf{h} = (3, 2.2, 0.1)$	0.9	$6.6924\mathsf{A}^2$	$Q_{\bar{X}}(0) = 0.55,\ Q_{\bar{X}}(s_2\mathsf{A}) = 0.45$
$\mathbf{h} = (3, 2.2, 1.1)$	0.7	$7.1001\mathsf{A}^2$	$Q_{\bar{X}}(0) = 0.7667,\ Q_{\bar{X}}(s_3\mathsf{A}) = 0.2333$
$\mathbf{h} = (3, 1.5, 0.3)$	0.95	$5.1158\mathsf{A}^2$	$Q_{\bar{X}}(0) = 0.5907,\ Q_{\bar{X}}(s_2\mathsf{A}) = 0.2780,$ $Q_{\bar{X}}(s_3\mathsf{A}) = 0.1313$

Chapter 5

MISO Channel Capacity Analysis

This chapter presents a new improved upper bound for the SISO channel and new lower and upper bounds for the MISO channel. Many results in this chapter are from [23], and included for completeness; Theorems 14 and 16 are the main new results of this thesis.

5.1 Equivalent Capacity Expression

In this section we first express the channel capacity in terms of $\bar{X}$. From Lemma 2 in Chapter 3, we define the random variable U over the alphabet $\{1, \ldots, n_{\mathrm{T}}\}$ to indicate in which interval $\bar{X}$ lies:

$$\bar{X} \in [\mathsf{A}s_{k-1}, \mathsf{A}s_k) \implies U = k, \tag{5.1}$$

and $U = n_{\mathrm{T}}$ if $\bar{X} = \mathsf{A}s_{n_{\mathrm{T}}}$. Let $\mathbf{p} = (p_1, \ldots, p_{n_{\mathrm{T}}})$ denote the probability vector of U:

$$p_k \triangleq \Pr[U = k], \qquad k \in \{1, \ldots, n_{\mathrm{T}}\}. \tag{5.2}$$

The expression of the channel capacity for the MISO case can then be simplified in the following lemma. The proof can be found in [23].

Lemma 13 (Proposition 3, [23]). *The MISO capacity satisfies*

$$\mathsf{C}_{\mathbf{h}}(\mathsf{A}, \alpha\mathsf{A}) = \max_{P_{\bar{X}}} \mathrm{I}(\bar{X}; Y), \tag{5.3}$$

where the maximization is over all laws on $\bar{X} \in \mathbb{R}_0^+$ satisfying

$$\Pr\big[\bar{X} > s_{n_{\mathrm{T}}}\mathsf{A}\big] = 0 \tag{5.4a}$$

and

$$\sum_{k=1}^{n_{\mathrm{T}}} p_k \left(\frac{\mathsf{E}[\bar{X} \,|\, U = k] - \mathsf{A}s_{k-1}}{h_k} + (k-1)\mathsf{A} \right) \leq \alpha\mathsf{A}. \tag{5.4b}$$

5.2 Capacity Results

5.2.1 A Duality-Based Upper Bound for the SISO Channel

Consider first the SISO channel, where $n_{\mathrm{T}} = 1$ and $h_1 = 1$. So here, the average-power constraint is active when $\alpha \leq \frac{1}{2}$. We have the following upper bound:

Theorem 14 (Upper Bound on SISO Capacity). *For any $\mu > 0$, the SISO capacity $\mathsf{C}_1(\mathsf{A}, \alpha\mathsf{A})$ under peak-power constraint A and average-power constraint $\alpha\mathsf{A}$ is upper-bounded as:*

$$\mathsf{C}_1(\mathsf{A}, \alpha\mathsf{A}) \leq \log\left(1 + \frac{\mathsf{A}}{\sqrt{2\pi e}} \frac{1 - e^{-\mu}}{\mu}\right) + \frac{1}{\sqrt{2\pi}} \frac{\mu}{\mathsf{A}} \left(1 - e^{-\frac{\mathsf{A}^2}{2}}\right) + \mu\alpha\left(1 - 2\mathcal{Q}\left(\frac{\mathsf{A}}{2}\right)\right), \tag{5.5}$$

where $\mathcal{Q}(\cdot)$ denotes the $\mathcal{Q}$-function associated with the standard normal distribution.

Proof: See Appendix A.4.1. □

5.2.2 A Duality-Based Upper Bound for the MISO Channel

In the following we present an analytic upper bound and compare it to numerical lower bounds. As we will see, the upper bound is asymptotically tight at high-SNR, and can improve on previous bounds in the regime of moderate SNR.

This upper bound is based on Theorem 5.5 and the following Proposition 15:

Proposition 15 (Sec. 6, Eq. (88), [23]). *Let $\mathbf{X}^*$ be a capacity-achieving input distribution for the MISO channel with gain vector $\mathbf{h}$. Define for all $k \in \{1, \ldots, n_{\mathrm{T}}\}$:*

$$p_k^* \triangleq \Pr_{\mathbf{X}^*}[U = k], \tag{5.6a}$$

$$\alpha_k^* \triangleq \mathsf{E}_{\mathbf{X}^*}\left[\frac{\bar{X} - s_{k-1}\mathsf{A}}{h_k \mathsf{A}} \middle| U = k\right]. \tag{5.6b}$$

The capacity of the MISO channel is upper-bounded as

$$\mathsf{C}_{\mathbf{h}}(\mathsf{A}, \alpha\mathsf{A}) \leq \mathsf{H}(\mathbf{p}^*) + \sum_{k=1}^{n_{\mathrm{T}}} p_k^* \mathsf{C}_1(h_k\mathsf{A}, \alpha_k^* h_k \mathsf{A}), \tag{5.7}$$

and it holds that

$$\sum_{k=1}^{n_{\mathrm{T}}} p_k^* \big(\alpha_k^* + (k-1)\big) \leq \alpha. \tag{5.8}$$

We can now state our new upper bound on the MISO capacity.

Theorem 16. *The MISO capacity is upper-bounded as:*

$$\mathsf{C}_{\mathbf{h}}(\mathsf{A}, \alpha\mathsf{A}) \leq \sup_{\mathbf{p}} \inf_{\mu > 0} \left\{ H(\mathbf{p}) + \sum_{k=1}^{n_T} p_k \log\left(1 + \frac{\mathsf{A}h_k}{\sqrt{2\pi e}} \cdot \frac{1 - e^{-\mu}}{\mu}\right) + \frac{\mu}{\sqrt{2\pi}\mathsf{A}} \sum_{k=1}^{n_T} \frac{p_k}{h_k} \left(1 - e^{-\frac{\mathsf{A}^2 h_k^2}{2}}\right) + \mu\left(\alpha - \sum_{k=1}^{n_T} p_k (k-1)\right) \right\} \tag{5.9}$$

where the supremum is over vectors $\mathbf{p} = (p_1, \ldots, p_{n_\mathrm{T}})$ *satisfying*

$$\sum_{k=1}^{n_T} p_k(k-1) \leq \alpha. \tag{5.10}$$

Proof: Combine Proposition 15 and Theorem 14, and use the bound $1 - 2\mathcal{Q}\big(\frac{\mathsf{A}}{2}\big) < 1$. □

5.3 Asymptotic Capacity at low SNR

Proposition 17. *The MISO capacity is upper-bounded as*

$$\mathsf{C}_{\mathbf{h}}(\mathsf{A}, \alpha\mathsf{A}) \leq \frac{1}{2}\log(1 + \mathsf{V}_{\max}(\mathsf{A}, \alpha\mathsf{A})). \tag{5.11}$$

Proof: Since $\bar{X}$ and Z are independent, we know that the variance of Y cannot exceed $\mathsf{V}_{\max}(\mathsf{A}, \alpha\mathsf{A}) + 1$, and therefore

$$\mathsf{h}(Y) \leq \frac{1}{2}\log 2\pi e(\mathsf{V}_{\max}(\mathsf{A}, \alpha\mathsf{A}) + 1). \tag{5.12}$$

The bound follows by subtracting $\mathsf{h}(Z) = \frac{1}{2}\log 2\pi e$ from the above. □

In fact, the asymptotic capacity slope at low SNR is only determined by two parameters A and $\mathsf{V}_{\max}(\mathsf{A}, \alpha\mathsf{A})$. It is shown that

Theorem 18 (Proposition 12, [23]). *The low-SNR asymptotic capacity slope is*

$$\lim_{\mathsf{A}\downarrow 0} \frac{\mathsf{C}_{\mathbf{h}}(\mathsf{A}, \alpha\mathsf{A})}{\mathsf{A}^2} = \frac{\gamma}{2}, \tag{5.13}$$

where γ *is defined in* (4.14).

5.4 Numerical Results

Example 19. Consider a SISO channel with $\alpha = 0.4$, the numerical results are shown in Figure 5.1. We compare the upper bound (5.5) with the lower and upper bounds in [23]. We also plot numerical lower bound with two, three, and four probability mass points. At low- and moderate-SNR regime, these numerical lower bounds are very close to the new upper bound. This indicates that it gives a good approximation to the capacity and dominates other existing upper bounds in the moderate-SNR regime. ♢

Example 20. Consider the 3-LED MISO channel with gains $\mathbf{h} = (3, 2, 1.5)$. The asymptotic low-SNR capacity slope is $\gamma/2 = 5.07$ and is attained by choosing $\bar{X}$ equal to 0 with probability $q_0 = 0.6$ and equal to $s_3\mathsf{A}$ with probability $q_3 = 0.4$. Figure 5.2 shows lower and upper bounds on the channel capacity at different SNR values. The blue lower bound is obtained by numerically evaluating $\mathrm{I}(\bar{X}; Y)$ for

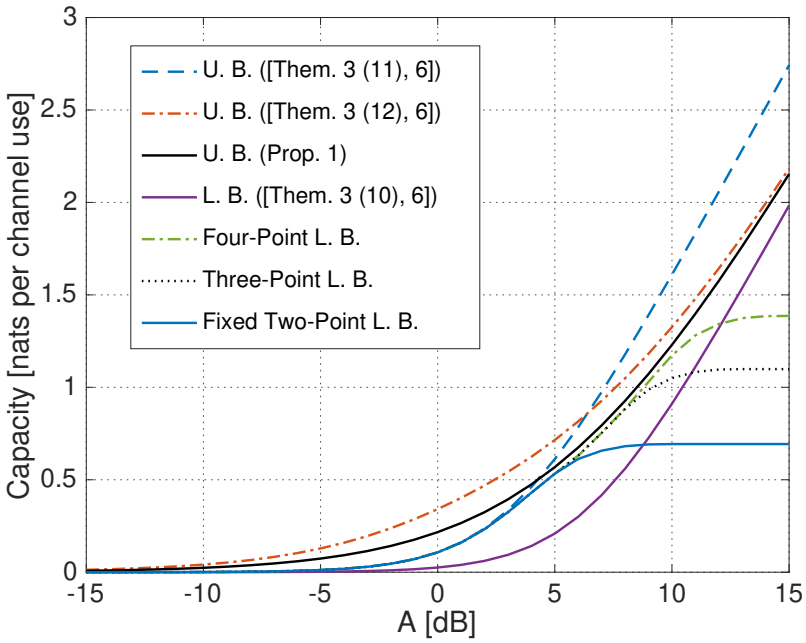

Figure 5.1: Bounds on capacity of SISO channel with $\alpha = 0.4$.

the choice of $\bar{X}$ that achieves the asymptotic low-SNR capacity. The magenta lower bound follows by numerically optimizing $\mathrm{I}(\bar{X};Y)$ over all choices of $\bar{X}$ that have positive probability on $\bar{X} = 0$ and on at most two point masses from $\{s_1\mathsf{A}, \ldots, s_{n_\mathrm{T}}\mathsf{A}\}$. In the low-SNR regime, these numerical lower bounds improve over the previous analytic lower bounds in [23] and are very close to the maximum-variance upper bound in [23, Prop. 9]. The gap between the best upper and lower bounds is larger in the moderate SNR regime. In this regime, the best upper bound (see the black line) is given in Theorem 16. ◊

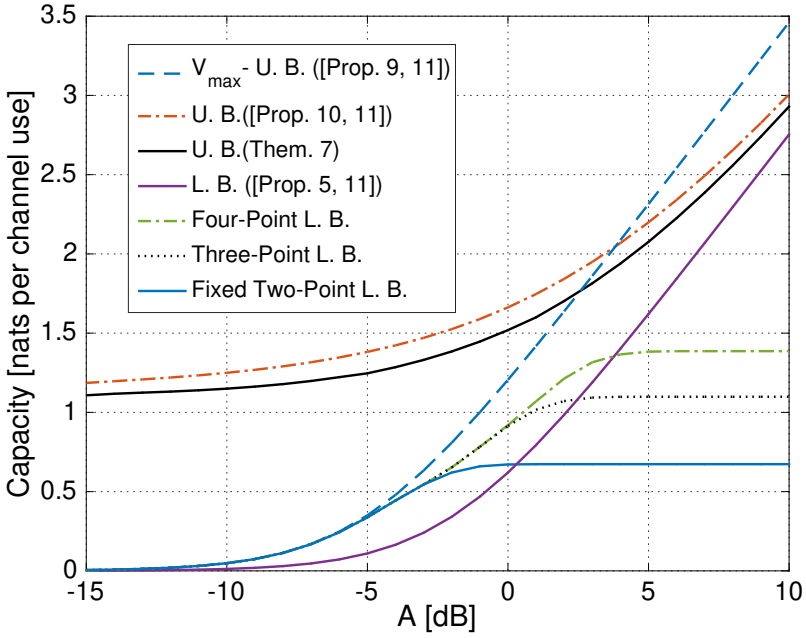

Figure 5.2: Bounds on capacity of MISO channel with gains $\mathbf{h} = (3, 2, 1.5)$ and average-to-peak power ratio $\alpha = 1.2$.

Chapter 6

MIMO Channel Capacity Analysis

In this chapter we present new upper and lower bounds on the capacity of the general MIMO channels. As byproducts, we also characterize the asymptotic capacity at low and high SNR. The results in this chapter are based on the results in [52], [53].

6.1 Equivalent Capacity Expression

We state an alternative expression for the capacity $\mathsf{C}_{\mathsf{H}}(\mathsf{A}, \alpha\mathsf{A})$ in terms of $\bar{\mathbf{X}}$ instead of $\mathbf{X}$. To that goal we define for each index set $\mathcal{I} \in \mathcal{U}$

$$s_{\mathcal{I}} \triangleq \sum_{j \in \mathcal{I}^{\mathrm{c}}} g_{\mathcal{I},j}, \quad \mathcal{I} \in \mathcal{U}, \tag{6.1}$$

which indicates the number of components of the input vector set to A in order to induce $\mathbf{v}_{\mathcal{I}}$.

Remark 21. It follows directly from Lemma 6 that

$$0 \leq s_{\mathcal{I}} \leq n_{\mathrm{T}} - n_{\mathrm{R}}. \tag{6.2}$$

△

Proposition 22. *The capacity* $\mathsf{C}_{\mathsf{H}}(\mathsf{A}, \alpha\mathsf{A})$ *defined in* (2.10) *is given by*

$$\mathsf{C}_{\mathsf{H}}(\mathsf{A}, \alpha\mathsf{A}) = \max_{P_{\bar{\mathbf{X}}}} \mathrm{I}(\bar{\mathbf{X}}; \mathbf{Y}) \tag{6.3}$$

where the maximization is over all distributions $P_{\bar{\mathbf{X}}}$ *over* $\mathcal{R}(\mathsf{H})$ *subject to the power constraint:*

$$\mathsf{E}_U\Big[\mathsf{A}s_U + \big\|\mathsf{H}_U^{-1}\big(\mathsf{E}[\bar{\mathbf{X}}\,|\,U] - \mathbf{v}_U\big)\big\|_1\Big] \leq \alpha\mathsf{A}, \tag{6.4}$$

where U is a random variable over $\mathcal{U}$ such that[1]

$$\big(U = \mathcal{I}\big) \implies \big(\bar{\mathbf{X}} \in (\mathbf{v}_{\mathcal{I}} + \mathcal{D}_{\mathcal{I}})\big). \tag{6.5}$$

Proof: Notice that we have a Markov chain $\mathbf{X} \multimap \bar{\mathbf{X}} \multimap \mathbf{Y}$, and that $\bar{\mathbf{X}}$ is a function of $\mathbf{X}$. Therefore, $\mathrm{I}(\bar{\mathbf{X}}; \mathbf{Y}) = \mathrm{I}(\mathbf{X}; \mathbf{Y})$. Moreover, by Lemma 6, the range of $\bar{\mathbf{X}}$ in $\mathcal{R}(\mathsf{H})$ can be decomposed into the shifted parallelepipeds $\{\mathbf{v}_{\mathcal{I}} + \mathcal{D}_{\mathcal{I}}\}_{\mathcal{I}\in\mathcal{U}}$. Again by Lemma 6, for any image point $\bar{\mathbf{x}}$ in $\mathbf{v}_{\mathcal{I}} + \mathcal{D}_{\mathcal{I}}$, the minimum energy required to induce $\bar{\mathbf{x}}$ is

$$\mathsf{A} s_{\mathcal{I}} + \big\|\mathsf{H}_{\mathcal{I}}^{-1}(\bar{\mathbf{x}} - \mathbf{v}_{\mathcal{I}})\big\|_1. \tag{6.6}$$

Without loss in optimality, we restrict ourselves to input vectors $\mathbf{x}$ that achieve some $\bar{\mathbf{x}}$ with minimum energy. Then, by the law of total expectation, the average power can be rewritten as

$$\begin{aligned}
\mathsf{E}\big[\|\mathbf{X}\|_1\big] &= \sum_{\mathcal{I}\in\mathcal{U}} p_{\mathcal{I}}\, \mathsf{E}\big[\|\mathbf{X}\|_1 \,\big|\, U = \mathcal{I}\big] && (6.7)\\
&= \sum_{\mathcal{I}\in\mathcal{U}} p_{\mathcal{I}}\, \mathsf{E}\Big[\mathsf{A} s_{\mathcal{I}} + \big\|\mathsf{H}_{\mathcal{I}}^{-1}(\bar{\mathbf{X}} - \mathbf{v}_{\mathcal{I}})\big\|_1 \,\Big|\, U = \mathcal{I}\Big] && (6.8)\\
&= \sum_{\mathcal{I}\in\mathcal{U}} p_{\mathcal{I}}\Big(\mathsf{A} s_{\mathcal{I}} + \big\|\mathsf{H}_{\mathcal{I}}^{-1}\big(\mathsf{E}[\bar{\mathbf{X}} \,|\, U = \mathcal{I}] - \mathbf{v}_{\mathcal{I}}\big)\big\|_1\Big) && (6.9)\\
&= \mathsf{E}_U\Big[\mathsf{A} s_U + \big\|\mathsf{H}_U^{-1}\big(\mathsf{E}[\bar{\mathbf{X}} \,|\, U] - \mathbf{v}_U\big)\big\|_1\Big]. && (6.10)
\end{aligned}$$

□

Remark 23. The term inside the expectation on the left-hand side (LHS) of (6.4) can be seen as a cost function for $\bar{\mathbf{X}}$, where the cost is linear within each of the parallelepipeds $\{\mathcal{D}_{\mathcal{I}} + \mathbf{v}_{\mathcal{I}}\}_{\mathcal{I}\in\mathcal{U}}$ (but not linear on the entire $\mathcal{R}(\mathsf{H})$). At very high SNR, the receiver can obtain an almost perfect guess of U. As a result, our channel can be seen as a set of almost parallel channels in the sense of [54, Exercise 7.28]. Each one of the parallel channels is an amplitude-constrained $n_{\mathrm{R}} \times n_{\mathrm{R}}$ MIMO channel, with a linear power constraint. This observation will help us obtain upper and lower bounds on capacity that are tight in the high-SNR limit. Specifically, for an upper bound, we reveal U to the receiver and then apply previous results on full-rank $n_{\mathrm{R}} \times n_{\mathrm{R}}$ MIMO channels [24]. For a lower bound, we choose the inputs in such a way that, on each parallelepiped $\mathcal{D}_{\mathcal{I}} + \mathbf{v}_{\mathcal{I}}$, the vector $\bar{\mathbf{X}}$ has the high-SNR-optimal distribution for the corresponding $n_{\mathrm{R}} \times n_{\mathrm{R}}$ channel. △

6.2 Capacity Results

Define

$$\mathsf{V}_{\mathsf{H}} \triangleq \sum_{\mathcal{I}\in\mathcal{U}} |\det(\mathsf{H}_{\mathcal{I}})|, \tag{6.11}$$

[1] The choice of U that satisfies (6.5) is not unique, but U under different choices are equal with probability 1.

and let $\mathbf{q}$ be a probability vector on $\mathcal{U}$ with entries

$$q_{\mathcal{I}} \triangleq \frac{|\det \mathsf{H}_{\mathcal{I}}|}{\mathsf{V}_{\mathsf{H}}}, \quad \mathcal{I} \in \mathcal{U}. \tag{6.12}$$

Further, define

$$\alpha_{\text{th}} \triangleq \frac{n_{\text{R}}}{2} + \sum_{\mathcal{I} \in \mathcal{U}} s_{\mathcal{I}}\, q_{\mathcal{I}}, \tag{6.13}$$

where $\{s_{\mathcal{I}}\}$ are defined in (6.1). Notice that α_{th} determines the threshold value for α above which $\bar{\mathbf{X}}$ can be made uniform over $\mathcal{R}(\mathsf{H})$. In fact, combining the minimum-energy signaling in Lemma 6 with a uniform distribution for $\bar{\mathbf{X}}$ over $\mathcal{R}(\mathsf{H})$, the expected input power is

$$\begin{aligned} \mathsf{E}[\|\mathbf{X}\|_1] &= \sum_{\mathcal{I} \in \mathcal{U}} \Pr[U = \mathcal{I}] \cdot \mathsf{E}[\|\mathbf{X}\|_1 \,|\, U = \mathcal{I}] && (6.14) \\ &= \sum_{\mathcal{I} \in \mathcal{U}} q_{\mathcal{I}} \left(\mathsf{A} s_{\mathcal{I}} + \frac{n_{\text{R}} \mathsf{A}}{2} \right) && (6.15) \\ &= \alpha_{\text{th}} \mathsf{A} && (6.16) \end{aligned}$$

where the random variable U indicates the parallelepiped containing $\bar{\mathbf{X}}$; see (6.5). Equality (6.15) holds because, when $\bar{\mathbf{X}}$ is uniform over $\mathcal{R}(\mathsf{H})$, $\Pr[U = \mathcal{I}] = q_{\mathcal{I}}$, and because, conditional on $U = \mathcal{I}$, using the minimum-energy signaling scheme, the input vector $\mathbf{X}$ is uniform over $\mathbf{v}_{\mathcal{I}} + \mathcal{D}_{\mathcal{I}}$.

Remark 24. Note that

$$\alpha_{\text{th}} \leq \frac{n_{\text{T}}}{2}, \tag{6.17}$$

as can be argued as follows. Let $\mathbf{X}$ be an input that achieves a uniform $\bar{\mathbf{X}}$ with minimum energy. According to (6.16) it consumes an input power $\alpha_{\text{th}}\mathsf{A}$. Define $\mathbf{X}'$ as

$$X'_i \triangleq \mathsf{A} - X_i, \quad i = 1, \ldots, n_{\text{T}}. \tag{6.18}$$

It must consume input power $(n_{\text{T}} - \alpha_{\text{th}})\mathsf{A}$. Note that $\mathbf{X}'$ also induces a uniform $\bar{\mathbf{X}}$ because the zonotope $\mathcal{R}(\mathsf{H})$ is point-symmetric. Since $\mathbf{X}$ consumes minimum energy, we know

$$\mathsf{E}[\|\mathbf{X}\|_1] \leq \mathsf{E}[\|\mathbf{X}'\|_1], \tag{6.19}$$

i.e.,

$$\alpha_{\text{th}}\mathsf{A} \leq (n_{\text{T}} - \alpha_{\text{th}})\mathsf{A}, \tag{6.20}$$

which implies (6.17). $\triangle$

6.2.1 EPI Lower Bounds

The proofs to the theorems in this section can be found in Appendix A.5.1.

Theorem 25. *If $\alpha \geq \alpha_{\text{th}}$, then*

$$\mathsf{C}_{\mathsf{H}}(\mathsf{A}, \alpha\mathsf{A}) \geq \frac{1}{2}\log\left(1 + \frac{\mathsf{A}^{2n_{\text{R}}}\mathsf{V}_{\mathsf{H}}^2}{(2\pi e)^{n_{\text{R}}}}\right). \tag{6.21}$$

Theorem 26. *If $\alpha < \alpha_{\text{th}}$, then*

$$\mathsf{C}_{\mathsf{H}}(\mathsf{A}, \alpha\mathsf{A}) \geq \frac{1}{2}\log\left(1 + \frac{\mathsf{A}^{2n_{\text{R}}}\mathsf{V}_{\mathsf{H}}^2}{(2\pi e)^{n_{\text{R}}}}\, e^{2\nu}\right) \tag{6.22}$$

with

$$\nu \triangleq \sup_{\lambda \in \left(\max\left\{0, \frac{n_{\text{R}}}{2} + \alpha - \alpha_{\text{th}}\right\}, \min\left\{\frac{n_{\text{R}}}{2}, \alpha\right\}\right)} \left\{ n_{\text{R}}\left(1 - \log\frac{\mu}{1 - e^{-\mu}} - \frac{\mu\, e^{-\mu}}{1 - e^{-\mu}}\right) - \inf_{\mathbf{p}} \mathsf{D}(\mathbf{p}\|\mathbf{q}) \right\}, \tag{6.23}$$

where μ is the unique solution to the following equation:

$$\frac{1}{\mu} - \frac{e^{-\mu}}{1 - e^{-\mu}} = \frac{\lambda}{n_{\text{R}}}, \tag{6.24}$$

and where the infimum is over all probability vectors $\mathbf{p}$ on $\mathcal{U}$ such that

$$\sum_{\mathcal{I} \in \mathcal{U}} p_{\mathcal{I}} s_{\mathcal{I}} = \alpha - \lambda \tag{6.25}$$

with $\{s_{\mathcal{I}}\}$ defined in (6.1).

The two lower bounds in Theorems 25 and 26 are derived by applying the EPI, and by maximizing the differential entropy $\mathsf{h}(\bar{\mathbf{X}})$ under constraints (6.4). When $\alpha \geq \alpha_{\text{th}}$, choosing $\bar{\mathbf{X}}$ to be uniformly distributed on $\mathcal{R}(\mathsf{H})$ satisfies (6.4), hence we can achieve $\mathsf{h}(\bar{\mathbf{X}}) = \log \mathsf{V}_{\mathsf{H}}$. When $\alpha < \alpha_{\text{th}}$, the uniform distribution is no longer an admissible distribution for $\bar{\mathbf{X}}$. In this case, we first select a PMF over the events $\{\bar{\mathbf{X}} \in (\mathbf{v}_{\mathcal{I}} + \mathcal{D}_{\mathcal{I}})\}_{\mathcal{I} \in \mathcal{U}}$, and, given $\bar{\mathbf{X}} \in \mathbf{v}_{\mathcal{I}} + \mathcal{D}_{\mathcal{I}}$, we choose the inputs $\{X_i \colon i \in \mathcal{I}\}$ according to a truncated exponential distribution rotated by the matrix $\mathsf{H}_{\mathcal{I}}$. Interestingly, it is optimal to choose the truncated exponential distributions for all sets $\mathcal{I} \in \mathcal{U}$ to have the same parameter μ. This parameter is determined by the power $\frac{\lambda}{n_{\text{R}}}$ allocated to the n_{R} signaling inputs $\{X_i \colon i \in \mathcal{I}\}$.

6.2.2 Duality-Based Upper Bounds

The proofs to the theorems in this section can be found in Appendix A.5.2.

The first upper bound is based on an analysis of the channel with peak-power constraint only, i.e., the average-power constraint (2.5b) is ignored.

Theorem 27. *For an arbitrary α,*

$$\mathsf{C}_{\mathsf{H}}(\mathsf{A},\alpha\mathsf{A}) \le \sup_{\mathbf{p}}\left\{\log \mathsf{V}_{\mathsf{H}} - \mathsf{D}(\mathbf{p}\|\mathbf{q}) + \sum_{\mathcal{I}\in\mathcal{U}} p_{\mathcal{I}} \sum_{\ell=1}^{n_{\mathrm{R}}} \log\left(\sigma_{\mathcal{I},\ell} + \frac{\mathsf{A}}{\sqrt{2\pi e}}\right)\right\}, \tag{6.26}$$

where $\sigma_{\mathcal{I},\ell}$ denotes the square root of the ℓth diagonal entry of the matrix $\mathsf{H}_{\mathcal{I}}^{-1}\mathsf{H}_{\mathcal{I}}^{-\mathsf{T}}$, and where the supremum is over all probability vectors $\mathbf{p}$ on $\mathcal{U}$.

The following two upper bounds in Theorems 28 and 29 hold only when $\alpha < \alpha_{\mathrm{th}}$.

Theorem 28. *If $\alpha < \alpha_{\mathrm{th}}$, then*

$$\begin{aligned}\mathsf{C}_{\mathsf{H}}(\mathsf{A},\alpha\mathsf{A}) \le \sup_{\mathbf{p}} \inf_{\mu>0}\Bigg\{&\log \mathsf{V}_{\mathsf{H}} - \mathsf{D}(\mathbf{p}\|\mathbf{q}) + \sum_{\mathcal{I}\in\mathcal{U}} p_{\mathcal{I}} \sum_{\ell=1}^{n_{\mathrm{R}}} \log\left(\sigma_{\mathcal{I},\ell} + \frac{\mathsf{A}}{\sqrt{2\pi e}}\frac{1-e^{-\mu}}{\mu}\right)\\ &+ \frac{\mu}{\mathsf{A}\sqrt{2\pi}} \sum_{\mathcal{I}\in\mathcal{U}} p_{\mathcal{I}} \sum_{\ell=1}^{n_{\mathrm{R}}} \sigma_{\mathcal{I},\ell}\left(1 - e^{-\frac{\mathsf{A}^2}{2\sigma_{\mathcal{I},\ell}^2}}\right) + \mu\left(\alpha - \sum_{\mathcal{I}\in\mathcal{U}} p_{\mathcal{I}} s_{\mathcal{I}}\right)\Bigg\},\end{aligned} \tag{6.27}$$

where the supremum is over all probability vectors $\mathbf{p}$ on $\mathcal{U}$ such that

$$\sum_{\mathcal{I}\in\mathcal{U}} p_{\mathcal{I}} s_{\mathcal{I}} \le \alpha. \tag{6.28}$$

Theorem 29. *If $\alpha < \alpha_{\mathrm{th}}$, then*

$$\begin{aligned}&\mathsf{C}_{\mathsf{H}}(\mathsf{A},\alpha\mathsf{A})\\ &\le \sup_{\mathbf{p}} \inf_{\delta,\mu>0}\Bigg\{\log \mathsf{V}_{\mathsf{H}} - \mathsf{D}(\mathbf{p}\|\mathbf{q}) + \sum_{\mathcal{I}\in\mathcal{U}} p_{\mathcal{I}} \sum_{\ell=1}^{n_{\mathrm{R}}} \log\left(\mathsf{A}\cdot\frac{e^{\frac{\mu\delta}{\mathsf{A}}} - e^{-\mu(1+\frac{\delta}{\mathsf{A}})}}{\sqrt{2\pi e}\mu\big(1-2\,\mathcal{Q}\big(\frac{\delta}{\sigma_{\mathcal{I},\ell}}\big)\big)}\right)\\ &\qquad+\sum_{\mathcal{I}\in\mathcal{U}} p_{\mathcal{I}} \sum_{\ell=1}^{n_{\mathrm{R}}} \mathcal{Q}\left(\frac{\delta}{\sigma_{\mathcal{I},\ell}}\right) + \sum_{\mathcal{I}\in\mathcal{U}} p_{\mathcal{I}} \sum_{\ell=1}^{n_{\mathrm{R}}} \frac{\delta}{\sqrt{2\pi}\sigma_{\mathcal{I},\ell}}\, e^{-\frac{\delta^2}{2\sigma_{\mathcal{I},\ell}^2}}\\ &\qquad+\frac{\mu}{\mathsf{A}\sqrt{2\pi}} \sum_{\mathcal{I}\in\mathcal{U}} p_{\mathcal{I}} \sum_{\ell=1}^{n_{\mathrm{R}}} \sigma_{\mathcal{I},\ell}\left(e^{-\frac{\delta^2}{2\sigma_{\mathcal{I},\ell}^2}} - e^{-\frac{(\mathsf{A}+\delta)^2}{2\sigma_{\mathcal{I},\ell}^2}}\right) + \mu\left(\alpha - \sum_{\mathcal{I}\in\mathcal{U}} p_{\mathcal{I}} s_{\mathcal{I}}\right)\Bigg\},\end{aligned} \tag{6.29}$$

where $\mathcal{Q}(\cdot)$ denotes the $\mathcal{Q}$-function associated with the standard normal distribution, and the supremum is over all probability vectors $\mathbf{p}$ on $\mathcal{U}$ satisfying (6.28).

The three upper bounds in Theorems 27, 28 and 29 are derived using the fact that capacity cannot be larger than over a channel where the receiver observes both $\mathbf{Y}$ and U. The mutual information corresponding to this channel $\mathsf{I}(\bar{\mathbf{X}};\mathbf{Y},U)$ decomposes as $\mathsf{H}(U) + \mathsf{I}(\bar{\mathbf{X}};\mathbf{Y}|U)$, where the term $\mathsf{H}(U)$ indicates the rate that can be achieved by coding over the choice of the parallelepiped to which $\bar{\mathbf{X}}$ belongs, and $\mathsf{I}(\bar{\mathbf{X}};\mathbf{Y}|U)$ indicates the average rate that can be achieved by coding over a single parallelepiped. By the results in Lemma 6, we can treat the channel matrix as an invertible matrix when knowing U, which greatly simplifies the bounding

on $\mathrm{I}(\bar{\mathbf{X}};\mathbf{Y}|U)$. The upper bounds are then obtained by optimizing over the probabilities assigned to the different parallelepipeds. As we will see later, the upper bounds are asymptotically tight at high SNR. The reason is that the additional term $\mathrm{I}(\bar{\mathbf{X}};\mathbf{Y},U)-\mathrm{I}(\bar{\mathbf{X}};\mathbf{Y})=\mathrm{I}(\bar{\mathbf{X}};U|\mathbf{Y})$ vanishes as the SNR grows large. To derive the asymptotic high-SNR capacity, we also use previous results in [24], which derived the high-SNR capacity of this channel when the channel matrix is invertible.

6.2.3 A Maximum-Variance Upper Bound

The upper bound in Theorem 30 is determined by the maximum trace of the covariance matrix of $\bar{\mathbf{X}}$ under the constraints (2.5).

Theorem 30. *For an arbitrary α,*

$$\mathsf{C}_{\mathsf{H}}(\mathsf{A},\alpha\mathsf{A}) \le \frac{n_{\mathrm{R}}}{2}\log\left(1+\frac{1}{n_{\mathrm{R}}}\max_{P_{\mathbf{X}}}\mathrm{tr}\big(\mathsf{K}_{\bar{\mathbf{X}}\bar{\mathbf{X}}}\big)\right), \tag{6.30}$$

where the maximization is over all input distributions $P_{\mathbf{X}}$ satisfying the power constraints (2.5)*.*

Note that Section 4.2 provides results that considerably simplify the maximization in (6.30). In particular, there exists a maximizing $P_{\mathbf{X}}$ that is a probability mass function over $\mathbf{0}$ and at most $n_{\mathrm{R}}+1$ other points on $\mathcal{F}_{\mathrm{CP}}$, where $\mathcal{F}_{\mathrm{CP}}$ is defined in (4.10).

6.3 Asymptotic Capacity

The proofs to the theorems in this section can be found in Appendix A.5.4.

Theorem 31 (High-SNR Asymptotics). *If $\alpha \ge \alpha_{\mathrm{th}}$, then*

$$\lim_{\mathsf{A}\to\infty}\big\{\mathsf{C}_{\mathsf{H}}(\mathsf{A},\alpha\mathsf{A})-n_{\mathrm{R}}\log\mathsf{A}\big\}=\frac{1}{2}\log\left(\frac{\mathsf{V}_{\mathsf{H}}^2}{(2\pi e)^{n_{\mathrm{R}}}}\right). \tag{6.31}$$

If $\alpha < \alpha_{\mathrm{th}}$, then

$$\lim_{\mathsf{A}\to\infty}\big\{\mathsf{C}_{\mathsf{H}}(\mathsf{A},\alpha\mathsf{A})-n_{\mathrm{R}}\log\mathsf{A}\big\}=\frac{1}{2}\log\left(\frac{\mathsf{V}_{\mathsf{H}}^2}{(2\pi e)^{n_{\mathrm{R}}}}\right)+\nu, \tag{6.32}$$

where $\nu<0$ is defined in (6.23)–(7.47)*.*

Recall that α_{th} is a threshold that determines whether $\bar{\mathbf{X}}$ can be uniformly distributed over $\mathcal{R}(\mathsf{H})$ or not. When $\alpha<\alpha_{\mathrm{th}}$, compared with the asymptotic capacity without active average-power constraint, the average-power constraint imposes a penalty on the channel capacity. This penalty is characterized by ν in (6.32). As shown in Figure 6.1, ν is a increasing function of α. When $\alpha<\alpha_{\mathrm{th}}$, ν is always negative, and reaches 0 when $\alpha\ge\alpha_{\mathrm{th}}$.

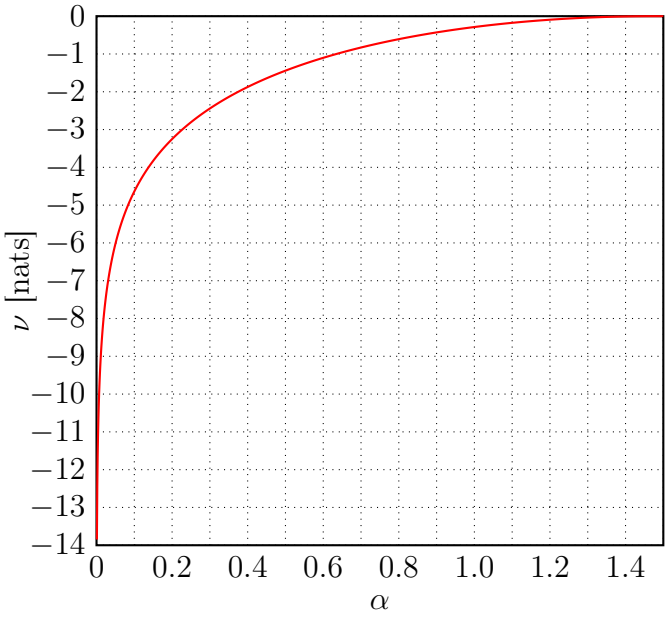

Figure 6.1: The parameter ν in (6.23) as a function of α, for a 2×3 MIMO channel with channel matrix $\mathsf{H} = [1, 1.5, 3; 2, 2, 1]$ with corresponding $\alpha_{\text{th}} = 1.4762$. Recall that ν is the asymptotic capacity gap to the case with no active average-power constraint.

Theorem 32 (Low-SNR Asymptotics, [28]). *For an arbitrary α,*

$$\lim_{\mathsf{A}\downarrow 0} \frac{\mathsf{C}_{\mathsf{H}}(\mathsf{A}, \alpha\mathsf{A})}{\mathsf{A}^2} = \frac{1}{2} \max_{P_{\mathbf{X}}} \operatorname{tr}\big(\mathsf{K}_{\bar{\mathbf{X}}\bar{\mathbf{X}}}\big), \tag{6.33}$$

where the maximization is over all input distributions $P_{\mathbf{X}}$ satisfying the power constraints

$$\Pr\big[X_k > 1\big] = 0, \quad \forall\, k \in \{1, \ldots, n_{\mathrm{T}}\}, \tag{6.34a}$$

$$\mathsf{E}\big[\|\mathbf{X}\|_1\big] \leq \alpha. \tag{6.34b}$$

Again, see the results in Section 4.2 about maximizing the trace of the covariance matrix $\mathsf{K}_{\bar{\mathbf{X}}\bar{\mathbf{X}}}$.

Example 33. Figure 6.2 plots the asymptotic slope, i.e., the right-hand side (RHS) of (6.33), as a function of α for a 2×3 MIMO channel. As we can see, the asymptotic slope is strictly increasing for all values of $\alpha < \frac{n_{\mathrm{T}}}{2}$. ◊

6.4 Numerical Results

In the following we present some numerical examples of our lower and upper bounds.

Example 34. Figures 6.3 and 6.4 depict the derived lower and upper bounds for a 2×3 MIMO channel (same channel as in Example 33) for $\alpha = 0.9$ and $\alpha = 0.3$ (both values are less than $\alpha_{\text{th}} = 1.4762$), respectively. Both upper bounds (6.27)

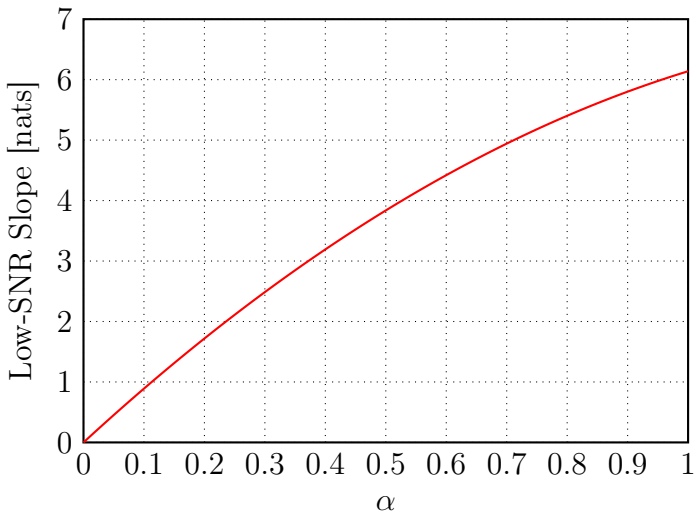

Figure 6.2: Low-SNR slope as a function of α, for a 2×3 MIMO channel with channel matrix $\mathsf{H} = [1, 1.5, 3; 2, 2, 1]$.

and (6.29) match with lower bound (6.22) asymptotically as A tends to infinity. Moreover, upper bound (6.26) gives a good approximation on capacity when the average-power constraint is weak (i.e., when α is close to α_{th}). Indeed, (6.26) is asymptotically tight at high SNR when $\alpha \geq \alpha_{\text{th}}$. We also plot three numerical lower bounds by optimizing $\mathrm{I}(\bar{\mathbf{X}}; \mathbf{Y})$ over all feasible choices of $\bar{\mathbf{X}}$ that have positive probability on two, three, or four distinct mass points. (One of the mass points is always at $\mathbf{0}$.) In the low-SNR regime, the upper bound (6.30) matches well with the two-point numerical lower bound. Actually (6.30) shares the same slope with capacity when the SNR tends to zero, which can be seen by comparing (6.30) with Theorem 32. ◊

Example 35. Figures 6.5 and 6.6 show similar trends in a 2×4 MIMO channel. Note that although in the 2×3 channel of Figures 6.3 and 6.4 the upper bound (6.27) is always tighter than (6.29), this does not hold in general, as can be seen in Figure 6.6. ◊

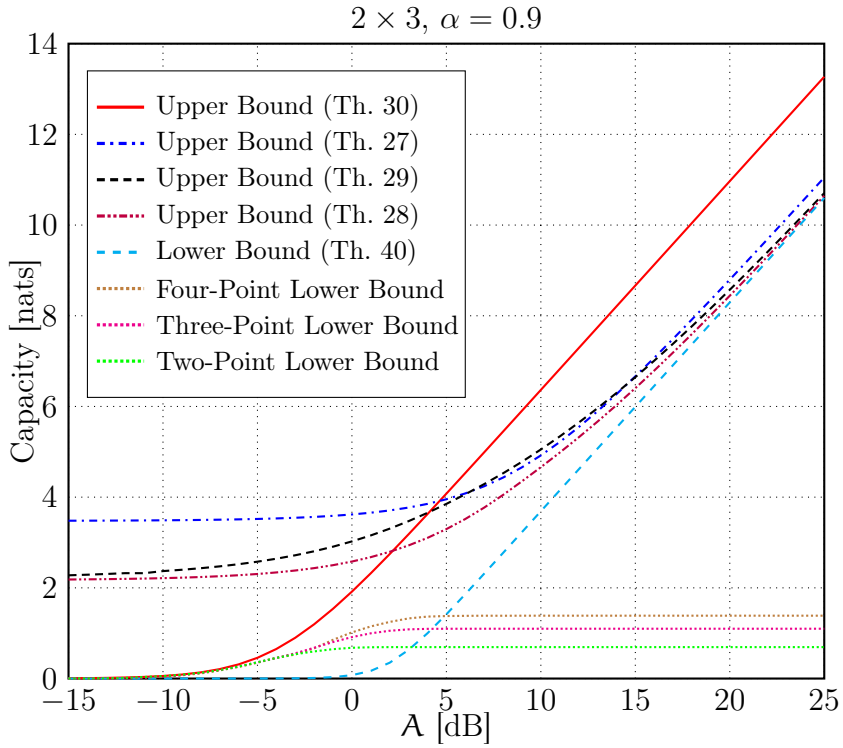

Figure 6.3: Bounds on capacity of 2×3 MIMO channel with channel matrix $\mathsf{H} = [1, 1.5, 3; 2, 2, 1]$, and average-to-peak power ratio $\alpha = 0.9$. Note that the threshold of the channel is $\alpha_{\text{th}} = 1.4762$.

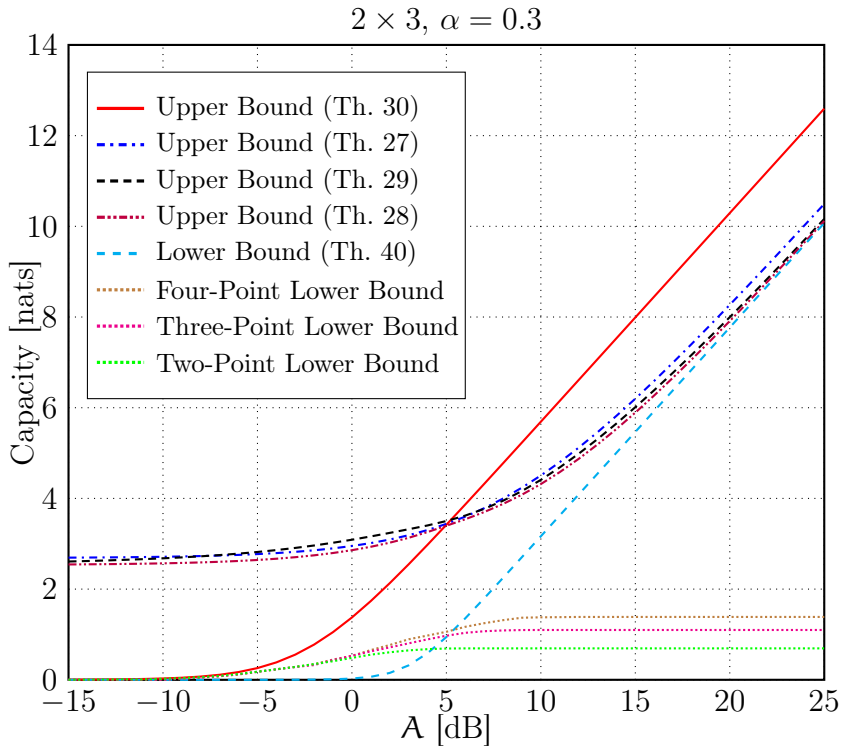

Figure 6.4: Bounds on capacity of the same 2×3 MIMO channel as discussed in Figure 6.3, and average-to-peak power ratio $\alpha = 0.3$.

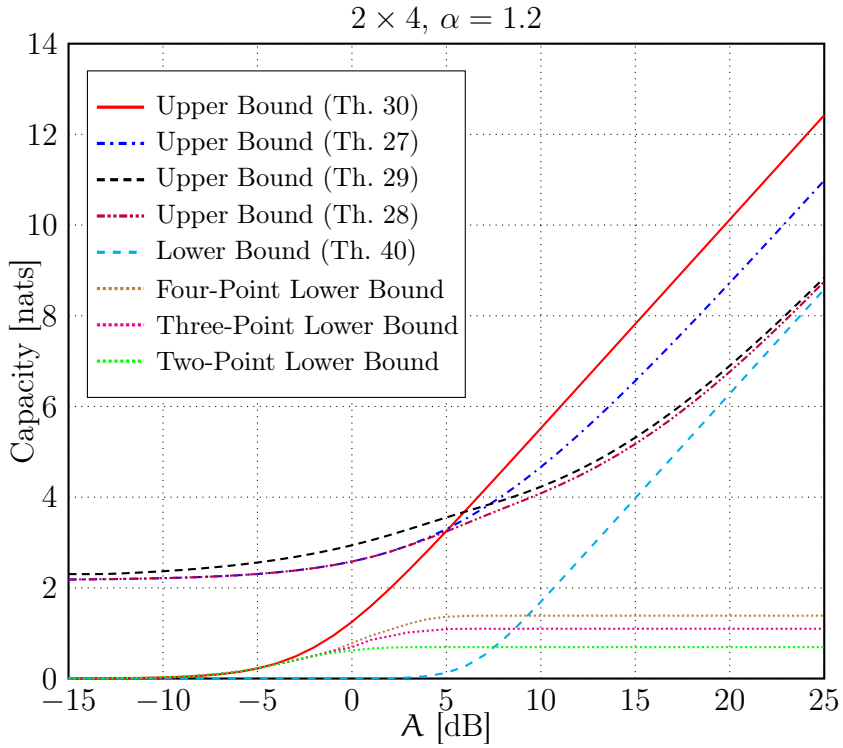

Figure 6.5: Bounds on capacity of 2×4 MIMO channel with channel matrix $\mathsf{H} = [1.5, 1, 0.75, 0.5; 0.5, 0.75, 1, 1.5]$, and average-to-peak power ratio $\alpha = 1.2$. Note that the threshold of the channel is $\alpha_{\text{th}} = 1.947$.

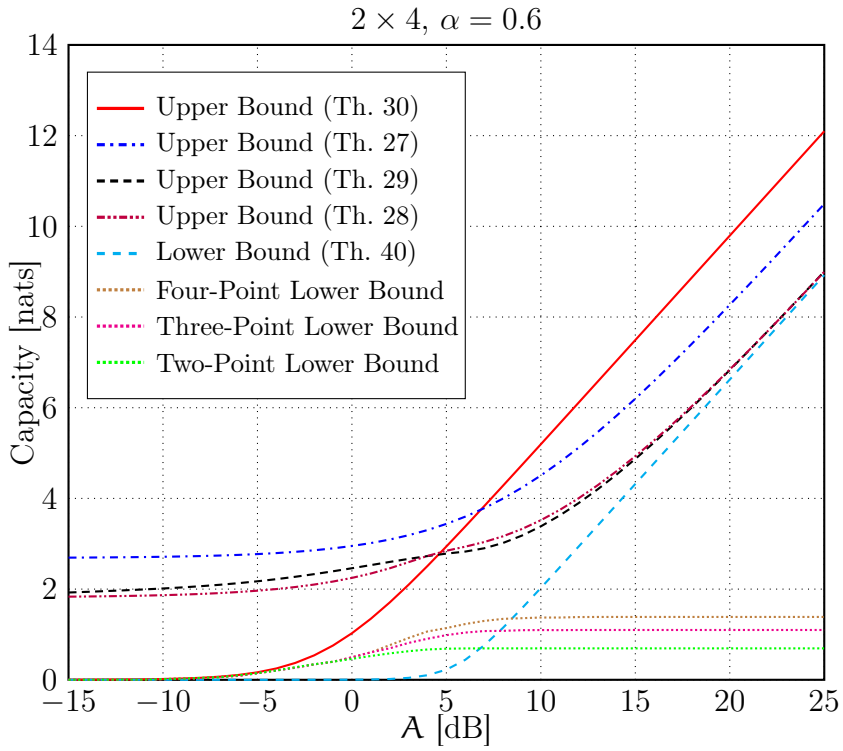

Figure 6.6: Bounds on capacity of the same 2×4 MIMO channel as discussed in Figure 6.5, and average-to-peak power ratio $\alpha = 0.6$.

Chapter 7

Block Fading Channel Capacity Analysis

The capacity of block fading FSOI channel is investigated in this chapter. With the assumption that the receiver always has perfect CSI, we present several upper and lower bounds on channel capacity when the transmitter has no CSI, perfect CSI, and limited CSI.

7.1 Channel Model

We first consider the following $n_{\mathrm{R}} \times n_{\mathrm{T}}$ block fading channel:

$$\mathbf{Y}_t[n] = \mathbb{H}_t \mathbf{x}_t[n] + \mathbf{Z}_t[n], \tag{7.1}$$

where $t \in \{1, 2, \ldots, \mathsf{B}\}$ denotes the block index, with B being the number of blocks; $n \in \{1, 2, \ldots, \mathsf{N}\}$ denotes the symbol index along a block, with N being the block length; $\mathbf{x}_t[n] = \left(x_t^{(1)}[n], \ldots, x_t^{(n_{\mathrm{T}})}[n]\right)^{\mathsf{T}}$ denotes the n_{T}-dimensional channel input vector; $\mathbf{Z}_t[n]$ denotes the n_{R}-dimensional noise vector with independent standard Gaussian entries,

$$\mathbf{Z}_t[n] \sim \mathcal{N}(0, \mathsf{I}); \tag{7.2}$$

and

$$\mathbb{H}_t = \left[\mathbf{H}_t^{(1)}, \mathbf{H}_t^{(2)}, \ldots, \mathbf{H}_t^{(n_{\mathrm{T}})}\right] \tag{7.3}$$

is a random $n_{\mathrm{R}} \times n_{\mathrm{T}}$ channel matrix with nonnegative entries. Thus, $\mathbf{H}_t^{(1)}, \ldots, \mathbf{H}_t^{(n_{\mathrm{T}})}$ are n_{R}-dimensional random column vectors. The channel noises $\{\mathbf{Z}_t[n]\}$ are independent and identically distributed (IID) inside and across blocks. The channel matrix $\mathbb{H}_t$ remains constant within each block and is IID across blocks. We assume it has finite density $f(\mathbb{H}_t)$ over the set of nonnegative real numbers (e.g., Rayleigh, Weibull, Pareto, or gamma distributions).

As before, since the channel inputs correspond to optical intensities, they are nonnegative:

$$x_t^{(k)}[n] \in \mathbb{R}_0^+, \quad k = 1, \dots, n_{\mathrm{T}}, \tag{7.4}$$

for all $t \in \{1, \dots, \mathsf{B}\}$ and $n \in \{1, \dots, \mathsf{N}\}$, and we assume that the inputs are subject to a peak-power (peak-intensity) and a *per-block* average-power (average-intensity) constraint:

$$\Pr\big[X_t^{(k)}[n] > \mathsf{A}\big] = 0, \quad \forall\, k \in \{1, \dots, n_{\mathrm{T}}\}, \tag{7.5a}$$

$$\frac{1}{\mathsf{N}}\,\mathsf{E}\left[\sum_{n=1}^{\mathsf{N}} \big\|\mathbf{X}_t[n]\big\|_1\right] \le \mathsf{E}, \quad \forall\, t \in \{1, 2, \dots, \mathsf{B}\}, \tag{7.5b}$$

for some fixed parameters $\mathsf{A}, \mathsf{E} > 0$. Here, the power allocation is permitted only inside each block. This restriction on power allocation is to prevent large, visible fluctuations in the light.

We still denote α as the ratio between the allowed average power and the allowed peak power:

$$\alpha \triangleq \frac{\mathsf{E}}{\mathsf{A}}. \tag{7.6}$$

The goal of the communication is to convey a random message $M \in \{1, 2, \dots, \mathsf{M}\}$ from the transmitter to the receiver over a fixed number of B blocks. Encoding is described separately for each kind of CSI. Decoding is as follows. Based on its observed NB outputs $\mathbf{Y}_1[1], \dots, \mathbf{Y}_{\mathsf{B}}[\mathsf{N}]$ and its knowledge of the B channel state matrices $\mathbb{H}_1, \dots, \mathbb{H}_{\mathsf{B}}$, it produces an estimate

$$\hat{M} \triangleq \psi(\mathbf{Y}_1[1], \dots, \mathbf{Y}_{\mathsf{B}}[\mathsf{N}], \mathbb{H}_1, \dots, \mathbb{H}_{\mathsf{B}}). \tag{7.7}$$

The probability of error is defined as

$$P_{\mathrm{e}}^{(\mathsf{NB})} = \Pr\big[\hat{M} \neq M\big], \tag{7.8}$$

and the communication rate is given as

$$\mathsf{R} = \frac{\log_2 \mathsf{M}}{\mathsf{NB}}. \tag{7.9}$$

A rate R is said to be achievable if there exists a sequence of codes such that $P_{\mathrm{e}}^{(\mathsf{NB})} \to 0$ as $\mathsf{B} \to \infty$ (N remains fixed). The ergodic capacity $\mathsf{C}_{\mathbb{H}}$ of the channel is defined as the supremum of all achievable rates.

7.2 No CSI at the Transmitter

In this section we assume that the transmitter has no CSI.[1] In this case, the channel input $\mathbf{X}_t[n]$ is just a function of the message M:

$$\mathbf{X}_t[n] = \phi_t(M), \tag{7.10}$$

and the ergodic capacity is given by the following proposition.

[1] Note that the channel *statistics* are always assumed to be known everywhere.

Proposition 36. *If the transmitter has no CSI, then*

$$\mathsf{C}_{\mathbb{H}} = \max_{P_{\mathbf{X}} \text{ satisfying (7.5)}} \mathsf{E}_{\mathbb{H}}\big[\mathrm{I}(\mathbf{X}; \bar{\mathbf{X}} + \mathbf{Z} | \mathbb{H} = \mathsf{H})\big], \tag{7.11}$$

where

$$\bar{\mathbf{X}} \triangleq \mathbb{H}\mathbf{X}. \tag{7.12}$$

Proof: By treating the CSI at the receiver as a part of the output of the channel, the mutual information between channel input and output can be expressed as

$$\begin{aligned} \mathrm{I}(\mathbf{X}; \mathbf{Y}, \mathbb{H}) &= \mathrm{I}(\mathbf{X}; \mathbb{H}) + \mathrm{I}(\mathbf{X}; \mathbf{Y} | \mathbb{H}) && (7.13)\\ &= \mathrm{I}(\mathbf{X}; \mathbf{Y} | \mathbb{H}). && (7.14)\\ &= \mathsf{E}_{\mathbb{H}}\big[\mathrm{I}(\mathbf{X}; \mathbf{Y} | \mathbb{H} = \mathsf{H})\big]. && (7.15) \end{aligned}$$

Hence the ergodic capacity is

$$\mathsf{C}_{\mathbb{H}} = \max_{P_{\mathbf{X}} \text{ satisfying (7.5)}} \mathsf{E}_{\mathbb{H}}\big[\mathrm{I}(\mathbf{X}; \mathbf{Y} | \mathbb{H} = \mathsf{H})\big]. \tag{7.16}$$

□

We first present a lower bound based on the EPI, whose proof is given in Appendix A.6.1.

Theorem 37. *If the transmitter has no CSI, then*

$$\mathsf{C}_{\mathbb{H}} \geq \frac{1}{2} \sup_{\lambda \in (0, \frac{n_{\mathrm{R}}}{2})} \sup_{\mathsf{G}} \mathsf{E}_{\mathbb{H}}\left[\log_2\left(1 + \frac{\mathsf{A}^{2n_{\mathrm{R}}} (\det \mathbb{H}\mathsf{G})^2 \, e^{2\nu}}{(2\pi e)^{n_{\mathrm{R}}}}\right)\right]. \tag{7.17}$$

Here, the supremum is over all $n_{\mathrm{T}} \times n_{\mathrm{R}}$ matrices G with nonnegative entries, with $\mathrm{rank}(\mathsf{G}) = n_{\mathrm{R}}$*, with $\|\mathsf{G}\|_1 \leq \alpha/\lambda$, and with row vectors satisfying $\|\mathbf{g}_i\|_1 \leq 1$, $\forall\, i \in \{1, \ldots, n_{\mathrm{T}}\}$; and ν is defined as*

$$\nu \triangleq n_{\mathrm{R}}\left(1 - \log_2 \frac{\mu}{1 - e^{-\mu}} - \frac{\mu \, e^{-\mu}}{1 - e^{-\mu}}\right) \tag{7.18}$$

with μ being the unique solution to (6.24)*.*

7.3 Perfect CSI at the Transmitter

In this section, we assume that the transmitter has perfect CSI, i.e., the channel input $\mathbf{X}_t[n]$ is a function of the message M and the channel matrix $\mathbb{H}_t$:[2]

$$\mathbf{X}_t[n] = \phi_t(M, \mathbb{H}_t). \tag{7.19}$$

The ergodic capacity in this scenario is characterized as follows.

[2]More generally, one could allow the channel input $\mathbf{X}_t[n]$ to depend on all previous channel matrices $\mathbb{H}_1, \ldots, \mathbb{H}_t$. But since we do not allow for power allocation across blocks and since the channel matrices are independent across blocks, the more general definition is not helpful.

Proposition 38. *If the transmitter has perfect CSI, then*

$$\mathsf{C}_{\mathbb{H}} = \mathsf{E}_{\mathbb{H}}\Big[\max_{P_{\mathbf{X}|\mathbb{H}=\mathsf{H}} \text{ satisfying (7.5)}} \mathrm{I}(\mathbf{X}; \bar{\mathbf{X}} + \mathbf{Z}|\mathbb{H} = \mathsf{H})\Big]. \tag{7.20}$$

Proof: The choice of the distribution of $\mathbf{X}$ can be dependent on each realization H of $\mathbb{H}$, and the mutual information for the given H can be expressed as, by treating the CSI at the receiver as a part of the output of the channel,

$$\mathrm{I}(\mathbf{X}, \mathbb{H} = \mathsf{H}; \mathbf{Y}, \mathbb{H} = \mathsf{H}) = \mathrm{I}(\mathbf{X}; \mathbf{Y}|\mathbb{H} = \mathsf{H}). \tag{7.21}$$

□

Remark 39. The difference between Propositions 36 and 38 lies in the optimization space of the input distributions. Here in Proposition 38, the input distribution $P_{\mathbf{X}|\mathbb{H}=\mathsf{H}}$ can depend on the channel realization H, which was not the case before. △

7.3.1 The Choice of $P_{\mathbf{X}|\mathbb{H}=\mathsf{H}}$

Fix an $n_{\mathrm{R}} \times n_{\mathrm{T}}$ channel matrix H for which every tuple of n_{R} columns is linearly independent.

The following parameters are important in this section. Let $\mathbf{q}$ be a probability vector on $\mathcal{U}$ with entries

$$q_{\mathcal{I}} \triangleq \frac{|\det \mathsf{H}_{\mathcal{I}}|}{\sum_{\mathcal{I}' \in \mathcal{U}} |\det \mathsf{H}_{\mathcal{I}'}|}, \quad \mathcal{I} \in \mathcal{U}, \tag{7.22}$$

and define

$$\alpha_{\mathrm{th}}(\mathsf{H}) \triangleq \frac{n_{\mathrm{R}}}{2} + \sum_{\mathcal{I} \in \mathcal{U}} s_{\mathcal{I}}\, q_{\mathcal{I}}. \tag{7.23}$$

If $\alpha \geq \alpha_{\mathrm{th}}(\mathsf{H})$, we choose $P_{\mathbf{X}}$ so that $\bar{\mathbf{X}}$ is uniform over $\mathcal{R}(\mathsf{H})$. This is obtained by defining a random variable over $\mathcal{U}$ with probability mass function (PMF) $\mathbf{q}$ and conditional on $\tilde{U} = \mathcal{I}$, choose $\mathbf{X}$ according to the minimum-energy signaling in (3.28) and so that $\bar{\mathbf{X}}$ is uniform over the shifted parallelepiped $\mathbf{v}_{\mathcal{I}} + \mathcal{D}_{\mathcal{I}}$.

If $\alpha < \alpha_{\mathrm{th}}(\mathsf{H})$, we fix a parameter

$$\lambda \in \Big(\max\Big\{0, \frac{n_{\mathrm{R}}}{2} + \alpha - \alpha_{\mathrm{th}}(\mathsf{H})\Big\}, \min\Big\{\frac{n_{\mathrm{R}}}{2}, \alpha\Big\}\Big) \tag{7.24}$$

and a PMF $\mathbf{p} = (p_{\mathcal{I}} \colon \mathcal{I} \in \mathcal{U})$ over the set $\mathcal{U}$ so that

$$\sum_{\mathcal{I} \in \mathcal{U}} p_{\mathcal{I}} s_{\mathcal{I}} = \alpha - \lambda. \tag{7.25}$$

Let then $\tilde{U}$ be a random variable over $\mathcal{U}$ with PMF $\mathbf{p}$, and conditional on $\tilde{U} = \mathcal{I}$, choose $\mathbf{X}$ according to the minimum-energy signaling in (3.28) and so that $\bar{\mathbf{X}}$ follows an n_{R}-dimensional truncated exponential distribution over the shifted parallelepiped

$\mathbf{v}_{\mathcal{I}} + \mathcal{D}_{\mathcal{I}}$. Specifically, given $\mathbb{H} = \mathsf{H}$ and $\tilde{U} = \mathcal{I}$, the inputs $\{X_i \colon i \in \mathcal{I}^{\mathrm{c}}\}$ are deterministically set to

$$X_i = \mathsf{A} \cdot g_{\mathcal{I},i}(\mathsf{H}), \quad i \in \mathcal{I}^{\mathrm{c}}, \tag{7.26}$$

where $g_{\mathcal{I},i}(\mathsf{H})$ is defined in (3.18), (3.23) or Algorithm 4, and the remaining inputs $\{X_i \colon i \in \mathcal{I}\}$ are chosen as the truncated exponential distribution,

$$f_{X_i|\tilde{U}=\mathcal{I}}(x_i) = \frac{\mu}{1-e^{-\mu}} e^{-\frac{\mu x_i}{\mathsf{A}}}, \quad \forall i \in \mathcal{I}. \tag{7.27}$$

Then at the receiver side, the image vector $\bar{\mathbf{X}} = \mathsf{H}\mathbf{X}$ is of conditional density

$$f_{\bar{\mathbf{X}}|\tilde{U}=\mathcal{I}}(\bar{\mathbf{x}}) = \frac{1}{\mathsf{A}^{n_{\mathrm{R}}}|\det \mathsf{H}_{\mathcal{I}}|} \cdot \left(\frac{\mu}{1-e^{-\mu}}\right)^{n_{\mathrm{R}}} e^{\frac{-\mu\|\mathsf{H}_{\mathcal{I}}^{-1}(\bar{\mathbf{x}}-\mathbf{v}_{\mathcal{I}})\|_1}{\mathsf{A}}}. \tag{7.28}$$

7.3.2 Capacity Results

We first present the following lower bound on capacity obtained with the EPI, whose proof is given in Appendix A.6.2.

Theorem 40. *If the transmitter has perfect CSI, then*

$$\mathsf{C}_{\mathbb{H}} \geq \frac{1}{2}\,\mathsf{E}_{\mathbb{H}}\left[\log_2\left(1 + \frac{\mathsf{A}^{2n_{\mathrm{R}}}\mathsf{V}_{\mathbb{H}}^2}{(2\pi e)^{n_{\mathrm{R}}}}\, e^{2\nu(\mathbb{H})}\right)\right], \tag{7.29}$$

where for each realization of the channel matrix H*:*

$$\mathsf{V}_{\mathsf{H}} \triangleq \sum_{\mathcal{I}\in\mathcal{U}} |\det \mathsf{H}_{\mathcal{I}}|, \tag{7.30}$$

and if $\alpha \geq \alpha_{\mathrm{th}}(\mathsf{H})$*, then*

$$\nu(\mathsf{H}) \triangleq 0, \tag{7.31}$$

whereas if $\alpha < \alpha_{\mathrm{th}}(\mathsf{H})$*, then*

$$\nu(\mathsf{H}) \triangleq \sup_{\lambda \in \left(\max\left\{0, \frac{n_{\mathrm{R}}}{2}+\alpha-\alpha_{\mathrm{th}}\right\}, \min\left\{\frac{n_{\mathrm{R}}}{2}, \alpha\right\}\right)} \left\{ n_{\mathrm{R}}\left(1 - \log_2 \frac{\mu}{1-e^{-\mu}} - \frac{\mu\, e^{-\mu}}{1-e^{-\mu}}\right) - \inf_{\mathbf{p}} \mathsf{D}(\mathbf{p}\|\mathbf{q}) \right\}. \tag{7.32}$$

Thus, $\nu(\mathsf{H})$ *is nonpositive and corresponds to the penalty due to* α*.*

Next, we present a duality-based upper bound on capacity, whose proof is given in Appendix A.6.3.

Theorem 41. *If the transmitter has perfect CSI, then*

$$\mathsf{C}_{\mathbb{H}} \leq \mathsf{E}_{\mathbb{H}}\Big[\mathsf{C}_{\mathbb{H},1}\,\mathbb{1}\big\{\alpha \geq \alpha_{\mathrm{th}}(\mathbb{H})\big\} + \mathsf{C}_{\mathbb{H},2}\,\mathbb{1}\big\{\alpha < \alpha_{\mathrm{th}}(\mathbb{H})\big\}\Big], \tag{7.33}$$

where for each realization of the channel matrix H*:* $\mathsf{C}_{\mathsf{H},1}$ *and* $\mathsf{C}_{\mathsf{H},2}$ *are defined the same as* $\mathsf{C}_{\mathsf{H}}(\mathsf{A}, \alpha\mathsf{A})$ *in* (6.26) *and* (6.27)*, respectively.*

Finally, we analyze the asymptotic capacity for $\mathsf{A}, \mathsf{E} \to \infty$ with α held fixed.

Theorem 42. *If the transmitter has perfect CSI, then*

$$\lim_{\mathsf{A}\to\infty} \big\{\mathsf{C}_{\mathbb{H}} - n_{\mathrm{R}} \log_2 \mathsf{A}\big\} = \frac{1}{2}\,\mathsf{E}_{\mathbb{H}}\left[\log_2\left(\frac{\mathsf{V}_{\mathbb{H}}^2}{(2\pi e)^{n_{\mathrm{R}}}}\right) + \nu(\mathbb{H})\,\mathbb{1}\big\{\alpha < \alpha_{\mathrm{th}}(\mathbb{H})\big\}\right], \tag{7.34}$$

where for each realization of the channel matrix H*,* $\nu(\mathsf{H})$ *is defined by* (7.31) *for* $\alpha \geq \alpha_{\mathrm{th}}(\mathsf{H})$ *and by* (7.32) *for* $\alpha < \alpha_{\mathrm{th}}(\mathsf{H})$*.*

Proof: See Appendix A.6.4. □

7.4 Limited CSI at the Transmitter

In this section we assume an instantaneous rate-limited *channel state feedback link* from the receiver to the transmitter. At the very beginning of each block, before transmission begins, the receiver learns $\mathbb{H}_t$ and sends a function of it,

$$\mathcal{F}_t(\mathbb{H}_t), \tag{7.35}$$

back to the transmitter.

The transmitter can thus compute its channel inputs $\mathbf{X}_t[n]$ as a function of the received feedback $\mathcal{F}_t(\mathbb{H}_t)$ and the message M:

$$\mathbf{X}_t[n] = \phi\big(\mathcal{F}_t(\mathbb{H}_t), M\big). \tag{7.36}$$

Of course, the capacity of this channel depends on the functions $\{\mathcal{F}_t\}_{t=1}^{\mathsf{B}}$. We will assume a *stationary* feedback policy where

$$\mathcal{F}_1 = \cdots = \mathcal{F}_{\mathsf{B}} = \mathcal{F}. \tag{7.37}$$

Proposition 43. *The capacity* $\mathsf{C}_{\mathbb{H},\mathcal{F}}$ *of a channel with limited CSI* $\mathcal{F}(\mathbb{H})$ *at the transmitter is:*

$$\mathsf{C}_{\mathbb{H},\mathcal{F}} = \mathsf{E}_{\mathbb{H}}\left[\max_{P_{\mathbf{X}|\mathcal{F}(\mathsf{H})} \text{ satisfying (7.5)}} \mathrm{I}(\mathbf{X};\mathbf{Y}|\mathbb{H}=\mathsf{H})\right]. \tag{7.38}$$

Proof: The choice of the distribution of $\mathbf{X}$ is dependent on $\mathcal{F}(\mathsf{H})$ for each realization H of $\mathbb{H}$, and the mutual information can be expressed as, by treating the CSI at the receiver as a part of the output of the channel,

$$\mathrm{I}(\mathbf{X}, \mathcal{F}(\mathsf{H}); \mathbf{Y}, \mathbb{H}=\mathsf{H}) = \mathrm{I}(\mathbf{X};\mathbf{Y}|\mathbb{H}=\mathsf{H}). \tag{7.39}$$

Then the ergodic capacity is

$$\mathsf{C}_{\mathbb{H}} = \mathsf{E}_{\mathbb{H}}\left[\max_{P_{\mathbf{X}|\mathcal{F}(\mathsf{H})} \text{ satisfying (7.5)}} \mathrm{I}(\mathbf{X};\mathbf{Y}|\mathbb{H}=\mathsf{H})\right]. \tag{7.40}$$

□

7.4.1 The Choice of $P_{\mathbf{X}|\mathcal{F}(\mathsf{H})}$

We present a choice of the function $\mathcal{F}$ with only $\binom{n_{\mathrm{T}}}{n_{\mathrm{R}}}^{n_{\mathrm{T}}-n_{\mathrm{R}}}$ function values, for which the corresponding capacity with limited CSI is close to the one with perfect CSI. Obviously, to implement this function it suffices that the receiver can feed back

$$\mathsf{R}_{\mathrm{FB}} = (n_{\mathrm{T}} - n_{\mathrm{R}}) \log_2 \binom{n_{\mathrm{T}}}{n_{\mathrm{R}}} \tag{7.41}$$

bits in each block.

Before describing our choice of $\mathcal{F}$, we first define a parameter:

$$a_{\mathcal{I},i}(\mathsf{H}) = \mathsf{A} \cdot g_{\mathcal{I},i}, \quad i \in \mathcal{I}^{\mathrm{c}}, \tag{7.42}$$

where $g_{\mathcal{I},i}$ is defined in (3.18), (3.23) or Algorithm 4.

Notice that to achieve the rates in Theorem 40, it suffices that the transmitter learns the binary values $\{a_{\mathcal{I},i}(\mathsf{H})\}_{\mathcal{I}\in\mathcal{U}}$ and the PMF $\mathbf{p}$ for each realization of H. Learning the PMF $\mathbf{p}$ at the transmitter requires the state-feedback to have infinite number of bits. In contrast, the binary values $\{a_{\mathcal{I},i}(\mathsf{H})\}_{\mathcal{I}\in\mathcal{U}}$ can be learned with only $(n_{\mathrm{T}} - n_{\mathrm{R}}) \log_2 \binom{n_{\mathrm{T}}}{n_{\mathrm{R}}}$ bits of feedback.

We thus propose to set

$$\mathcal{F}(\mathsf{H}) \triangleq \{a_{\mathcal{I},i}(\mathsf{H}) \colon \mathcal{I} \in \mathcal{U}, i \in \mathcal{I}^{\mathrm{c}}\}. \tag{7.43}$$

The transmitter then uses the following conditional distribution $P_{\mathbf{X}|\mathcal{F}}$ to generate its (random) codebook for transmitting the desired message M. For each realization $\mathcal{F} = \mathrm{f}$, pick an arbitrary positive number $\lambda \in (0, \frac{n_{\mathrm{R}}}{2})$ and let μ denote the solution to (6.24) for the picked value of λ. Then for this λ, pick an arbitrary PMF $\mathbf{p}$ over $\mathcal{U}$ satisfying (7.25), and let $\tilde{U} \sim \mathbf{p}$. (By (6.1) and (7.43), the parameters $\{s_{\mathcal{I}}\}_{\mathcal{I}\in\mathcal{U}}$ in condition (7.25) depend on H only through $\mathcal{F}(\mathsf{H})$, and thus the proposed $\mathbf{p}$ can be used as a parameter for the distribution $P_{\mathbf{X}|\mathcal{F}(\mathsf{H})}$.) Similarly to before, given that $\mathcal{F} = \mathrm{f}$ and $\tilde{U} = \mathcal{I}$, we deterministically set

$$X_i = a_{\mathcal{I},i}(\mathsf{H}), \quad i \in \mathcal{I}^{\mathrm{c}}, \tag{7.44}$$

and choose the remaining inputs $\{X_i \colon i \in \mathcal{I}\}$ according to the distribution in (7.27).

7.4.2 Capacity Results

We now present the following lower bound, whose proof is given in Appendix A.6.5.

Theorem 44. *For the limited CSI function $\mathcal{F}$ in* (7.43)*:*

$$\mathsf{C}_{\mathbb{H},\mathcal{F}} \geq \mathsf{E}_{\mathcal{F}(\mathbb{H})}\left[\sup_{\lambda\in(0,\frac{n_{\mathrm{R}}}{2})} \sup_{\mathbf{p}} \mathsf{E}_{\mathbb{H}|\mathcal{F}}\left[\frac{1}{2}\log\left(1 + \frac{\mathsf{A}^{2n_{\mathrm{R}}}\mathsf{V}_{\mathbb{H}}{}^{2}\, e^{2\nu^\star}}{(2\pi e)^{n_{\mathrm{R}}}}\right)\right]\right] \tag{7.45}$$

where

$$\nu^\star \triangleq n_{\mathrm{R}}\left(1 - \log_2 \frac{\mu}{1-e^{-\mu}} - \frac{\mu\, e^{-\mu}}{1-e^{-\mu}}\right) - \mathsf{D}(\mathbf{p}\|\mathbf{q}), \tag{7.46}$$

with μ satisfying (6.24)*, and where the supremum over $\mathbf{p}$ is over all PMFs satisfying*

$$\sum_{\mathcal{I}\in\mathcal{U}} p_{\mathcal{I}} s_{\mathcal{I}} = \alpha - \lambda. \tag{7.47}$$

7.5 Numerical Results

Figure 7.1 illustrates the derived upper and lower bounds on the capacities for a 1×3 MISO channel where the entries $\{h_i\}_{i\in\{1,2,3\}}$ in the channel matrix $\mathbb{H}$ are IID and follow a Rayleigh distribution:

$$f(h_i) = 2h_i e^{-h_i^2} \mathbb{1}\{h_i \geq 0\}, \ \forall i \in \{1,2,3\}. \tag{7.48}$$

When the SNR tends to infinity, the lower bound in Theorem 40 coincides with the upper bound in Theorem 41. Furthermore, the gap between the lower bound in Theorem 44 below and the upper bound in Theorem 41 tends to a small constant at high SNR. Thus, at high SNR a relatively small number of feedback bits is sufficient to approach the perfect CSI capacity.

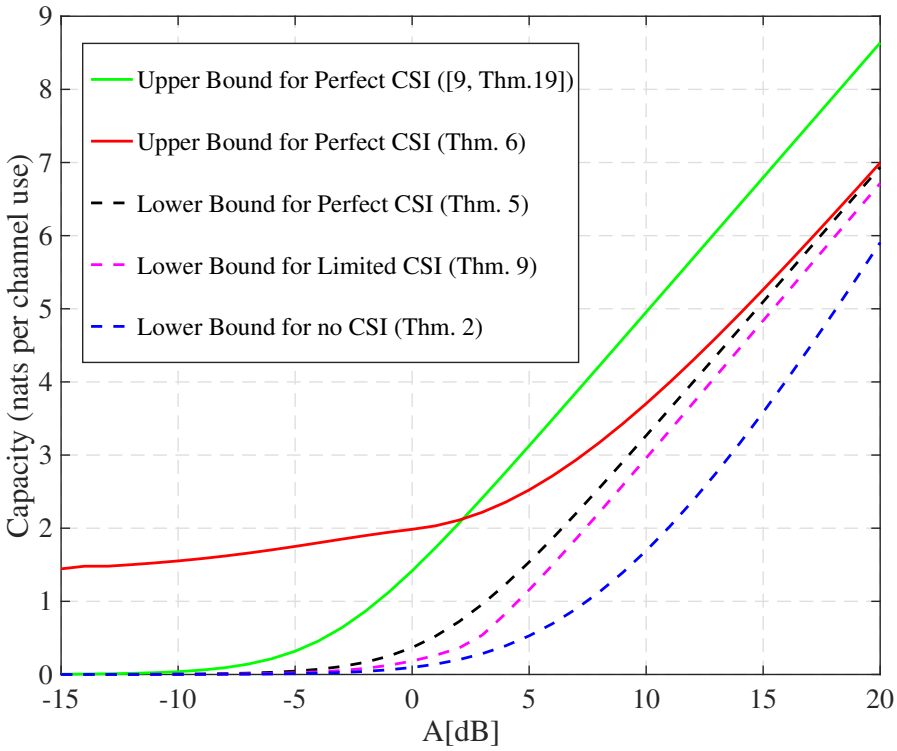

Figure 7.1: A 1×3 MISO channel, where entries in $\mathbb{H}_{1\times 3}$ follow a Rayleigh distribution, with $\alpha = 0.4$.

Chapter 8

Conclusions and Perspectives

8.1 MIMO FSOI Channels

In this thesis we investigated the capacity of a general $n_{\mathrm{R}} \times n_{\mathrm{T}}$ MIMO FSOI channel with $n_{\mathrm{R}} > n_{\mathrm{T}}$. We first expressed capacity as a maximization problem over distributions for the image vector $\bar{\mathbf{X}} = \mathsf{H}\mathbf{X}$. The main challenge there is to transform the total average-power constraint on $\mathbf{X}$ to a constraint on $\bar{\mathbf{X}}$, as the mapping from $\mathbf{x}$ to $\bar{\mathbf{x}}$ is many-to-one. This problem is solved by identifying, for each $\bar{\mathbf{x}}$, the input vector $\mathbf{x}_{\min}$ that induces this $\bar{\mathbf{x}}$ with minimum energy. Specifically, we showed that the range of the image vectors $\bar{\mathbf{x}}$ can be decomposed into a number of parallelepipeds such that, for all $\bar{\mathbf{x}}$ within one parallelepiped, the minimum-energy input vectors $\mathbf{x}_{\min}$ have a similar form.

At high SNR, the above minimum-energy signaling result allows the transmitter to decompose the channel into several "almost parallel" channels, each of which being an $n_{\mathrm{R}} \times n_{\mathrm{R}}$ MIMO channel in itself. This is because, at high SNR, the output $\mathbf{y}$ allows the receiver to obtain a good estimate of which of the parallelepipeds $\bar{\mathbf{x}}$ lies in. We can then apply previous results on the capacity of the MIMO channel with full column rank. The remaining steps in deriving our results on the high-SNR asymptotic capacity can be understood, on a high level, as optimizing probabilities and energy constraints assigned to each of the parallel channels.

In the low-SNR regime, the capacity slope is shown to be proportional to the trace of the covariance matrix of $\bar{\mathbf{X}}$ under the given power constraints. We proved several properties of the input distribution that maximizes this trace. For example, each entry in $\mathbf{X}$ should be either zero or the maximum value A, and the total number of values of $\mathbf{X}$ with nonzero probabilities need not exceed $n_{\mathrm{R}} + 2$.

We also derived new upper and lower bounds on the capacity of SISO and MISO FSOI channels. At low SNR, we characterized the capacity slope, and showed that for almost all channel gains, the distribution to achieve the asymptotic low-SNR

capacity slope only contains two or three positive probability mass points. These mass points correspond to setting all input antennas to 0 or to setting some strongest antennas to the maximum allowed peak power and the remaining weaker antennas to 0. We also present improved upper bounds which are asymptotically tight at high SNR and beat other existing upper bounds in large regimes of moderate- and high-SNR regime. For certain parameters, these upper bounds also match well with our derived numerical lower bounds indicating that these bounds give good approximations to the channel capacity.

8.2 Block Fading FSOI Channel

We considered the scenario when the channel suffers from block fading. Lower bounds were derived on the capacity of block fading channels in the three cases where the transmitter has no CSI, perfect CSI, and limited CSI, respectively. For perfect and limited CSI, our lower bounds are based on the proposed minimum-energy signaling. In particular, for limited CSI, in each block, the receiver only sends a finite set of binary values, which can be exactly characterized by $(n_{\mathrm{T}}-n_{\mathrm{R}})\log_2\binom{n_{\mathrm{T}}}{n_{\mathrm{R}}}$ bits per block, but the corresponding lower bound performs close to the lower bound with perfect CSI. In the case of perfect CSI we also provided an upper bound on capacity and showed that it approaches the proposed lower bound asymptotically in the high-SNR regime. In this regime, the perfect CSI capacity can thus be closely approached with only a small number of feedback bits per block.

8.3 Future Work

Smith's seminal paper [14] showed that the optimal input distribution is discrete with finite support. However, the exact capacity-achieving input distribution is itself unknown to date, and even estimating the number of positive mass points is currently insurmountable. Interestingly, the results in [55] seem to be related with this involved problem. They show that for fixed m mass points, the so-called Gauss quadrature constellation is capacity-achieving in the low SNR regime. The peak power for the Gauss quadrature constellation is $\sqrt{m}$, so it seems reasonable to conjecture that the number of mass point in the capacity-achieving input distribution may scale as square of the peak power. This is a potentially interesting research problem.

In the general MIMO FSOI channels, although the asymptotic capacities at low and high SNR have been exactly characterized, existing lower and upper bounds still have a large gap for small average-to-noise ratio in the finite SNR regime. New methods and techniques may be introduced to get improved upper and lower bounds in the MIMO case.

When the channel suffers from fading, in this thesis we only consider the scenario when the receiver sends $(n_{\mathrm{T}}-n_{\mathrm{R}})\log_2\binom{n_{\mathrm{T}}}{n_{\mathrm{R}}}$ bits-feedback per channel block to the transmitter. However, if the feedback capacity is less or larger than $(n_{\mathrm{T}}-n_{\mathrm{R}})\log_2\binom{n_{\mathrm{T}}}{n_{\mathrm{R}}}$ bits per channel block, how to choose the feedback function, such that

it can most efficiently describe the channel matrix in the rate-limited feedback link to the transmitter, is an interesting extension to our current work.

Appendix A

Proofs

A.1 Proofs of Chapter 2

A.1.1 A Proof of Proposition 1

Fix a capacity-achieving input $\mathbf{X}$ and let

$$\alpha^* \triangleq \mathsf{E}\big[\|\mathbf{X}\|_1\big]\mathsf{A}^{-1}. \tag{A.1}$$

Define $\mathbf{a} \triangleq (A, A, \ldots, A)^\mathsf{T}$ and

$$\mathbf{X}' \triangleq \mathbf{a} - \mathbf{X}. \tag{A.2}$$

We have

$$\mathsf{E}\big[\|\mathbf{X}'\|_1\big] = \mathsf{A}(n_\mathrm{T} - \alpha^*) \tag{A.3}$$

and

$$\begin{aligned}
\mathrm{I}(\mathbf{X};\mathbf{Y}) &= \mathrm{I}(\mathbf{X};\mathsf{H}\mathbf{a} - \mathbf{Y}) && \text{(A.4)}\\
&= \mathrm{I}(\mathbf{X};\mathsf{H}\mathbf{a} - \mathsf{H}\mathbf{X} - \mathbf{Z}) && \text{(A.5)}\\
&= \mathrm{I}(\mathbf{a} - \mathbf{X};\mathsf{H}(\mathbf{a} - \mathbf{X}) - \mathbf{Z}) && \text{(A.6)}\\
&= \mathrm{I}(\mathbf{a} - \mathbf{X};\mathsf{H}(\mathbf{a} - \mathbf{X}) + \mathbf{Z}) && \text{(A.7)}\\
&= \mathrm{I}(\mathbf{X}';\mathsf{H}\mathbf{X}' + \mathbf{Z}) && \text{(A.8)}\\
&= \mathrm{I}(\mathbf{X}';\mathbf{Y}') && \text{(A.9)}
\end{aligned}$$

where $\mathbf{Y}' \triangleq \mathsf{H}\mathbf{X}' + \mathbf{Z}$, and where (A.7) follows because $\mathbf{Z}$ is symmetric around $\mathbf{0}$ and independent of $\mathbf{X}$.

Define another random vector $\tilde{\mathbf{X}}$ as follows:

$$\tilde{\mathbf{X}} \triangleq \begin{cases} \mathbf{X} & \text{with probability } p, \\ \mathbf{X}' & \text{with probability } 1-p. \end{cases} \tag{A.10}$$

Notice that, since $\mathrm{I}(\mathbf{X};\mathbf{Y})$ is concave in $P_\mathbf{X}$ for a fixed channel law, we have

$$\mathrm{I}(\tilde{\mathbf{X}};\tilde{\mathbf{Y}}) \geq p\,\mathrm{I}(\mathbf{X};\mathbf{Y}) + (1-p)\,\mathrm{I}(\mathbf{X}';\mathbf{Y}'). \tag{A.11}$$

Therefore, by (A.9),

$$\mathrm{I}(\tilde{\mathbf{X}};\tilde{\mathbf{Y}}) \geq \mathrm{I}(\mathbf{X};\mathbf{Y}) \tag{A.12}$$

for all $p \in [0,1]$. Combined with the assumption that $\mathbf{X}$ achieves capacity, (A.12) implies that $\tilde{\mathbf{X}}$ must also achieve capacity.

We are now ready to prove the two claims in the proposition. We first prove that for $\alpha > \frac{n_\mathrm{T}}{2}$ the average-power constraint is inactive. To this end, we choose $p = \frac{1}{2}$, which yields

$$\mathsf{E}\big[\|\tilde{\mathbf{X}}\|_1\big] = \frac{n_\mathrm{T}}{2}\mathsf{A}. \tag{A.13}$$

Since $\tilde{\mathbf{X}}$ achieves capacity (see above), we conclude that capacity is unchanged if one strengthens the average-power constraint from $\alpha\mathsf{A}$ to $\frac{n_\mathrm{T}}{2}\mathsf{A}$.

We now prove that, if $\alpha \leq \frac{n_\mathrm{T}}{2}$, then there exists a capacity-achieving input distribution for which the average-power constraint is met with equality. Assume that $\alpha^* < \alpha$ (otherwise $\mathbf{X}$ is itself such an input), then choose

$$p = \frac{n_\mathrm{T} - \alpha^* - \alpha}{n_\mathrm{T} - 2\alpha^*}. \tag{A.14}$$

With this choice,

$$\begin{aligned}
\mathsf{E}\big[\|\tilde{\mathbf{X}}\|_1\big] &= p\,\mathsf{E}\big[\|\mathbf{X}\|_1\big] + (1-p)\,\mathsf{E}\big[\|\mathbf{X}'\|_1\big] && \text{(A.15)}\\
&= \big(p\alpha^* + (1-p)(n_\mathrm{T} - \alpha^*)\big)\mathsf{A} && \text{(A.16)}\\
&= \alpha\mathsf{A}. && \text{(A.17)}
\end{aligned}$$

Hence $\tilde{\mathbf{X}}$ (which achieves capacity) meets the average-power constraint with equality.

A.2 Proofs of Chapter 3

A.2.1 A Proof of Lemma 6

We first restrict ourselves to the case where the condition in (3.22) is satisfied. The implications caused if (3.22) is violated are discussed at the end.

We start with Part 2. The minimization problem under consideration,

$$\min_{\mathbf{x}' \in \mathcal{S}(\bar{\mathbf{x}})} \|\mathbf{x}'\|_1, \tag{A.18}$$

is over a compact set and the objective function is continuous, so a minimum must exist. We are now going to prove that in fact the minimum is unique and is achieved by the input vector $\mathbf{x}$ defined in (3.28). To that goal, we first link the components β_i in (3.28) with the components of some arbitrary input vector $\mathbf{x}' \in \mathcal{S}(\bar{\mathbf{x}})$, $\mathbf{x}' \neq \mathbf{x}$, and then use this to show that $\mathbf{x}'$ consumes more energy than $\mathbf{x}$.

In the following, $\mathcal{I}_i$ denotes the ith entry in $\mathcal{I}$ for $i \in \{1,\ldots,n_\mathrm{R}\}$. Thus, we can restate (3.19) as

$$\mathbf{h}_j = \mathsf{H}_\mathcal{I}\boldsymbol{\gamma}_{\mathcal{I},j} = \sum_{i=1}^{n_\mathrm{R}} \gamma_{\mathcal{I},j}^{(i)}\,\mathbf{h}_{\mathcal{I}_i}, \quad \forall\, j \in \mathcal{I}^\mathrm{c}, \tag{A.19}$$

where $\gamma_{\mathcal{I},j}^{(i)}$, $i = 1, \dots, n_{\mathrm{R}}$, denote the components of $\boldsymbol{\gamma}_{\mathcal{I},j}$.

So, we choose an arbitrary $\mathbf{x}' \triangleq (x'_1, \dots, x'_{n_{\mathrm{T}}})^{\mathsf{T}} \in \mathcal{S}(\bar{\mathbf{x}})$ and notice that

$$\bar{\mathbf{x}} = \mathsf{H}\mathbf{x}' \tag{A.20}$$

$$= \sum_{j=1}^{n_{\mathrm{T}}} x'_j \mathbf{h}_j \tag{A.21}$$

$$= \sum_{j \in \mathcal{I}} x'_j \mathbf{h}_j + \sum_{\substack{j \in \mathcal{I}^{\mathrm{c}}: \\ a_{\mathcal{I},j} < 1}} x'_j \mathbf{h}_j + \sum_{\substack{j \in \mathcal{I}^{\mathrm{c}}: \\ a_{\mathcal{I},j} > 1}} x'_j \mathbf{h}_j \tag{A.22}$$

$$= \sum_{j \in \mathcal{I}} x'_j \mathbf{h}_j + \sum_{\substack{j \in \mathcal{I}^{\mathrm{c}}: \\ a_{\mathcal{I},j} < 1}} x'_j \mathbf{h}_j + \sum_{\substack{j \in \mathcal{I}^{\mathrm{c}}: \\ a_{\mathcal{I},j} > 1}} \mathsf{A}\mathbf{h}_j - \sum_{\substack{j \in \mathcal{I}^{\mathrm{c}}: \\ a_{\mathcal{I},j} > 1}} \big(\mathsf{A} - x'_j\big)\mathbf{h}_j \tag{A.23}$$

$$= \sum_{i=1}^{n_{\mathrm{R}}} x'_{\mathcal{I}_i} \mathbf{h}_{\mathcal{I}_i} + \sum_{\substack{j \in \mathcal{I}^{\mathrm{c}}: \\ a_{\mathcal{I},j} < 1}} x'_j \sum_{i=1}^{n_{\mathrm{R}}} \gamma_{\mathcal{I},j}^{(i)} \, \mathbf{h}_{\mathcal{I}_i} + \sum_{\substack{j \in \mathcal{I}^{\mathrm{c}}: \\ a_{\mathcal{I},j} > 1}} \mathsf{A}\mathbf{h}_j - \sum_{\substack{j \in \mathcal{I}^{\mathrm{c}}: \\ a_{\mathcal{I},j} > 1}} \big(\mathsf{A} - x'_j\big) \sum_{i=1}^{n_{\mathrm{R}}} \gamma_{\mathcal{I},j}^{(i)} \, \mathbf{h}_{\mathcal{I}_i} \tag{A.24}$$

$$= \sum_{i=1}^{n_{\mathrm{R}}} \left(x'_{\mathcal{I}_i} + \sum_{\substack{j \in \mathcal{I}^{\mathrm{c}}: \\ a_{\mathcal{I},j} < 1}} \gamma_{\mathcal{I},j}^{(i)} \, x'_j - \sum_{\substack{j \in \mathcal{I}^{\mathrm{c}}: \\ a_{\mathcal{I},j} > 1}} \gamma_{\mathcal{I},j}^{(i)} \, \big(\mathsf{A} - x'_j\big) \right) \mathbf{h}_{\mathcal{I}_i} + \sum_{\substack{j \in \mathcal{I}^{\mathrm{c}}: \\ a_{\mathcal{I},j} > 1}} \mathsf{A}\mathbf{h}_j \tag{A.25}$$

$$= \sum_{i=1}^{n_{\mathrm{R}}} \left(x'_{\mathcal{I}_i} + \sum_{\substack{j \in \mathcal{I}^{\mathrm{c}}: \\ a_{\mathcal{I},j} < 1}} \gamma_{\mathcal{I},j}^{(i)} \, x'_j - \sum_{\substack{j \in \mathcal{I}^{\mathrm{c}}: \\ a_{\mathcal{I},j} > 1}} \gamma_{\mathcal{I},j}^{(i)} \, \big(\mathsf{A} - x'_j\big) \right) \mathbf{h}_{\mathcal{I}_i} + \mathbf{v}_{\mathcal{I}}, \tag{A.26}$$

where in (A.24) we used (A.19) and where the last equality follows from (3.23) and (3.21).

Since $\{\mathbf{h}_i \colon i \in \mathcal{I}\}$ are linearly independent, they must span $\mathbb{R}^{n_{\mathrm{R}}}$, and hence the coefficients

$$\left\{ x'_{\mathcal{I}_i} + \sum_{\substack{j \in \mathcal{I}^{\mathrm{c}}: \\ a_{\mathcal{I},j} < 1}} \gamma_{\mathcal{I},j}^{(i)} \, x'_j - \sum_{\substack{j \in \mathcal{I}^{\mathrm{c}}: \\ a_{\mathcal{I},j} > 1}} \gamma_{\mathcal{I},j}^{(i)} \, \big(\mathsf{A} - x'_j\big) \right\}_{i \in \{1, \dots, n_{\mathrm{R}}\}} \tag{A.27}$$

uniquely determine $\bar{\mathbf{x}} - \mathbf{v}_{\mathcal{I}}$. Thus it follows from (3.29) that (A.27) must be equal to $\{\beta_i\}_{i \in \{1, \dots, n_{\mathrm{R}}\}}$, i.e. by (3.28), to $\{x_{\mathcal{I}_i}\}_{i \in \{1, \dots, n_{\mathrm{R}}\}}$.

Next we argue that, if $\mathbf{x}' \neq \mathbf{x}$, then

$$\|\mathbf{x}\|_1 < \|\mathbf{x}'\|_1. \tag{A.28}$$

To that goal notice that, because the components of $\mathbf{x}$ are nonnegative,

$$\|\mathbf{x}\|_1 = \sum_{j=1}^{n_{\mathrm{T}}} x_j \tag{A.29}$$

$$= \sum_{\substack{i \in \mathcal{I}^{\mathrm{c}}: \\ a_{\mathcal{I},i} > 1}} x_i + \sum_{\substack{i \in \mathcal{I}^{\mathrm{c}}: \\ a_{\mathcal{I},i} < 1}} x_i + \sum_{i=1}^{n_{\mathrm{R}}} x_{\mathcal{I}_i} \tag{A.30}$$

$$= \sum_{\substack{i\in\mathcal{I}^{\mathrm{c}}:\\ a_{\mathcal{I},i}>1}} \mathsf{A} + \sum_{\substack{i\in\mathcal{I}^{\mathrm{c}}:\\ a_{\mathcal{I},i}<1}} 0 + \sum_{i=1}^{n_{\mathrm{R}}} \left(x'_{\mathcal{I}_i} + \sum_{\substack{j\in\mathcal{I}^{\mathrm{c}}:\\ a_{\mathcal{I},j}<1}} \gamma^{(i)}_{\mathcal{I},j}\, x'_j - \sum_{\substack{j\in\mathcal{I}^{\mathrm{c}}:\\ a_{\mathcal{I},j}>1}} \gamma^{(i)}_{\mathcal{I},j} \left(\mathsf{A} - x'_j\right) \right) \tag{A.31}$$

$$= \sum_{\substack{j\in\mathcal{I}^{\mathrm{c}}:\\ a_{\mathcal{I},j}>1}} \mathsf{A} + \sum_{i=1}^{n_{\mathrm{R}}} x'_{\mathcal{I}_i} + \sum_{\substack{j\in\mathcal{I}^{\mathrm{c}}:\\ a_{\mathcal{I},j}<1}} \sum_{i=1}^{n_{\mathrm{R}}} \gamma^{(i)}_{\mathcal{I},j}\, x'_j - \sum_{\substack{j\in\mathcal{I}^{\mathrm{c}}:\\ a_{\mathcal{I},j}>1}} \sum_{i=1}^{n_{\mathrm{R}}} \gamma^{(i)}_{\mathcal{I},j} \left(\mathsf{A} - x'_j\right) \tag{A.32}$$

$$= \sum_{\substack{j\in\mathcal{I}^{\mathrm{c}}:\\ a_{\mathcal{I},j}>1}} \mathsf{A} + \sum_{j\in\mathcal{I}} x'_j + \sum_{\substack{j\in\mathcal{I}^{\mathrm{c}}:\\ a_{\mathcal{I},j}<1}} \underbrace{a_{\mathcal{I},j}}_{<1}\, x'_j - \sum_{\substack{j\in\mathcal{I}^{\mathrm{c}}:\\ a_{\mathcal{I},j}>1}} \underbrace{a_{\mathcal{I},j}}_{>1} \left(\mathsf{A} - x'_j\right) \tag{A.33}$$

$$< \sum_{\substack{j\in\mathcal{I}^{\mathrm{c}}:\\ a_{\mathcal{I},j}>1}} \mathsf{A} + \sum_{j\in\mathcal{I}} x'_j + \sum_{\substack{j\in\mathcal{I}^{\mathrm{c}}:\\ a_{\mathcal{I},j}<1}} x'_j - \sum_{\substack{j\in\mathcal{I}^{\mathrm{c}}:\\ a_{\mathcal{I},j}>1}} \left(\mathsf{A} - x'_j\right) \tag{A.34}$$

$$= \sum_{j=1}^{n_{\mathrm{T}}} x'_j = \|\mathbf{x}'\|_1. \tag{A.35}$$

Here (A.31) follows from (3.23) and because $\{x_{\mathcal{I}_i}\}$ are identical to (A.27); (A.33) follows from (3.20); and (A.34) holds because, since $\mathbf{x}' \neq \mathbf{x}$, there must exist some $j \in \mathcal{I}^{\mathrm{c}}$, $a_{\mathcal{I},j} < 1$, such that $x'_j > 0$, or some $j \in \mathcal{I}^{\mathrm{c}}$, $a_{\mathcal{I},j} > 1$, such that $x'_j < \mathsf{A}$. This completes the proof of Part 2.

We now prove Part 1. Fix $\mathcal{I}, \mathcal{J} \in \mathcal{U}$ with $\mathcal{I} \neq \mathcal{J}$, and a point $\bar{\mathbf{x}}$ in the interior of $(\mathbf{v}_{\mathcal{I}} + \mathcal{D}_{\mathcal{I}})$. We argue by contradiction that $\bar{\mathbf{x}}$ cannot be in $(\mathbf{v}_{\mathcal{J}} + \mathcal{D}_{\mathcal{J}})$. To this end, choose an index $i \in \{1, \ldots, n_{\mathrm{T}}\}$ such that the channel vector $\mathbf{h}_i$ is in $\mathsf{H}_{\mathcal{I}}$ but not in $\mathsf{H}_{\mathcal{J}}$. Since $\mathcal{I} \neq \mathcal{J}$, such an index must exist. By definition of $\boldsymbol{\beta}$ in (3.29), any $\mathbf{x}$ that is a solution to the minimization in (A.18) has x_i lying in the open interval $(0, \mathsf{A})$. If $\bar{\mathbf{x}}$ is also in $(\mathbf{v}_{\mathcal{J}} + \mathcal{D}_{\mathcal{J}})$, then x_i must be 0 or A since $i \in \mathcal{J}^{\mathrm{c}}$. Since we have shown that the solution to the minimization in (A.18) is unique, we have arrived at a contradiction. Thus, no point can be in the interior of both $(\mathbf{v}_{\mathcal{I}} + \mathcal{D}_{\mathcal{I}})$ and $(\mathbf{v}_{\mathcal{J}} + \mathcal{D}_{\mathcal{J}})$, and therefore their intersection has Lebesgue measure zero.

Furthermore, clearly,

$$\bigcup_{\mathcal{I}\in\mathcal{U}} (\mathbf{v}_{\mathcal{I}} + \mathcal{D}_{\mathcal{I}}) \subseteq \mathcal{R}(\mathsf{H}). \tag{A.36}$$

Since the intersection of $\mathbf{v}_{\mathcal{I}} + \mathcal{D}_{\mathcal{I}}$ and $\mathbf{v}_{\mathcal{J}} + \mathcal{D}_{\mathcal{J}}$ has Lebesgue measure zero, the reverse direction follows immediately by noting that both sets are closed and

$$\mathrm{vol}\big(\mathcal{R}(\mathsf{H})\big) = \sum_{\mathcal{I}\in\mathcal{U}} \mathrm{vol}(\mathbf{v}_{\mathcal{I}} + \mathcal{D}_{\mathcal{I}}). \tag{A.37}$$

This latter equality holds because

$$\mathrm{vol}(\mathbf{v}_{\mathcal{I}} + \mathcal{D}_{\mathcal{I}}) = \mathsf{A}^{n_{\mathrm{R}}} |\det \mathsf{H}_{\mathcal{I}}| \tag{A.38}$$

and by [56], [57]

$$\mathrm{vol}\big(\mathcal{R}(\mathsf{H})\big) = \mathsf{A}^{n_{\mathrm{R}}} \sum_{\mathcal{I}\in\mathcal{U}} |\det \mathsf{H}_{\mathcal{I}}|. \tag{A.39}$$

This completes the proof of Part 1.

Finally, we argue that the lemma holds also when (3.22) is violated. Note that when $a_{\mathcal{I},j} = 1$ for some $\mathcal{I}$ and j, then the solution to (A.18) is not necessarily unique anymore. To circumvent this problem, note that Algorithm 4 can be interpreted as generating a small perturbation of the matrix H. We fix some small values $\epsilon_1 > \cdots > \epsilon_{n_\mathrm{T}} > 0$ and check through all $a_{\mathcal{I},j}$, $j \in \{1, \ldots, n_\mathrm{T}\}$. When we encounter a first tie $a_{\mathcal{I},j} = 1$, we multiply the corresponding vector $\mathbf{h}_j$ by a factor $(1 + \epsilon_1)$ and thereby break the tie (ϵ_1 is chosen to be small enough so that it does not affect any other choices). If a second tie shows up, we use the next perturbation factor $(1 + \epsilon_2)$ (which is smaller than $(1 + \epsilon_1)$, so we do not inadvertently revert our first perturbation); and so on. The lemma is then proven with a continuity argument by letting all of $\epsilon_1, \ldots, \epsilon_{n_\mathrm{T}}$ go to zero. We omit the details.

A.3 Proofs of Chapter 4

A.3.1 A Proof of Lemma 8

The ith diagonal element of $\mathsf{K}_{\bar{\mathbf{X}}\bar{\mathbf{X}}}$ can be decomposed as follows:

$$(\mathsf{K}_{\bar{\mathbf{X}}\bar{\mathbf{X}}})_{i,i} = \mathsf{E}\Big[\big(\bar{X}_i - \mathsf{E}[\bar{X}_i]\big)^2\Big] \tag{A.40}$$

$$= \mathsf{E}\left[\left(\sum_{k=1}^{n_\mathrm{T}} h_{i,k}\big(X_k - \mathsf{E}[X_k]\big)\right)^2\right] \tag{A.41}$$

$$= \sum_{k=1}^{n_\mathrm{T}} h_{i,k}^2\, \mathsf{E}\Big[\big(X_k - \mathsf{E}[X_k]\big)^2\Big] + \sum_{k=1}^{n_\mathrm{T}} \sum_{\substack{\ell=1 \\ \ell \neq k}}^{n_\mathrm{T}} h_{i,k} h_{i,\ell}\big(\mathsf{E}[X_k X_\ell] - \mathsf{E}[X_k]\,\mathsf{E}[X_\ell]\big). \tag{A.42}$$

Thus, the objective function in (4.2) is

$$\sum_{i=1}^{n_\mathrm{R}} \sum_{k=1}^{n_\mathrm{T}} h_{i,k}^2\, \mathsf{E}\Big[\big(X_k - \mathsf{E}[X_k]\big)^2\Big] + \sum_{i=1}^{n_\mathrm{R}} \sum_{k=1}^{n_\mathrm{T}} \sum_{\substack{\ell=1 \\ \ell \neq k}}^{n_\mathrm{T}} h_{i,k} h_{i,\ell}\big(\mathsf{E}[X_k X_\ell] - \mathsf{E}[X_k]\,\mathsf{E}[X_\ell]\big). \tag{A.43}$$

If we fix a joint distribution on $(X_1, \ldots, X_{n_\mathrm{T}-1})$ and choose with probability 1 a conditional mean $\mathsf{E}[X_{n_\mathrm{T}} \,|\, X_1, \ldots, X_{n_\mathrm{T}-1}]$, then the consumed total average input power is fixed and every summand on the RHS of (A.43) is determined except for

$$\mathsf{E}\Big[\big(X_{n_\mathrm{T}} - \mathsf{E}[X_{n_\mathrm{T}}]\big)^2\Big]. \tag{A.44}$$

This value is maximized—for any choice of joint distribution on $(X_1, \ldots, X_{n_\mathrm{T}-1})$ and conditional mean $\mathsf{E}[X_{n_\mathrm{T}} \,|\, X_1, \ldots, X_{n_\mathrm{T}-1}]$—if X_{n_T} takes value only in the set $\{0, \mathsf{A}\}$. We conclude that, to maximize the expression in (4.2) subject to a constraint on the average input power, it is optimal to restrict X_{n_T} to taking value only in $\{0, \mathsf{A}\}$.

Repeating this argument for $X_{n_\mathrm{T}-1}$, $X_{n_\mathrm{T}-2}$, etc., we conclude that every X_k, $k = 1, \ldots, n_\mathrm{T}$, should take value only in $\{0, \mathsf{A}\}$.

A.3.2 A Proof of Lemma 9

Some steps in our proof are inspired by [28]. We start by rewriting the objective function in (4.2) as:

$$\begin{aligned}
\operatorname{tr}\big(\mathsf{K}_{\bar{\mathbf{X}}\bar{\mathbf{X}}}\big) &= \sum_{i=1}^{n_{\mathrm{R}}} \mathsf{E}\Big[\big(\bar{X}_i - \mathsf{E}[\bar{X}_i]\big)^2\Big] && \text{(A.45)}\\
&= \sum_{i=1}^{n_{\mathrm{R}}} \mathsf{E}\left[\left(\sum_{k=1}^{n_{\mathrm{T}}} h_{i,k}\big(X_k - \mathsf{E}[X_k]\big)\right)^2\right] && \text{(A.46)}\\
&= \sum_{i=1}^{n_{\mathrm{R}}} \sum_{k=1}^{n_{\mathrm{T}}} \sum_{k'=1}^{n_{\mathrm{T}}} h_{i,k}\, h_{i,k'}\, \mathsf{E}\big[\big(X_k - \mathsf{E}[X_k]\big)\big(X_{k'} - \mathsf{E}[X_{k'}]\big)\big] && \text{(A.47)}\\
&= \sum_{k=1}^{n_{\mathrm{T}}} \sum_{k'=1}^{n_{\mathrm{T}}} \underbrace{\sum_{i=1}^{n_{\mathrm{R}}} h_{i,k}\, h_{i,k'}}_{\triangleq \kappa_{k,k'}} \cdot \mathsf{Cov}[X_k, X_{k'}] && \text{(A.48)}\\
&= \sum_{k=1}^{n_{\mathrm{T}}} \sum_{k'=1}^{n_{\mathrm{T}}} \kappa_{k,k'}\, \mathsf{Cov}[X_k, X_{k'}]. && \text{(A.49)}
\end{aligned}$$

Thus, we need to maximize $\mathsf{Cov}[X_k, X_{k'}]$. Assume that we have fixed the average power E_k, $k = 1, \ldots, n_{\mathrm{T}}$, assigned to each input antenna, and further assume that we reorder the antennas such that

$$\mathsf{E}_1 \geq \cdots \geq \mathsf{E}_{n_{\mathrm{T}}}. \tag{A.50}$$

Note that since each antenna only uses a binary input $X_k \in \{0, \mathsf{A}\}$, the assignment $\mathsf{E}[X_k] = \mathsf{E}_k$ determines the probabilities:

$$\Pr[X_k = \mathsf{A}] = \frac{\mathsf{E}_k}{\mathsf{A}} \tag{A.51}$$

and the variances:

$$\mathsf{Cov}[X_k, X_k] = \mathsf{Var}[X_k] = \mathsf{E}\big[X_k^2\big] - \mathsf{E}_k^2 = \mathsf{E}_k\mathsf{A} - \mathsf{E}_k^2. \tag{A.52}$$

For the covariances with $k < k'$ we obtain

$$\begin{aligned}
\mathsf{Cov}[X_k, X_{k'}] &= \mathsf{E}[X_k X_{k'}] - \mathsf{E}_k\mathsf{E}_{k'} && \text{(A.53)}\\
&= \mathsf{A}^2 \Pr[X_k = X_{k'} = \mathsf{A}] - \mathsf{E}_k\mathsf{E}_{k'} && \text{(A.54)}\\
&= \mathsf{A}^2 \Pr[X_{k'} = \mathsf{A}] \underbrace{\Pr[X_k = \mathsf{A} \,|\, X_{k'} = \mathsf{A}]}_{\leq 1} - \mathsf{E}_k\mathsf{E}_{k'} && \text{(A.55)}\\
&\leq \mathsf{A}\mathsf{E}_{k'} - \mathsf{E}_k\mathsf{E}_{k'} && \text{(A.56)}\\
&= \big(\mathsf{A} - \mathsf{E}_k\big)\mathsf{E}_{k'}. && \text{(A.57)}
\end{aligned}$$

The upper bound holds with equality if

$$\Pr[X_k = \mathsf{A} \,|\, X_{k'} = \mathsf{A}] = 1. \tag{A.58}$$

This choice is allowed, because for $k < k'$ the ordering (A.50) is compatible with Condition (A.58). This proves that the mass points can be ordered in such a way that (4.4) holds.

We next prove by contradiction that the first mass point must be $\mathbf{0}$. By Lemma 8, if $\mathbf{x}_1^* \neq \mathbf{0}$, then $\mathbf{x}_1^*$ must contain at least one entry that equals A. By (4.4), that entry must be A for all mass points used by the optimal input. Clearly, changing its value from A to 0 for all mass points will not affect the trace of (4.1), but will reduce the total input power. Hence we conclude that an input with $\mathbf{x}_1^* \neq \mathbf{0}$ (or with zero probability on $\mathbf{0}$) must be suboptimal.

A.3.3 A Proof of Lemma 10

We investigate the Karush-Kuhn-Tucker (KKT) conditions of the optimization problem (4.2). Using the definition of $\mathcal{T}$ and $r_{\mathcal{J},i}$ we rewrite the objective function of (4.2) as

$$\operatorname{tr}\big(\mathsf{K}_{\bar{\mathbf{X}}\bar{\mathbf{X}}}\big) = \sum_{i=1}^{n_{\mathrm{R}}} \Big(\mathsf{E}\big[\bar{X}_i^2\big] - \big(\mathsf{E}[\bar{X}_i]\big)^2 \Big) \tag{A.59}$$

$$= \mathsf{A}^2 \sum_{i=1}^{n_{\mathrm{R}}} \left(\sum_{\mathcal{J}\in\mathcal{T}} p_{\mathcal{J}}\, r_{\mathcal{J},i}^2 - \left(\sum_{\mathcal{J}\in\mathcal{T}} p_{\mathcal{J}}\, r_{\mathcal{J},i} \right)^2 \right). \tag{A.60}$$

Taking into account the constraints (2.5), the Lagrangian is obtained as:

$$\begin{aligned} \mathsf{L}(\mathbf{p}, \mu_0, \mu_1, \boldsymbol{\mu}) = \mathsf{A}^2 \sum_{i=1}^{n_{\mathrm{R}}} \left(\sum_{\mathcal{J}\in\mathcal{T}} p_{\mathcal{J}}\, r_{\mathcal{J},i}^2 - \left(\sum_{\mathcal{J}\in\mathcal{T}} p_{\mathcal{J}}\, r_{\mathcal{J},i} \right)^2 \right) - \mu_0 \left(\sum_{\mathcal{J}\in\mathcal{T}} p_{\mathcal{J}} - 1 \right) \\ - \mu_1 \left(\sum_{\mathcal{J}\in\mathcal{T}} p_{\mathcal{J}} |\mathcal{J}| - \alpha \right) - \sum_{\mathcal{J}\in\mathcal{T}} \mu_{\mathcal{J}} (0 - p_{\mathcal{J}}). \end{aligned} \tag{A.61}$$

The KKT conditions for the optimal PMF $\{p_{\mathcal{K}}^*\}_{\mathcal{K}\in\mathcal{U}}$ are as follows:

$$\mathsf{A}^2 \sum_{i=1}^{n_{\mathrm{R}}} \left(r_{\mathcal{K},i}^2 - 2 r_{\mathcal{K},i} \sum_{\mathcal{J}\in\mathcal{T}} p_{\mathcal{J}}^*\, r_{\mathcal{J},i} \right) - \mu_0 - \mu_1 |\mathcal{K}| + \mu_{\mathcal{K}} = 0, \quad \mathcal{K} \in \mathcal{T}, \tag{A.62a}$$

$$\mu_0 \left(\sum_{\mathcal{J}\in\mathcal{T}} p_{\mathcal{J}}^* - 1 \right) = 0, \tag{A.62b}$$

$$\mu_1 \left(\sum_{\mathcal{J}\in\mathcal{T}} p_{\mathcal{J}}^* |\mathcal{J}| - \alpha \right) = 0, \tag{A.62c}$$

$$\mu_{\mathcal{K}} p_{\mathcal{K}}^* = 0, \quad \mathcal{K} \in \mathcal{T}, \tag{A.62d}$$

$$\mu_0 \geq 0, \tag{A.62e}$$

$$\mu_1 \geq 0, \tag{A.62f}$$

$$\mu_{\mathcal{K}} \geq 0, \quad \mathcal{K} \in \mathcal{T}, \tag{A.62g}$$

$$\sum_{\mathcal{J}\in\mathcal{T}} p_{\mathcal{J}}^* \leq 1, \tag{A.62h}$$

$$\sum_{\mathcal{J}\in\mathcal{T}} p^*_{\mathcal{J}}|\mathcal{J}| \le \alpha, \tag{A.62i}$$

$$p^*_{\mathcal{K}} \ge 0, \quad \mathcal{K}\in\mathcal{T}. \tag{A.62j}$$

We define the vector $\mathbf{m} = (m_1, \dots, m_{n_\mathrm{R}})$ with components

$$m_i \triangleq \sum_{\mathcal{J}\in\mathcal{T}} p^*_{\mathcal{J}} r_{\mathcal{J},i}, \quad i = 1, \dots, n_\mathrm{R}, \tag{A.63}$$

and rewrite (A.62a) as

$$\mathsf{A}^2\|\mathbf{r}_{\mathcal{K}}\|_2^2 - 2\mathsf{A}^2\mathbf{r}_{\mathcal{K}}^\mathsf{T}\mathbf{m} - \mu_0 - \mu_1|\mathcal{K}| + \mu_{\mathcal{K}} = 0, \quad \mathcal{K}\in\mathcal{T}. \tag{A.64}$$

Since by Lemma 9 $P^*_{\mathbf{X}}(\mathbf{0}) > 0$, it must hold that (A.62h) holds with strict inequality and it thus follows from (A.62b) that $\mu_0 = 0$.

Next, assume by contradiction that there exist $n_\mathrm{R}+2$ choices $\mathcal{K}_1, \dots, \mathcal{K}_{n_\mathrm{R}+2} \in \mathcal{T}$ with positive probability $p^*_{\mathcal{K}_\ell} > 0$. Then, by (A.62d), $\mu_{\mathcal{K}_\ell} = 0$ for all $\ell \in \{1, \dots, n_\mathrm{R}+2\}$. From (A.64) we thus have

$$2\mathbf{r}_{\mathcal{K}_\ell}^\mathsf{T}\mathbf{m} + \tilde{\mu}_1|\mathcal{K}_\ell| = \|\mathbf{r}_{\mathcal{K}_\ell}\|_2^2, \quad \ell \in \{1, \dots, n_\mathrm{R}+2\}, \tag{A.65}$$

with $\tilde{\mu}_1 \triangleq \mu_1/\mathsf{A}^2$, which can be written in matrix form:

$$\begin{pmatrix} 2r_{\mathcal{K}_1,1} & \cdots & 2r_{\mathcal{K}_1,n_\mathrm{R}} & |\mathcal{K}_1| \\ 2r_{\mathcal{K}_2,1} & \cdots & 2r_{\mathcal{K}_2,n_\mathrm{R}} & |\mathcal{K}_2| \\ \vdots & \ddots & \vdots & \vdots \\ 2r_{\mathcal{K}_{n_\mathrm{R}+2},1} & \cdots & 2r_{\mathcal{K}_{n_\mathrm{R}+2},n_\mathrm{R}} & |\mathcal{K}_{n_\mathrm{R}+2}| \end{pmatrix} \begin{pmatrix} m_1 \\ m_2 \\ \vdots \\ m_{n_\mathrm{R}} \\ \tilde{\mu}_1 \end{pmatrix} = \begin{pmatrix} \|\mathbf{r}_{\mathcal{K}_1}\|_2^2 \\ \|\mathbf{r}_{\mathcal{K}_2}\|_2^2 \\ \vdots \\ \|\mathbf{r}_{\mathcal{K}_{n_\mathrm{R}+2}}\|_2^2 \end{pmatrix}. \tag{A.66}$$

This is an over-determined system of linear equations in $n_\mathrm{R}+1$ variables $m_1, \dots, m_{n_\mathrm{R}}$, $\tilde{\mu}_1$, which has a solution if, and only if,

$$\begin{aligned} &\operatorname{rank}\begin{pmatrix} 2r_{\mathcal{K}_1,1} & \cdots & 2r_{\mathcal{K}_1,n_\mathrm{R}} & |\mathcal{K}_1| \\ 2r_{\mathcal{K}_2,1} & \cdots & 2r_{\mathcal{K}_2,n_\mathrm{R}} & |\mathcal{K}_2| \\ \vdots & \ddots & \vdots & \vdots \\ 2r_{\mathcal{K}_{n_\mathrm{R}+2},1} & \cdots & 2r_{\mathcal{K}_{n_\mathrm{R}+2},n_\mathrm{R}} & |\mathcal{K}_{n_\mathrm{R}+2}| \end{pmatrix} \\ &= \operatorname{rank}\begin{pmatrix} 2r_{\mathcal{K}_1,1} & \cdots & 2r_{\mathcal{K}_1,n_\mathrm{R}} & |\mathcal{K}_1| & \|\mathbf{r}_{\mathcal{K}_1}\|_2^2 \\ 2r_{\mathcal{K}_2,1} & \cdots & 2r_{\mathcal{K}_2,n_\mathrm{R}} & |\mathcal{K}_2| & \|\mathbf{r}_{\mathcal{K}_2}\|_2^2 \\ \vdots & \ddots & \vdots & \vdots & \vdots \\ 2r_{\mathcal{K}_{n_\mathrm{R}+2},1} & \cdots & 2r_{\mathcal{K}_{n_\mathrm{R}+2},n_\mathrm{R}} & |\mathcal{K}_{n_\mathrm{R}+2}| & \|\mathbf{r}_{\mathcal{K}_{n_\mathrm{R}+2}}\|_2^2 \end{pmatrix}. \end{aligned} \tag{A.67}$$

However, since the matrix on the LHS has only $n_\mathrm{R}+1$ columns, its rank can be at most $n_\mathrm{R}+1$. The matrix on the RHS, on the other hand, has by assumption (see (4.9)) rank $n_\mathrm{R}+2$. This is a contradiction. We have proven that there exist at most $n_\mathrm{R}+1$ values $p_{\mathcal{K}}$ with positive values. Together with $\mathbf{0}$, there are at most $n_\mathrm{R}+2$ mass points in total.

A.3.4 A Proof of Lemma 12

The proof of Part 1 follows the same arguments as in the proof of Lemma 10. To prove Part 2, we notice that a solution $\mathbf{q}^* = (q_1^*, \ldots, q_{n_\mathrm{T}}^*)$ to (4.14) has to satisfy $\sum_{k=1}^{n_\mathrm{T}} q_k^* < 1$ because any $\bar{X}$ that achieves maximum variance $\mathsf{V}_{\max}$ puts nonzero probability on $\bar{X} = 0$. We further notice that the optimization problem (4.14) is convex because $s_1, \ldots, s_{n_\mathrm{T}} > 0$. Consider the KKT conditions for this optimization problem, and account for the fact that the linear constraint $\sum_{k=1}^{n_\mathrm{T}} q_k^* \leq 1$ is not active. The KKT conditions are then given by the following six (in)equalities:

$$-s_k(s_k - 2\mathbf{s}^\mathsf{T}\mathbf{q}) + \mu_0 \cdot k - \mu_k = 0, \quad k \in \{1, \ldots, n_\mathrm{T}\}, \tag{A.68a}$$

$$\mu_k q_k = 0, \quad k \in \{1, \ldots, n_\mathrm{T}\}, \tag{A.68b}$$

$$\mu_0 \left(\sum_{k=1}^{n_\mathrm{T}} k \cdot q_k - \alpha \right) = 0 \tag{A.68c}$$

$$\mu_i \geq 0, \quad i \in \{0, 1, \ldots, n_\mathrm{T}\}, \tag{A.68d}$$

$$\sum_{k=1}^{n_\mathrm{T}} k \cdot q_k \leq \alpha, \tag{A.68e}$$

$$q_k \geq 0, \quad k \in \{1, \ldots, n_\mathrm{T}\}. \tag{A.68f}$$

A solution to this convex optimization always exists. Assume now that for such a solution the inequality constraint $\sum_{k=1}^{n_\mathrm{T}} k \cdot q_k^* \leq \alpha$ holds with strict inequality. The corresponding Lagrange multiplier μ_0 must then equal 0. Now, since for any $q_i^* > 0$, $\mu_i = 0$, (A.68a) then implies

$$s_i = 2\mathbf{s}^\mathsf{T}\mathbf{q}^*. \tag{A.69}$$

But this can hold at most for a single $i \in \{1, \ldots, n_\mathrm{T}\}$ because all values of s_i are different ($h_{n_\mathrm{T}} > 0$). Moreover, it can hold only for $k = n_\mathrm{T}$. Indeed, if (A.69) holds for some $i < n_\mathrm{T}$, then the KKT condition (A.68a) cannot be satisfied for all $k > i$ because $\mu_k \geq 0$. To conclude, if the inequality constraint $\sum_{k=1}^{n_\mathrm{T}} k \cdot q_k^* \leq \alpha$ holds with strict inequality, then the optimal $\mathbf{q}^*$ satisfies $q_1^* = q_2^* = \ldots = q_{n_\mathrm{T}-1}^*$ and $q_{n_\mathrm{T}} = 1/2$. But this choice is only feasible for $\alpha = \frac{n_\mathrm{T}}{2}$, in which case the inequality constraint $\sum_{k=1}^{n_\mathrm{T}} k \cdot q_k^* \leq \alpha$ holds with equality. We have thus reached the desired contradiction, irrespective of the value of $\alpha \leq \frac{n_\mathrm{T}}{2}$.

We now prove Part 3 of the lemma by contradiction. Assume that for positive integers $k > i > j$ the optimal solution $\mathbf{q}^*$ satisfies $q_k^*, q_i^*, q_j^* > 0$. Then, by (A.68b), $\mu_k = \mu_j = \mu_i = 0$, and (A.68a) implies

$$\begin{pmatrix} 1 & \frac{j}{s_j} \\ 1 & \frac{i}{s_i} \\ 1 & \frac{k}{s_k} \end{pmatrix} \begin{pmatrix} 2\mathbf{s}^\mathsf{T}\mathbf{q} \\ \mu_0 \end{pmatrix} = \begin{pmatrix} s_j \\ s_i \\ s_k \end{pmatrix}. \tag{A.70}$$

This is an overdetermined system of linear equations in the two "variables" $(2\mathbf{s}^\mathsf{T}\mathbf{q})$ and $\mu_0 \geq 0$, and it has a solution if, and only if,

$$\operatorname{rank} \begin{pmatrix} 1 & \frac{j}{s_j} \\ 1 & \frac{i}{s_i} \\ 1 & \frac{k}{s_k} \end{pmatrix} = \operatorname{rank} \begin{pmatrix} 1 & \frac{j}{s_j} & s_j \\ 1 & \frac{i}{s_i} & s_i \\ 1 & \frac{k}{s_k} & s_k \end{pmatrix} \tag{A.71}$$

The proof follows then by noticing that this is only possible if the rank of both matrices in (A.71) is 2. In particular, the left-most matrix cannot have rank 1. And neither can the matrix in (4.15).

A.4 Proofs of Chapter 5

A.4.1 A Proof of Theorem 14

Let $Q(\cdot)$ denote the capacity-achieving input distribution. Then we evaluate the upper bound [58]

$$\mathsf{C}_1(\mathsf{A}, \alpha\mathsf{A}) \le \int \mathsf{D}(W(\cdot|x)\|R(\cdot))\,\mathrm{d}Q(x) \tag{A.72}$$

for the test density

$$R(y) = \begin{cases} (1-\beta)\cdot R_1(y) & \text{if } y \in [0, \mathsf{A}], \\ \beta \cdot R_2(y) & \text{otherwise,} \end{cases} \tag{A.73}$$

where $R_1(y)$ is a density over $[0, \mathsf{A}]$,

$$R_1(y) = \frac{1}{\mathsf{A}} \cdot \frac{\mu}{1-e^{-\mu}} \cdot e^{-\frac{\mu y}{\mathsf{A}}}, \quad y \in [0, \mathsf{A}], \tag{A.74}$$

for some $\mu > 0$; $R_2(y)$ is a density over $\mathbb{R}\backslash[0, \mathsf{A}]$,

$$R_2(y) = \begin{cases} \frac{1}{\sqrt{2\pi}}\, e^{-\frac{y^2}{2}} & \text{if } y < 0, \\ \frac{1}{\sqrt{2\pi}}\, e^{-\frac{(y-\mathsf{A})^2}{2}} & y > \mathsf{A}; \end{cases} \tag{A.75}$$

and $\beta \in (0,1)$ will be specified later.

For any $X = x \in [0, A]$, we have

$$\begin{aligned} D(W(\cdot|x)||R(\cdot)) &= \int_{-\infty}^{\infty} W(y|x) \log \frac{W(y|x)}{R(y)}\,\mathrm{d}y \\ &= -\int_{-\infty}^{\infty} W(y|x)\log R(y)\,\mathrm{d}y - \log\sqrt{2\pi e}. \end{aligned} \tag{A.76}$$

We first expand the first term in the RHS of (A.76) as

$$\begin{aligned} &-\int_{-\infty}^{-\infty} W(y|x)\log R(y)\,\mathrm{d}y \\ &= -\int_{-\infty}^{0} W(y|x)\log R(y)\,\mathrm{d}y - \int_{0}^{A} W(y|x)\log R(y)\,\mathrm{d}y - \int_{A}^{\infty} W(y|x)\log R(y)\,\mathrm{d}y \end{aligned} \tag{A.77}$$

We notice that

$$\begin{aligned} &-\int_{-\infty}^{0} W(y|x)\log R(y)\,\mathrm{d}y \\ &\quad = -\int_{-\infty}^{0} \frac{1}{\sqrt{2\pi}}\, e^{-\frac{(y-x)^2}{2}} \left(\log\frac{\beta}{\sqrt{2\pi}} - \frac{y^2}{2}\right)\mathrm{d}y \end{aligned} \tag{A.78}$$

$$= -\log\frac{\beta}{\sqrt{2\pi}}\mathcal{Q}(x) + \frac{1}{2}\big(\mathcal{Q}(x) + x^2\mathcal{Q}(x) - x\phi(x)\big) \tag{A.79}$$

$$\leq -\left(\log\frac{\beta}{\sqrt{2\pi}} - \frac{1}{2}\right)\mathcal{Q}(x), \tag{A.80}$$

where

$$\phi(x) \triangleq \frac{1}{\sqrt{2\pi}}\, e^{-\frac{x^2}{2}}, \tag{A.81}$$

and (A.80) holds because of [59, Prop. A.8]

$$\xi\mathcal{Q}(\xi) \leq \phi(\xi), \quad \xi \geq 0. \tag{A.82}$$

Similarly,

$$-\int_{\mathsf{A}}^{\infty} W_{\mathcal{I},\ell}(y|x)\log R_{\mathcal{I},\ell}(y)\,\mathrm{d}y \leq -\log\frac{\beta}{\sqrt{2\pi e}\sigma_{\mathcal{I},\ell}}\cdot\mathcal{Q}\left(\frac{\mathsf{A}-x}{\sigma_{\mathcal{I},\ell}}\right). \tag{A.83}$$

Following the same arguments, we also obtain:

$$-\int_{\mathsf{A}}^{\infty} W(y|x)\log R(y)\,\mathrm{d}y \leq -\left(\log\frac{\beta}{\sqrt{2\pi}} - \frac{1}{2}\right)\mathcal{Q}(\mathsf{A}-x). \tag{A.84}$$

Moreover,

$$-\int_0^{\mathsf{A}} W(y|x)\log R(y)\,\mathrm{d}y$$

$$= -\int_0^{\mathsf{A}} \frac{1}{\sqrt{2\pi}}\, e^{-\frac{(y-x)^2}{2}}\left(\log\frac{(1-\beta)}{\mathsf{A}}\frac{\mu}{1-e^{-\mu}} - \frac{\mu}{\mathsf{A}}y\right)\mathrm{d}y \tag{A.85}$$

$$= -\log\left(\frac{1-\beta}{\mathsf{A}}\frac{\mu}{1-e^{-\mu}}\right)\big(1-\mathcal{Q}(x)-\mathcal{Q}(\mathsf{A}-x)\big)$$
$$+\frac{\mu}{\mathsf{A}}\Big(\phi(x)-\phi(\mathsf{A}-x)+x\big(1-\mathcal{Q}(x)-\mathcal{Q}(\mathsf{A}-x)\big)\Big) \tag{A.86}$$

$$\leq -\log\left(\frac{1-\beta}{\mathsf{A}}\frac{\mu}{1-e^{-\mu}}\right)\big(1-\mathcal{Q}(x)-\mathcal{Q}(\mathsf{A}-x)\big)$$
$$+\frac{\mu}{\mathsf{A}}\left(\phi(0)-\phi(\mathsf{A})+x\left(1-2\,\mathcal{Q}\left(\frac{\mathsf{A}}{2}\right)\right)\right), \tag{A.87}$$

where (A.87) follows from the fact that $1-\mathcal{Q}(x)-\mathcal{Q}(\mathsf{A}-x)$ achieves the maximum value at $x=\frac{\mathsf{A}}{2}$ when $x\in[0,\mathsf{A}]$.

Combining (A.80), (A.84), and (A.87) with (A.72), and choosing

$$\beta = \frac{\mu\sqrt{2\pi e}}{\mathsf{A}\cdot(1-e^{-\mu})+\mu\sqrt{2\pi e}}, \tag{A.88}$$

now yields the desired upper bound in the theorem.

A.4.2 A proof of Theorem 18

The converse follows immediately from the maximum-variance upper bound in Theorem 17. Achievability follows from [60, Thm. 2], which states that

$$\mathsf{C}_{\mathbf{h}}(\mathsf{A}, \alpha\mathsf{A}) \geq \mathsf{V}_{\max}(\mathsf{A}, \alpha\mathsf{A}) + o(\mathsf{A}^2), \tag{A.89}$$

where $o(\mathsf{A}^2)$ decreases to 0 faster than A^2, i.e.,

$$\lim_{\mathsf{A}\downarrow 0} \frac{o(\mathsf{A}^2)}{\mathsf{A}^2} = 0. \tag{A.90}$$

Note that the MISO channel under consideration in this paper satisfies the technical conditions A–F in [60].

A.5 Proofs of Chapter 6

A.5.1 Derivation of Lower Bounds

For any choice of the random vector $\bar{\mathbf{X}}$ over $\mathcal{R}(\mathsf{H})$, the following holds:

$$\begin{aligned}
\mathsf{C}_{\mathsf{H}}(\mathsf{A}, \alpha\mathsf{A}) &\geq \mathrm{I}(\bar{\mathbf{X}}; \bar{\mathbf{X}} + \mathbf{Z}) && \text{(A.91)}\\
&= \mathsf{h}(\bar{\mathbf{X}} + \mathbf{Z}) - \mathsf{h}(\mathbf{Z}) && \text{(A.92)}\\
&\geq \frac{1}{2}\log\Big(e^{2\,\mathsf{h}(\bar{\mathbf{X}})} + e^{2\,\mathsf{h}(\mathbf{Z})}\Big) - \mathsf{h}(\mathbf{Z}) && \text{(A.93)}\\
&= \frac{1}{2}\log\left(1 + \frac{e^{2\,\mathsf{h}(\bar{\mathbf{X}})}}{(2\pi e)^{n_{\mathrm{R}}}}\right), && \text{(A.94)}
\end{aligned}$$

where (A.93) follows from the EPI [54].

Proof of Theorem 25

We choose $\bar{\mathbf{X}}$ to be uniformly distributed over $\mathcal{R}(\mathsf{H})$. To verify that this uniform distribution satisfies the average-power constraint (6.4), we define

$$p_{\mathcal{I}} \triangleq \Pr[U = \mathcal{I}] \tag{A.95}$$

and derive

$$\begin{aligned}
&\mathsf{E}_U\big[\mathsf{A}s_U + \big\|\mathsf{H}_U^{-1}\big(\mathsf{E}\big[\bar{\mathbf{X}}\,\big|\,U\big] - \mathbf{v}_U\big)\big\|_1\big]\\
&\quad= \mathsf{A}\sum_{\mathcal{I}\in\mathcal{U}} p_{\mathcal{I}}\, s_{\mathcal{I}} + \sum_{\mathcal{I}\in\mathcal{U}} p_{\mathcal{I}}\big\|\mathsf{H}_{\mathcal{I}}^{-1}\big(\mathsf{E}[\bar{\mathbf{X}}\,|\,U=\mathcal{I}] - \mathbf{v}_{\mathcal{I}}\big)\big\|_1 && \text{(A.96)}\\
&\quad= \mathsf{A}\sum_{\mathcal{I}\in\mathcal{U}} q_{\mathcal{I}}\, s_{\mathcal{I}} + \sum_{\mathcal{I}\in\mathcal{U}} q_{\mathcal{I}}\cdot\frac{n_{\mathrm{R}}\mathsf{A}}{2} && \text{(A.97)}\\
&\quad= \alpha_{\mathrm{th}}\mathsf{A} && \text{(A.98)}\\
&\quad\leq \alpha\mathsf{A}. && \text{(A.99)}
\end{aligned}$$

Here, (A.97) follows because when $\bar{\mathbf{X}}$ is uniformly distributed in $\mathcal{R}(\mathsf{H})$, we have

$$\mathsf{H}_{\mathcal{I}}^{-1}\big(\mathsf{E}[\bar{\mathbf{X}}\,|\,U=\mathcal{I}]-\mathbf{v}_{\mathcal{I}}\big)=\frac{\mathsf{A}}{2}\cdot\mathbf{1}_{n_{\mathrm{R}}} \tag{A.100}$$

and

$$p_{\mathcal{I}}=q_{\mathcal{I}},\quad \mathcal{I}\in\mathcal{U}. \tag{A.101}$$

The last inequality (A.99) holds by the assumption in the theorem.

The uniform distribution of $\bar{\mathbf{X}}$ results in

$$\mathsf{h}(\bar{\mathbf{X}})=\log(\mathsf{A}^{n_{\mathrm{R}}}\cdot\mathsf{V}_{\mathsf{H}}), \tag{A.102}$$

which, by (A.94), leads to (6.21).

Proof of Theorem 26

We choose

$$\lambda\in\Big(\max\Big\{0,\frac{n_{\mathrm{R}}}{2}+\alpha-\alpha_{\mathrm{th}}\Big\},\min\Big\{\frac{n_{\mathrm{R}}}{2},\alpha\Big\}\Big), \tag{A.103}$$

a probability vector $\mathbf{p}$ satisfying (7.47), and μ as the unique solution to (6.24).

Note that such choices are always possible as can be argued as follows. From (A.103) one directly sees that $0<\lambda<\frac{n_{\mathrm{R}}}{2}$. Thus, $0<\frac{\lambda}{n_{\mathrm{R}}}<\frac{1}{2}$, which corresponds exactly to the range where (6.24) has a unique solution. From (A.103) it also follows that $\frac{n_{\mathrm{R}}}{2}+\alpha-\alpha_{\mathrm{th}}<\lambda<\alpha$ and thus

$$0<\alpha-\lambda<\alpha_{\mathrm{th}}-\frac{n_{\mathrm{R}}}{2}\le\frac{n_{\mathrm{T}}}{2}-\frac{n_{\mathrm{R}}}{2}, \tag{A.104}$$

where the inequality follows from (6.17). So the RHS of (6.25) takes value within the interval $\big(0,\frac{n_{\mathrm{T}}-n_{\mathrm{R}}}{2}\big)$. By Remark 21, the LHS of (7.47) can take value in the interval $[0,n_{\mathrm{T}}-n_{\mathrm{R}}]$, which covers the range of the RHS. The existence of $\mathbf{p}$ satisfying (6.25) now follows from the continuity of the LHS of (6.25) in $\mathbf{p}$.

For each $\mathcal{I}$ we now pick the probability density function (PDF) $f_{\bar{\mathbf{X}}|U=\mathcal{I}}$ to be the n_{R}-dimensional product truncated exponential distribution rotated by the matrix $\mathsf{H}_{\mathcal{I}}$:

$$f_{\bar{\mathbf{X}}|U=\mathcal{I}}(\bar{\mathbf{x}})=\frac{1}{\mathsf{A}^{n_{\mathrm{R}}}|\det\mathsf{H}_{\mathcal{I}}|}\cdot\left(\frac{\mu}{1-e^{-\mu}}\right)^{n_{\mathrm{R}}}e^{\frac{-\mu\|\mathsf{H}_{\mathcal{I}}^{-1}(\bar{\mathbf{x}}-\mathbf{v}_{\mathcal{I}})\|_1}{\mathsf{A}}}. \tag{A.105}$$

Note that this corresponds to the entropy-maximizing distribution under a total average-power constraint. The average-power constraint (6.4) is satisfied because

$$\begin{aligned}&\mathsf{E}_U\big[\mathsf{A}s_U+\big\|\mathsf{H}_U^{-1}\big(\mathsf{E}\big[\bar{\mathbf{X}}\,\big|\,U\big]-\mathbf{v}_U\big)\big\|_1\big]\\&\quad=\sum_{\mathcal{I}\in\mathcal{U}}p_{\mathcal{I}}\Big(\mathsf{A}s_{\mathcal{I}}+\big\|\mathsf{H}_{\mathcal{I}}^{-1}\big(\mathsf{E}[\bar{\mathbf{X}}\,|\,U=\mathcal{I}]-\mathbf{v}_{\mathcal{I}}\big)\big\|_1\Big) &\text{(A.106)}\\&\quad=\sum_{\mathcal{I}\in\mathcal{U}}p_{\mathcal{I}}\left(\mathsf{A}s_{\mathcal{I}}+n_{\mathrm{R}}\mathsf{A}\left(\frac{1}{\mu}-\frac{e^{-\mu}}{1-e^{-\mu}}\right)\right) &\text{(A.107)}\end{aligned}$$

$$= \sum_{\mathcal{I}\in\mathcal{U}} p_{\mathcal{I}}\big(\mathsf{A}s_{\mathcal{I}} + \mathsf{A}\lambda\big) \tag{A.108}$$

$$= \mathsf{A}\sum_{\mathcal{I}\in\mathcal{U}} p_{\mathcal{I}}s_{\mathcal{I}} + \mathsf{A}\lambda \tag{A.109}$$

$$= \mathsf{A}(\alpha - \lambda) + \mathsf{A}\lambda \tag{A.110}$$

$$= \alpha\mathsf{A}. \tag{A.111}$$

Here, (A.107) follows from the expected value of the truncated exponential distribution; (A.108) is due to (6.24); and (A.110) follows from (6.25).

Furthermore,

$$\mathsf{h}(\bar{\mathbf{X}}) = \mathsf{I}(\bar{\mathbf{X}}; U) + \mathsf{h}(\bar{\mathbf{X}}|U) \tag{A.112}$$

$$= \mathsf{H}(U) + \mathsf{h}(\bar{\mathbf{X}}|U) \tag{A.113}$$

$$= \mathsf{H}(\mathbf{p}) + \sum_{\mathcal{I}\in\mathcal{U}} p_{\mathcal{I}}\,\mathsf{h}(\bar{\mathbf{X}}|U = \mathcal{I}) \tag{A.114}$$

$$= \mathsf{H}(\mathbf{p}) + \sum_{\mathcal{I}\in\mathcal{U}} p_{\mathcal{I}}\log|\det\mathsf{H}_{\mathcal{I}}| + n_{\mathrm{R}}\log\mathsf{A} - n_{\mathrm{R}}\log\frac{\mu}{1-e^{-\mu}} + n_{\mathrm{R}}\left(1 - \frac{\mu\,e^{-\mu}}{1-e^{-\mu}}\right) \tag{A.115}$$

$$= -\sum_{\mathcal{I}\in\mathcal{U}} p_{\mathcal{I}}\log p_{\mathcal{I}} + \sum_{\mathcal{I}\in\mathcal{U}} p_{\mathcal{I}}\log\frac{|\det\mathsf{H}_{\mathcal{I}}|}{\mathsf{V}_{\mathsf{H}}} + \log\mathsf{V}_{\mathsf{H}} + n_{\mathrm{R}}\log\mathsf{A} + n_{\mathrm{R}}\left(1 - \log\frac{\mu}{1-e^{-\mu}} - \frac{\mu\,e^{-\mu}}{1-e^{-\mu}}\right) \tag{A.116}$$

$$= -\mathsf{D}(\mathbf{p}\|\mathbf{q}) + \log\mathsf{V}_{\mathsf{H}} + n_{\mathrm{R}}\log\mathsf{A} + n_{\mathrm{R}}\left(1 - \log\frac{\mu}{1-e^{-\mu}} - \frac{\mu\,e^{-\mu}}{1-e^{-\mu}}\right). \tag{A.117}$$

Here, (A.113) holds because $\mathsf{H}(U|\bar{\mathbf{X}}) = 0$; (A.115) follows from the differential entropy of a truncated exponential distribution; and in (A.117) we used the definition of $\mathbf{q}$ in (6.12). Then, (6.22) follows by plugging (A.117) into (A.94).

A.5.2 Derivation of Upper Bounds

Let $\bar{\mathbf{X}}^\star$ be a maximizer in (6.3) and let $U^\star$ be defined by $\bar{\mathbf{X}}^\star$ as in (6.5). Then,

$$\mathsf{C}_{\mathsf{H}}(\mathsf{A}, \alpha\mathsf{A}) = \mathsf{I}\big(\bar{\mathbf{X}}^\star; \bar{\mathbf{X}}^\star + \mathbf{Z}\big) \tag{A.118}$$

$$\leq \mathsf{I}\big(\bar{\mathbf{X}}^\star; \bar{\mathbf{X}}^\star + \mathbf{Z}, U^\star\big) \tag{A.119}$$

$$= \mathsf{H}(U^\star) + \mathsf{I}\big(\bar{\mathbf{X}}^\star; \bar{\mathbf{X}}^\star + \mathbf{Z}\big|U^\star\big). \tag{A.120}$$

For each set $\mathcal{I} \in \mathcal{U}$, we have

$$\mathsf{I}\big(\bar{\mathbf{X}}^\star; \bar{\mathbf{X}}^\star + \mathbf{Z}\big|U^\star = \mathcal{I}\big) = \mathsf{I}\big(\bar{\mathbf{X}}^\star - \mathbf{v}_{\mathcal{I}}; (\bar{\mathbf{X}}^\star - \mathbf{v}_{\mathcal{I}}) + \mathbf{Z}\big|U^\star = \mathcal{I}\big) \tag{A.121}$$

$$= \mathsf{I}\big(\mathsf{H}_{\mathcal{I}}^{-1}(\bar{\mathbf{X}}^\star - \mathbf{v}_{\mathcal{I}}); \mathsf{H}_{\mathcal{I}}^{-1}(\bar{\mathbf{X}}^\star - \mathbf{v}_{\mathcal{I}}) + \mathsf{H}_{\mathcal{I}}^{-1}\mathbf{Z}\big|U^\star = \mathcal{I}\big) \tag{A.122}$$

$$= \mathrm{I}(\mathbf{X}_{\mathcal{I}}; \mathbf{X}_{\mathcal{I}} + \mathbf{Z}_{\mathcal{I}} | U^\star = \mathcal{I}) \tag{A.123}$$

where we have defined

$$\mathbf{Z}_{\mathcal{I}} \triangleq \mathsf{H}_{\mathcal{I}}^{-1} \mathbf{Z}, \tag{A.124}$$

$$\mathbf{X}_{\mathcal{I}} \triangleq \mathsf{H}_{\mathcal{I}}^{-1} (\mathbf{X}^\star - \mathbf{v}_{\mathcal{I}}). \tag{A.125}$$

It should be noted that

$$\mathbf{Z}_{\mathcal{I}} \sim \mathcal{N}\big(0, \mathsf{H}_{\mathcal{I}}^{-1} \mathsf{H}_{\mathcal{I}}^{-\mathsf{T}}\big). \tag{A.126}$$

Moreover, $\mathbf{X}_{\mathcal{I}}$ is subject to the following peak- and average-power constraints:

$$\Pr\big[\bar{X}_{\mathcal{I},\ell} > \mathsf{A}\big] = 0, \quad \forall\, \ell \in \{1, \ldots, n_{\mathrm{R}}\}, \tag{A.127a}$$

$$\mathsf{E}\big[\|\mathbf{X}_{\mathcal{I}}\|_1\big] = \mathsf{E}_{\mathcal{I}}, \tag{A.127b}$$

for some $\mathsf{E}_{\mathcal{I}} \geq 0$, where the set $\{\mathsf{E}_{\mathcal{I}} \colon \mathcal{I} \in \mathcal{U}\}$ satisfies

$$\sum_{\mathcal{I} \in \mathcal{U}} p_{\mathcal{I}}(s_{\mathcal{I}} \mathsf{A} + \mathsf{E}_{\mathcal{I}}) \leq \alpha \mathsf{A}. \tag{A.128}$$

To further bound the RHS of (A.123), we use the duality-based upper-bounding technique using a product output distribution

$$R_{\mathcal{I}}(\mathbf{y}_{\mathcal{I}}) = \prod_{\ell=1}^{n_{\mathrm{R}}} R_{\mathcal{I},\ell}(y_{\mathcal{I},\ell}). \tag{A.129}$$

Denoting by $W_{\mathcal{I}}(\cdot|\mathbf{X}_{\mathcal{I}})$ the transition law of the $n_{\mathrm{R}} \times n_{\mathrm{R}}$ MIMO channel with input $\mathbf{X}_{\mathcal{I}}$ and output $\mathbf{Y}_{\mathcal{I}} \triangleq \mathbf{X}_{\mathcal{I}} + \mathbf{Z}_{\mathcal{I}}$, and by $W_{\mathcal{I},\ell}(\cdot|\bar{X}_{\mathcal{I},\ell})$ the marginal transition law of its ℓth component, we have:

$$\begin{aligned}
&\mathrm{I}(\mathbf{X}_{\mathcal{I}}; \mathbf{X}_{\mathcal{I}} + \mathbf{Z}_{\mathcal{I}} | U^\star = \mathcal{I}) \\
&\quad \leq \mathsf{E}_{\mathbf{X}_{\mathcal{I}}|U^\star=\mathcal{I}}\big[\mathsf{D}\big(W_{\mathcal{I}}(\cdot|\mathbf{X}_{\mathcal{I}}) \big\| R_{\mathcal{I}}(\cdot)\big)\big] && \text{(A.130)} \\
&\quad = -\mathsf{h}\big(\mathbf{X}_{\mathcal{I}} + \mathbf{Z}_{\mathcal{I}} \big| \mathbf{X}_{\mathcal{I}}, U^\star = \mathcal{I}\big) - \mathsf{E}_{\mathbf{X}_{\mathcal{I}}|U^\star=\mathcal{I}}\left[\sum_{\ell=1}^{n_{\mathrm{R}}} \mathsf{E}_{W_{\mathcal{I}}(\mathbf{Y}_{\mathcal{I}}|\mathbf{X}_{\mathcal{I}})}[\log R_{\mathcal{I},\ell}(Y_{\mathcal{I},\ell})]\right] && \text{(A.131)} \\
&\quad = -\frac{n_{\mathrm{R}}}{2} \log 2\pi e + \log|\det \mathsf{H}_{\mathcal{I}}| - \sum_{\ell=1}^{n_{\mathrm{R}}} \mathsf{E}_{\bar{X}_{\mathcal{I},\ell}|U^\star=\mathcal{I}}\Big[\mathsf{E}_{W_{\mathcal{I},\ell}(Y_{\mathcal{I},\ell}|\bar{X}_{\mathcal{I},\ell})}[\log R_{\mathcal{I},\ell}(Y_{\mathcal{I},\ell})]\Big], && \text{(A.132)}
\end{aligned}$$

where the last equality holds because

$$\mathsf{h}(\mathbf{X}_{\mathcal{I}} + \mathbf{Z}_{\mathcal{I}} | \mathbf{X}_{\mathcal{I}}, U^\star = \mathcal{I}) = \mathsf{h}(\mathbf{Z}_{\mathcal{I}}) = \frac{1}{2} \log\big((2\pi e)^{n_{\mathrm{R}}} \det \mathsf{H}_{\mathcal{I}}^{-1} \mathsf{H}_{\mathcal{I}}^{-\mathsf{T}}\big). \tag{A.133}$$

We finally combine (A.120) with (A.123) and (A.132) to obtain

$$\begin{aligned}
\mathsf{C}_{\mathsf{H}}(\mathsf{A}, \alpha\mathsf{A}) \leq \mathsf{H}(\mathbf{p}^*) &- \sum_{\ell=1}^{n_{\mathrm{R}}} \sum_{\mathcal{I} \in \mathcal{U}} p_{\mathcal{I}}^* \, \mathsf{E}_{\bar{X}_{\mathcal{I},\ell}|U^\star=\mathcal{I}}\Big[\mathsf{E}_{W_{\mathcal{I},\ell}(Y_{\mathcal{I},\ell}|\bar{X}_{\mathcal{I},\ell})}[\log R_{\mathcal{I},\ell}(Y_{\mathcal{I},\ell})]\Big] \\
&+ \sum_{\mathcal{I} \in \mathcal{U}} p_{\mathcal{I}}^* \log|\det \mathsf{H}_{\mathcal{I}}| - \frac{n_{\mathrm{R}}}{2} \log 2\pi e,
\end{aligned} \tag{A.134}$$

where $\mathbf{p}^*$ denotes the probability vector of $U^\star$. The bounds in Section 6.2.2 are then found by picking appropriate choices for the distribution on the output alphabet $R_{\mathcal{I},\ell}(\cdot)$. We elaborate on this in the following.

Proof of Theorem 27

Inspired by [17] and [20], we choose

$$R_{\mathcal{I},\ell}(y) = \begin{cases} \frac{\beta}{\sqrt{2\pi}\sigma_{\mathcal{I},\ell}} \cdot e^{-\frac{y^2}{2\sigma_{\mathcal{I},\ell}^2}} & \text{if } y \in (-\infty, 0), \\ (1-\beta) \cdot \frac{1}{\mathsf{A}} & \text{if } y \in [0, \mathsf{A}], \\ \frac{\beta}{\sqrt{2\pi}\sigma_{\mathcal{I},\ell}} \cdot e^{-\frac{(y-\mathsf{A})^2}{2\sigma_{\mathcal{I},\ell}^2}} & \text{if } y \in (\mathsf{A}, \infty), \end{cases} \tag{A.135}$$

where $\beta \in (0,1)$ will be specified later. Recall that $\sigma_{\mathcal{I},\ell}$ is the square root of the ℓth diagonal entry of the matrix $\mathsf{H}_{\mathcal{I}}^{-1}\mathsf{H}_{\mathcal{I}}^{-\mathsf{T}}$, i.e.,

$$\sigma_{\mathcal{I},\ell} = \sqrt{\mathsf{Var}[Z_{\mathcal{I},\ell}]}. \tag{A.136}$$

We notice that

$$\begin{aligned} &-\int_{-\infty}^{0} W_{\mathcal{I},\ell}(y|x) \log R_{\mathcal{I},\ell}(y)\, \mathrm{d}y \\ &= -\int_{-\infty}^{0} \frac{1}{\sqrt{2\pi}\sigma_{\mathcal{I},\ell}} e^{-\frac{(y-x)^2}{2\sigma_{\mathcal{I},\ell}^2}} \left(\log \frac{\beta}{\sqrt{2\pi}\sigma_{\mathcal{I},\ell}} - \frac{y^2}{2\sigma_{\mathcal{I},\ell}^2} \right) \mathrm{d}y && \text{(A.137)} \\ &= -\log\left(\frac{\beta}{\sqrt{2\pi}\sigma_{\mathcal{I},\ell}}\right) \mathcal{Q}\left(\frac{x}{\sigma_{\mathcal{I},\ell}}\right) + \frac{1}{2}\,\mathcal{Q}\left(\frac{x}{\sigma_{\mathcal{I},\ell}}\right) \\ &\quad + \frac{1}{2}\left(\frac{x}{\sigma_{\mathcal{I},\ell}}\right)^2 \mathcal{Q}\left(\frac{x}{\sigma_{\mathcal{I},\ell}}\right) - \frac{x}{2\sigma_{\mathcal{I},\ell}}\phi\left(\frac{x}{\sigma_{\mathcal{I},\ell}}\right) && \text{(A.138)} \\ &\le -\left(\log \frac{\beta}{\sqrt{2\pi}\sigma_{\mathcal{I},\ell}} - \frac{1}{2}\right) \mathcal{Q}\left(\frac{x}{\sigma_{\mathcal{I},\ell}}\right) && \text{(A.139)} \\ &= -\log \frac{\beta}{\sqrt{2\pi e}\sigma_{\mathcal{I},\ell}} \cdot \mathcal{Q}\left(\frac{x}{\sigma_{\mathcal{I},\ell}}\right), && \text{(A.140)} \end{aligned}$$

where $\phi(\cdot)$ is defined in (A.81), and (A.139) holds because of (A.82).

Similarly,

$$-\int_{\mathsf{A}}^{\infty} W_{\mathcal{I},\ell}(y|x) \log R_{\mathcal{I},\ell}(y)\, \mathrm{d}y \le -\log \frac{\beta}{\sqrt{2\pi e}\sigma_{\mathcal{I},\ell}} \cdot \mathcal{Q}\left(\frac{\mathsf{A}-x}{\sigma_{\mathcal{I},\ell}}\right). \tag{A.141}$$

Moreover, we have

$$\begin{aligned} -\int_{0}^{\mathsf{A}} W_{\mathcal{I},\ell}(y|x) \log R_{\mathcal{I},\ell}(y)\, \mathrm{d}y &= -\int_{0}^{\mathsf{A}} \frac{1}{\sqrt{2\pi}\sigma_{\mathcal{I},\ell}} e^{-\frac{(y-x)^2}{2\sigma_{\mathcal{I},\ell}^2}} \log \frac{(1-\beta)}{\mathsf{A}}\, \mathrm{d}y && \text{(A.142)} \\ &= \log\left(\frac{\mathsf{A}}{1-\beta}\right) \cdot \left(1 - \mathcal{Q}\left(\frac{x}{\sigma_{\mathcal{I},\ell}}\right) - \mathcal{Q}\left(\frac{\mathsf{A}-x}{\sigma_{\mathcal{I},\ell}}\right)\right). && \text{(A.143)} \end{aligned}$$

We choose

$$\beta = \frac{\sqrt{2\pi e}\sigma_{\mathcal{I},\ell}}{\mathsf{A} + \sqrt{2\pi e}\sigma_{\mathcal{I},\ell}} \tag{A.144}$$

and obtain from (A.140), (A.141), and (A.143)

$$-\mathsf{E}_{W_{\mathcal{I},\ell}(Y_{\mathcal{I},\ell}|\bar{X}_{\mathcal{I},\ell})}[\log R_{\mathcal{I},\ell}(Y_{\mathcal{I},\ell})] \le \log\bigl(\mathsf{A}+\sqrt{2\pi e}\sigma_{\mathcal{I},\ell}\bigr). \tag{A.145}$$

Substituting (A.145) into (A.134) then yields

$$\begin{aligned}\mathsf{C}_{\mathsf{H}}(\mathsf{A},\alpha\mathsf{A}) &\le \sup_{\mathbf{p}}\Biggl\{\mathsf{H}(\mathbf{p})-\frac{n_{\mathrm{R}}}{2}\log 2\pi e+\sum_{\mathcal{I}\in\mathcal{U}}p_{\mathcal{I}}\log|\det\mathsf{H}_{\mathcal{I}}| \\ &\qquad +\sum_{\mathcal{I}\in\mathcal{U}}p_{\mathcal{I}}\sum_{\ell=1}^{n_{\mathrm{R}}}\log\Bigl(\mathsf{A}+\sqrt{2\pi e}\sigma_{\mathcal{I},\ell}\Bigr)\Biggr\} \qquad (\text{A.146})\\ &= \sup_{\mathbf{p}}\Biggl\{\mathsf{H}(\mathbf{p})+\sum_{\mathcal{I}\in\mathcal{U}}p_{\mathcal{I}}\log\frac{|\det\mathsf{H}_{\mathcal{I}}|}{\mathsf{V}_{\mathsf{H}}}+\log\mathsf{V}_{\mathsf{H}} \\ &\qquad +\sum_{\mathcal{I}\in\mathcal{U}}p_{\mathcal{I}}\sum_{\ell=1}^{n_{\mathrm{R}}}\log\Bigl(\sigma_{\mathcal{I},\ell}+\frac{\mathsf{A}}{\sqrt{2\pi e}}\Bigr)\Biggr\} \qquad (\text{A.147})\\ &= \sup_{\mathbf{p}}\Biggl\{\log\mathsf{V}_{\mathsf{H}}-\mathsf{D}(\mathbf{p}\|\mathbf{q})+\sum_{\mathcal{I}\in\mathcal{U}}p_{\mathcal{I}}\sum_{\ell=1}^{n_{\mathrm{R}}}\log\Bigl(\sigma_{\mathcal{I},\ell}+\frac{\mathsf{A}}{\sqrt{2\pi e}}\Bigr)\Biggr\}. \qquad (\text{A.148})\end{aligned}$$

Proof of Theorem 28

We choose

$$R_{\mathcal{I},\ell}(y)=\begin{cases}\frac{\beta}{\sqrt{2\pi}\sigma_{\mathcal{I},\ell}}\,e^{-\frac{y^2}{2\sigma^2_{\mathcal{I},\ell}}} & \text{if } y\in(-\infty,0),\\ \frac{1-\beta}{\mathsf{A}}\cdot\frac{\mu}{1-e^{-\mu}}\,e^{-\frac{\mu y}{\mathsf{A}}} & \text{if } y\in[0,\mathsf{A}],\\ \frac{\beta}{\sqrt{2\pi}\sigma_{\mathcal{I},\ell}}\,e^{-\frac{(y-\mathsf{A})^2}{2\sigma^2_{\mathcal{I},\ell}}} & \text{if } y\in(\mathsf{A},\infty),\end{cases} \tag{A.149}$$

where $\beta\in(0,1)$ and $\mu>0$ will be specified later.

We notice that the inequalities in (A.140) and (A.141) still hold, while

$$\begin{aligned}&-\int_0^{\mathsf{A}}W_{\mathcal{I},\ell}(y|x)\log R_{\mathcal{I},\ell}(y)\,\mathrm{d}y\\ &\quad=-\int_0^{\mathsf{A}}\frac{1}{\sqrt{2\pi}\sigma_{\mathcal{I},\ell}}\,e^{-\frac{(y-x)^2}{2\sigma^2_{\mathcal{I},\ell}}}\left(\log\frac{1-\beta}{\mathsf{A}}\frac{\mu}{1-e^{-\mu}}-\frac{\mu}{\mathsf{A}}y\right)\mathrm{d}y \qquad (\text{A.150})\\ &\quad=-\log\left(\frac{1-\beta}{\mathsf{A}}\frac{\mu}{1-e^{-\mu}}\right)\left(1-\mathcal{Q}\left(\frac{x}{\sigma_{\mathcal{I},\ell}}\right)-\mathcal{Q}\left(\frac{\mathsf{A}-x}{\sigma_{\mathcal{I},\ell}}\right)\right)\\ &\qquad+\frac{\mu\sigma_{\mathcal{I},\ell}}{\mathsf{A}}\left(\phi\left(\frac{x}{\sigma_{\mathcal{I},\ell}}\right)-\phi\left(\frac{\mathsf{A}-x}{\sigma_{\mathcal{I},\ell}}\right)\right)+\frac{\mu}{\mathsf{A}}x\left(1-\mathcal{Q}\left(\frac{x}{\sigma_{\mathcal{I},\ell}}\right)-\mathcal{Q}\left(\frac{\mathsf{A}-x}{\sigma_{\mathcal{I},\ell}}\right)\right) \qquad (\text{A.151})\\ &\quad\le-\log\left(\frac{1-\beta}{\mathsf{A}}\frac{\mu}{1-e^{-\mu}}\right)\left(1-\mathcal{Q}\left(\frac{x}{\sigma_{\mathcal{I},\ell}}\right)-\mathcal{Q}\left(\frac{\mathsf{A}-x}{\sigma_{\mathcal{I},\ell}}\right)\right)\end{aligned}$$

$$+\frac{\mu\sigma_{\mathcal{I},\ell}}{\mathsf{A}}\left(\phi(0)-\phi\left(\frac{\mathsf{A}}{\sigma_{\mathcal{I},\ell}}\right)\right)+\frac{\mu}{\mathsf{A}}x\left(1-2\,\mathcal{Q}\left(\frac{\mathsf{A}}{2\sigma_{\mathcal{I},\ell}}\right)\right) \tag{A.152}$$

$$\leq -\log\left(\frac{1-\beta}{\mathsf{A}}\frac{\mu}{1-e^{-\mu}}\right)\left(1-\mathcal{Q}\left(\frac{x}{\sigma_{\mathcal{I},\ell}}\right)-\mathcal{Q}\left(\frac{\mathsf{A}-x}{\sigma_{\mathcal{I},\ell}}\right)\right)$$
$$+\frac{\mu\sigma_{\mathcal{I},\ell}}{\mathsf{A}}\left(\phi(0)-\phi\left(\frac{\mathsf{A}}{\sigma_{\mathcal{I},\ell}}\right)\right)+\frac{\mu}{\mathsf{A}}x. \tag{A.153}$$

Here (A.152) follows from the fact that, for $\xi\in[0,\mathsf{A}]$, $1-\mathcal{Q}(\xi)-\mathcal{Q}(\mathsf{A}-\xi)$ achieves the maximum value at $\xi=\frac{\mathsf{A}}{2}$, and that $\phi(\xi)$ is monotonically decreasing; and (A.153) holds because $1-2\,\mathcal{Q}(\xi)\leq 1$ and because $x\geq 0$.

Combining (A.140), (A.141), and (A.153), and choosing

$$\beta=\frac{\mu\sqrt{2\pi e}\sigma_{\mathcal{I},\ell}}{\mathsf{A}(1-e^{-\mu})+\mu\sqrt{2\pi e}\sigma_{\mathcal{I},\ell}} \tag{A.154}$$

now yield

$$-\mathsf{E}_{W_{\mathcal{I},\ell}(Y_{\mathcal{I},\ell}|\bar{x}_{\mathcal{I},\ell})}[\log R_{\mathcal{I},\ell}(Y_{\mathcal{I},\ell})]$$
$$\leq\log\left(\sqrt{2\pi e}\sigma_{\mathcal{I},\ell}+\mathsf{A}\cdot\frac{1-e^{-\mu}}{\mu}\right)+\frac{\mu\sigma_{\mathcal{I},\ell}}{\mathsf{A}\sqrt{2\pi}}\left(1-e^{-\frac{\mathsf{A}^2}{2\sigma^2_{\mathcal{I},\ell}}}\right)+\frac{\mu}{\mathsf{A}}\bar{x}_{\mathcal{I},\ell}. \tag{A.155}$$

Substituting (A.155) into (A.134), we have

$$\mathsf{C}_{\mathsf{H}}(\mathsf{A},\alpha\mathsf{A})$$
$$\leq\mathsf{H}(\mathbf{p}^*)+\sum_{\mathcal{I}\in\mathcal{U}}p^*_{\mathcal{I}}\log|\det\mathsf{H}_{\mathcal{I}}|-\frac{n_{\mathrm{R}}}{2}\log 2\pi e+\sum_{\mathcal{I}\in\mathcal{U}}p^*_{\mathcal{I}}\sum_{\ell=1}^{n_{\mathrm{R}}}\log\left(\sqrt{2\pi e}\sigma_{\mathcal{I},\ell}+\mathsf{A}\cdot\frac{1-e^{-\mu}}{\mu}\right)$$
$$+\frac{\mu}{\mathsf{A}\sqrt{2\pi}}\sum_{\mathcal{I}\in\mathcal{U}}p^*_{\mathcal{I}}\sum_{\ell=1}^{n_{\mathrm{R}}}\sigma_{\mathcal{I},\ell}\left(1-e^{-\frac{\mathsf{A}^2}{2\sigma^2_{\mathcal{I},\ell}}}\right)+\frac{\mu}{\mathsf{A}}\sum_{\mathcal{I}\in\mathcal{U}}p^*_{\mathcal{I}}\sum_{\ell=1}^{n_{\mathrm{R}}}\mathsf{E}\left[\bar{X}_{\mathcal{I},\ell}\,\middle|\,U^\star=\mathcal{I}\right] \tag{A.156}$$
$$=\mathsf{H}(\mathbf{p}^*)+\sum_{\mathcal{I}\in\mathcal{U}}p^*_{\mathcal{I}}\log\frac{|\det\mathsf{H}_{\mathcal{I}}|}{\mathsf{V}_{\mathsf{H}}}+\log\mathsf{V}_{\mathsf{H}}+\sum_{\mathcal{I}\in\mathcal{U}}p^*_{\mathcal{I}}\sum_{\ell=1}^{n_{\mathrm{R}}}\log\left(\sigma_{\mathcal{I},\ell}+\frac{\mathsf{A}}{\sqrt{2\pi e}}\cdot\frac{1-e^{-\mu}}{\mu}\right)$$
$$+\frac{\mu}{\mathsf{A}\sqrt{2\pi}}\sum_{\mathcal{I}\in\mathcal{U}}p^*_{\mathcal{I}}\sum_{\ell=1}^{n_{\mathrm{R}}}\sigma_{\mathcal{I},\ell}\left(1-e^{-\frac{\mathsf{A}^2}{2\sigma^2_{\mathcal{I},\ell}}}\right)+\frac{\mu}{\mathsf{A}}\sum_{\mathcal{I}\in\mathcal{U}}p^*_{\mathcal{I}}\left\|\mathsf{H}_{\mathcal{I}}^{-1}\big(\mathsf{E}[\mathbf{X}^\star\,|\,U^\star=\mathcal{I}]-\mathbf{v}_{\mathcal{I}}\big)\right\|_1 \tag{A.157}$$
$$\leq\log\mathsf{V}_{\mathsf{H}}-\mathsf{D}(\mathbf{p}^*\|\mathbf{q})+\sum_{\mathcal{I}\in\mathcal{U}}p^*_{\mathcal{I}}\sum_{\ell=1}^{n_{\mathrm{R}}}\log\left(\sigma_{\mathcal{I},\ell}+\frac{\mathsf{A}}{\sqrt{2\pi e}}\cdot\frac{1-e^{-\mu}}{\mu}\right)$$
$$+\frac{\mu}{\mathsf{A}\sqrt{2\pi}}\sum_{\mathcal{I}\in\mathcal{U}}p^*_{\mathcal{I}}\sum_{\ell=1}^{n_{\mathrm{R}}}\sigma_{\mathcal{I},\ell}\left(1-e^{-\frac{\mathsf{A}^2}{2\sigma^2_{\mathcal{I},\ell}}}\right)+\mu\left(\alpha-\sum_{\mathcal{I}\in\mathcal{U}}p^*_{\mathcal{I}}s_{\mathcal{I}}\right), \tag{A.158}$$

where (A.157) follows from (A.125), and (A.158) from (6.4). Theorem 28 is proven by taking the supremum over the probability vector $\mathbf{p}$ and the infimum over $\mu>0$.

Proof of Theorem 29

We choose

$$R_{\mathcal{I},\ell}(y) = \begin{cases} \frac{1}{\sqrt{2\pi}\sigma_{\mathcal{I},\ell}}\, e^{-\frac{y^2}{2\sigma^2_{\mathcal{I},\ell}}} & \text{if } y \in (-\infty, -\delta), \\ \frac{\mu}{\mathsf{A}} \cdot \frac{1-2\,\mathcal{Q}\left(\frac{\delta}{\sigma_{\mathcal{I},\ell}}\right)}{e^{\frac{\mu\delta}{\mathsf{A}}} - e^{-\mu(1+\frac{\delta}{\mathsf{A}})}}\, e^{-\frac{\mu y}{\mathsf{A}}} & \text{if } y \in [-\delta, \mathsf{A}+\delta], \\ \frac{1}{\sqrt{2\pi}\sigma_{\mathcal{I},\ell}}\, e^{-\frac{(y-\mathsf{A})^2}{2\sigma^2_{\mathcal{I},\ell}}} & \text{if } y \in (\mathsf{A}+\delta, \infty), \end{cases} \tag{A.159}$$

where $\delta, \mu > 0$ are free parameters. Following the steps in the proof of [16, App. B.B] and bounding $1 - \mathcal{Q}(\xi_1) - \mathcal{Q}(\xi_2) \leq 1$, we obtain:

$$\begin{aligned} &- \mathsf{E}_{\bar{X}_{\mathcal{I},\ell}|U^\star=\mathcal{I}}\Big[\mathsf{E}_{W_{\mathcal{I},\ell}(Y_{\mathcal{I},\ell}|\bar{X}_{\mathcal{I},\ell})}\big[\log R_{\mathcal{I},\ell}(Y_{\mathcal{I},\ell})\big]\Big] \\ &\quad \leq \log\left(\mathsf{A} \cdot \frac{e^{\frac{\mu\delta}{\mathsf{A}}} - e^{-\mu(1+\frac{\delta}{\mathsf{A}})}}{\mu\Big(1 - 2\,\mathcal{Q}\Big(\frac{\delta}{\sigma_{\mathcal{I},\ell}}\Big)\Big)}\right) + \frac{\delta}{\sqrt{2\pi}\sigma_{\mathcal{I},\ell}}\, e^{-\frac{\delta^2}{2\sigma^2_{\mathcal{I},\ell}}} + \mathcal{Q}\left(\frac{\delta}{\sigma_{\mathcal{I},\ell}}\right) \\ &\qquad + \frac{\mu\sigma_{\mathcal{I},\ell}}{\mathsf{A}\sqrt{2\pi}}\left(e^{-\frac{\delta^2}{2\sigma^2_{\mathcal{I},\ell}}} - e^{-\frac{(\mathsf{A}+\delta)^2}{2\sigma^2_{\mathcal{I},\ell}}}\right) + \frac{\mu}{\mathsf{A}}\,\mathsf{E}\big[\bar{X}_{\mathcal{I},\ell}\,\big|\,U^\star = \mathcal{I}\big]. \end{aligned} \tag{A.160}$$

Plugging (A.160) into (A.134) and using a derivation analogous to (A.156)–(A.158) then results in the given bound.

A.5.3 Derivation of Maximum-Variance Upper Bounds

Proof of Theorem 30

Using that

$$\mathsf{h}(\mathbf{Y}) \leq \frac{1}{2}\log\big((2\pi e)^{n_\mathrm{R}} \det \mathsf{K}_{\mathbf{YY}}\big), \tag{A.161}$$

where

$$\mathsf{K}_{\mathbf{YY}} = \mathsf{K}_{\bar{\mathbf{X}}\bar{\mathbf{X}}} + \mathsf{I}, \tag{A.162}$$

we have

$$\begin{aligned} \mathsf{C}_\mathsf{H}(\mathsf{A}, \alpha\mathsf{A}) &= \max_{P_\mathbf{X}} \big\{\mathsf{h}(\mathbf{Y}) - \mathsf{h}(\mathbf{Z})\big\} && \text{(A.163)} \\ &\leq \max_{P_\mathbf{X}} \left\{\frac{1}{2}\log\big((2\pi e)^{n_\mathrm{R}} \det(\mathsf{K}_{\bar{\mathbf{X}}\bar{\mathbf{X}}} + \mathsf{I})\big) - \frac{1}{2}\log(2\pi e)^{n_\mathrm{R}}\right\} && \text{(A.164)} \\ &= \max_{P_\mathbf{X}} \frac{1}{2}\log\det(\mathsf{I} + \mathsf{K}_{\bar{\mathbf{X}}\bar{\mathbf{X}}}) && \text{(A.165)} \\ &\leq \max_{P_\mathbf{X}} \frac{1}{2}\log\prod_{i=1}^{n_\mathrm{R}} \big(\mathsf{I} + \mathsf{K}_{\bar{\mathbf{X}}\bar{\mathbf{X}}}\big)_{i,i} && \text{(A.166)} \end{aligned}$$

$$= \max_{P_{\mathbf{X}}} \frac{n_{\mathrm{R}}}{2} \sum_{i=1}^{n_{\mathrm{R}}} \frac{1}{n_{\mathrm{R}}} \log\Big(1 + \big(\mathsf{K}_{\bar{\mathbf{X}}\bar{\mathbf{X}}}\big)_{i,i}\Big) \tag{A.167}$$

$$\leq \max_{P_{\mathbf{X}}} \frac{n_{\mathrm{R}}}{2} \log\left(1 + \sum_{i=1}^{n_{\mathrm{R}}} \frac{1}{n_{\mathrm{R}}} \big(\mathsf{K}_{\bar{\mathbf{X}}\bar{\mathbf{X}}}\big)_{i,i}\right) \tag{A.168}$$

$$= \max_{P_{\mathbf{X}}} \frac{n_{\mathrm{R}}}{2} \log\left(1 + \frac{1}{n_{\mathrm{R}}} \operatorname{tr}\big(\mathsf{K}_{\bar{\mathbf{X}}\bar{\mathbf{X}}}\big)\right) \tag{A.169}$$

$$= \frac{n_{\mathrm{R}}}{2} \log\left(1 + \frac{1}{n_{\mathrm{R}}} \max_{P_{\mathbf{X}}} \operatorname{tr}\big(\mathsf{K}_{\bar{\mathbf{X}}\bar{\mathbf{X}}}\big)\right). \tag{A.170}$$

Here, (A.166) follows from Hadamard's inequality, and (A.168) follows from Jensen's inequality.

A.5.4 Derivation of Asymptotic Results

Proof of Theorem 31

It follows directly from Theorem 25 that the RHS of (6.31) is a lower bound to its LHS. To prove the other direction, using that $\mathsf{D}(\mathbf{p}\|\mathbf{q}) \geq 0$, we have from Theorem 27 that

$$\mathsf{C}_{\mathsf{H}}(\mathsf{A}, \alpha\mathsf{A}) \leq \log \mathsf{V}_{\mathsf{H}} + n_{\mathrm{R}} \log\left(\sigma_{\max} + \frac{\mathsf{A}}{\sqrt{2\pi e}}\right) \tag{A.171}$$

where

$$\sigma_{\max} \triangleq \max_{\substack{\mathcal{I}\in\mathcal{U} \\ \ell\in\{1,\ldots,n_{\mathrm{R}}\}}} \sigma_{\mathcal{I},\ell}. \tag{A.172}$$

This proves that the RHS of (6.31) is also an upper bound to its LHS, and hence completes the proof of (6.31).

Next, we prove (6.32). Again, that its RHS is a lower bound to its LHS follows immediately from Theorem 26. To prove the other direction, we define for any $\mathbf{p}$:

$$\lambda(\mathbf{p}) \triangleq \alpha - \sum_{\mathcal{I}\in\mathcal{U}} p_{\mathcal{I}} s_{\mathcal{I}} \leq \alpha. \tag{A.173}$$

We then fix $\mathsf{A} \geq 1$ and choose μ depending on $\lambda(\mathbf{p})$ to be

$$\mu = \begin{cases} \mu^*(\mathbf{p}) & \text{if } \mathsf{A}^{-(1-\zeta)} < \frac{\lambda(\mathbf{p})}{n_{\mathrm{R}}} < \frac{1}{2}, \\ \mathsf{A}^{1-\zeta} & \text{if } \frac{\lambda(\mathbf{p})}{n_{\mathrm{R}}} \leq \mathsf{A}^{-(1-\zeta)}, \\ \frac{1}{\mathsf{A}} & \text{if } \frac{\lambda(\mathbf{p})}{n_{\mathrm{R}}} \geq \frac{1}{2}, \end{cases} \tag{A.174}$$

where $0 < \zeta < 1$ is a free parameter and $\mu^*(\mathbf{p})$ is the unique solution to

$$\frac{1}{\mu^*} - \frac{e^{-\mu^*}}{1 - e^{-\mu^*}} = \frac{\lambda(\mathbf{p})}{n_{\mathrm{R}}}. \tag{A.175}$$

Note that in the first case of (A.174),

$$\mathsf{A}^{-(1-\zeta)} < \frac{\lambda(\mathbf{p})}{n_{\mathrm{R}}} = \frac{1}{\mu^*(\mathbf{p})} - \frac{e^{-\mu^*(\mathbf{p})}}{1-e^{-\mu^*(\mathbf{p})}} < \frac{1}{\mu^*(\mathbf{p})}, \tag{A.176}$$

i.e.,

$$\mu^*(\mathbf{p}) < \mathsf{A}^{1-\zeta}, \tag{A.177}$$

and thus the choice (A.174) makes sure that in all three cases, irrespective of $\mathbf{p}$:

$$\mu \le \mathsf{A}^{1-\zeta}, \quad \text{for } \mathsf{A} \ge 1. \tag{A.178}$$

Then, for $\mathsf{A} \ge 1$, the upper bound (6.27) can be loosened as follows:

$$\mathsf{C}_{\mathsf{H}}(\mathsf{A}, \alpha\mathsf{A}) \le \frac{1}{2}\log\left(\frac{\mathsf{A}^{2n_{\mathrm{R}}}\mathsf{V}_{\mathsf{H}}^2}{(2\pi e)^{n_{\mathrm{R}}}}\right) + f(\mathsf{A}) + \sup_{\mathbf{p}} g(\mathsf{A}, \mathbf{p}, \mu) \tag{A.179}$$

where

$$f(\mathsf{A}) \triangleq \frac{n_{\mathrm{R}}\sigma_{\max}}{\mathsf{A}^{\zeta}\sqrt{2\pi}}\left(1 - e^{-\frac{\mathsf{A}^2}{2\sigma_{\min}^2}}\right), \tag{A.180}$$

$$g(\mathsf{A}, \mathbf{p}, \mu) \triangleq n_{\mathrm{R}}\log\left(\frac{\sqrt{2\pi e}\sigma_{\max}}{\mathsf{A}} + \frac{1-e^{-\mu}}{\mu}\right) + \mu\lambda(\mathbf{p}) - \mathsf{D}(\mathbf{p}\|\mathbf{q}) \tag{A.181}$$

with $\sigma_{\max}$ defined in (A.172) and with

$$\sigma_{\min} \triangleq \min_{\substack{\mathcal{I}\in\mathcal{U} \\ \ell\in\{1,\ldots,n_{\mathrm{R}}\}}} \sigma_{\mathcal{I},\ell}. \tag{A.182}$$

Note that

$$\lim_{\mathsf{A}\to\infty} f(\mathsf{A}) = 0. \tag{A.183}$$

Next, we upper-bound $g(\mathsf{A}, \mathbf{p}, \mu)$ individually for each of the three different cases in (A.174) to obtain a bound of the form

$$g(\mathsf{A}, \mathbf{p}, \mu) \le \begin{cases} g_1(\mathsf{A}) & \text{if } \mathsf{A}^{-(1-\zeta)} < \frac{\lambda(\mathbf{p})}{n_{\mathrm{R}}} < \frac{1}{2}, \\ g_2(\mathsf{A}) & \text{if } \frac{\lambda(\mathbf{p})}{n_{\mathrm{R}}} \le \mathsf{A}^{-(1-\zeta)}, \\ g_3(\mathsf{A}) & \text{if } \frac{\lambda(\mathbf{p})}{n_{\mathrm{R}}} \ge \frac{1}{2}, \end{cases} \tag{A.184}$$

for three functions g_1, g_2, and g_3 that only depend on A but not on $\mathbf{p}$ or μ. Thus, we shall then obtain the bound

$$g(\mathsf{A}, \mathbf{p}, \mu) \le \max\{g_1(\mathsf{A}), g_2(\mathsf{A}), g_3(\mathsf{A})\}, \quad \mathsf{A} \ge 1. \tag{A.185}$$

The functions g_1, g_2, and g_3 are introduced in the following.

For the first case where $\frac{\lambda(\mathbf{p})}{n_{\mathrm{R}}} \in \left(\mathsf{A}^{-(1-\zeta)}, \frac{1}{2}\right)$, we have

$$g(\mathsf{A}, \mathbf{p}, \mu) = n_{\mathrm{R}}\log\left(\frac{\sqrt{2\pi e}\sigma_{\max}}{\mathsf{A}} + \frac{1-e^{-\mu^*(\mathbf{p})}}{\mu^*(\mathbf{p})}\right) + \mu^*(\mathbf{p})\lambda(\mathbf{p}) - \mathsf{D}(\mathbf{p}\|\mathbf{q}) \tag{A.186}$$

$$= n_{\mathrm{R}} \log\left(1 + \frac{\mu^*(\mathbf{p})}{1 - e^{-\mu^*(\mathbf{p})}} \cdot \frac{\sqrt{2\pi e}\sigma_{\max}}{\mathsf{A}}\right)$$
$$+ n_{\mathrm{R}}\left(1 - \log\left(\frac{\mu^*(\mathbf{p})}{1 - e^{-\mu^*(\mathbf{p})}}\right) - \frac{\mu^*(\mathbf{p})\, e^{-\mu^*(\mathbf{p})}}{1 - e^{-\mu^*(\mathbf{p})}}\right) - \mathsf{D}(\mathbf{p}\|\mathbf{q}) \tag{A.187}$$
$$\leq \sup_{\mathbf{p}\colon \frac{\lambda(\mathbf{p})}{n_{\mathrm{R}}} \in \left(\mathsf{A}^{\zeta-1}, \frac{1}{2}\right)} \left\{ -\mathsf{D}(\mathbf{p}\|\mathbf{q}) + n_{\mathrm{R}} \log\left(1 + \frac{\mu^*(\mathbf{p})}{1 - e^{-\mu^*(\mathbf{p})}} \cdot \frac{\sqrt{2\pi e}\sigma_{\max}}{\mathsf{A}}\right) \right.$$
$$\left. + n_{\mathrm{R}}\left(1 - \log\left(\frac{\mu^*(\mathbf{p})}{1 - e^{-\mu^*(\mathbf{p})}}\right) - \frac{\mu^*(\mathbf{p})\, e^{-\mu^*(\mathbf{p})}}{1 - e^{-\mu^*(\mathbf{p})}}\right)\right\} \tag{A.188}$$
$$\triangleq g_1(\mathsf{A}). \tag{A.189}$$

Here, in (A.187) we have used (A.175).

For the second case where $\frac{\lambda(\mathbf{p})}{n_{\mathrm{R}}} \leq \mathsf{A}^{-(1-\zeta)}$, we use this inequality in combination with (A.174) to bound

$$\mu\lambda(\mathbf{p}) \leq \mathsf{A}^{1-\zeta} \cdot n_{\mathrm{R}} \mathsf{A}^{-(1-\zeta)} = n_{\mathrm{R}}. \tag{A.190}$$

Because $\mathsf{D}(\mathbf{p}\|\mathbf{q}) \geq 0$, we thus obtain

$$g(\mathsf{A}, \mathbf{p}, \mu) \leq n_{\mathrm{R}} \log\left(\frac{\sqrt{2\pi e}\sigma_{\max}}{\mathsf{A}} + \frac{1 - e^{-\mu}}{\mu}\right) + n_{\mathrm{R}} \tag{A.191}$$
$$= n_{\mathrm{R}} \log\left(\frac{\sqrt{2\pi e}\sigma_{\max}}{\mathsf{A}} + \frac{1 - e^{-\mathsf{A}^{1-\zeta}}}{\mathsf{A}^{1-\zeta}}\right) + n_{\mathrm{R}} \tag{A.192}$$
$$\triangleq g_2(\mathsf{A}). \tag{A.193}$$

For the third case where $\frac{\lambda(\mathbf{p})}{n_{\mathrm{R}}} \geq \frac{1}{2}$, we have

$$g(\mathsf{A}, \mathbf{p}, \mu) = n_{\mathrm{R}} \log\left(\frac{\sqrt{2\pi e}\sigma_{\max}}{\mathsf{A}} + \frac{1 - e^{-\frac{1}{\mathsf{A}}}}{\frac{1}{\mathsf{A}}}\right) + \frac{\lambda(\mathbf{p})}{\mathsf{A}} - \mathsf{D}(\mathbf{p}\|\mathbf{q}) \tag{A.194}$$
$$\leq n_{\mathrm{R}} \log\left(\frac{\sqrt{2\pi e}\sigma_{\max}}{\mathsf{A}} + \frac{1 - e^{-\frac{1}{\mathsf{A}}}}{\frac{1}{\mathsf{A}}}\right) + \frac{\alpha}{\mathsf{A}} - \inf_{\mathbf{p}\colon \frac{\lambda(\mathbf{p})}{n_{\mathrm{R}}} > \frac{1}{2}} \mathsf{D}(\mathbf{p}\|\mathbf{q}) \tag{A.195}$$
$$\triangleq g_3(\mathsf{A}). \tag{A.196}$$

Here, we used (A.173) to bound $\lambda(\mathbf{p}) \leq \alpha$.

We have now established (A.185) for the three functions defined in (A.189), (A.193), and (A.196), respectively. We now analyze the maximum in (A.185) when $\mathsf{A} \to \infty$. Since $g_2(\mathsf{A})$ tends to $-\infty$ as $\mathsf{A} \to \infty$, and since $g_1(\mathsf{A})$ and $g_3(\mathsf{A})$ are both bounded from below for $\mathsf{A} \geq 1$, we know that, for large enough A, $g_2(\mathsf{A})$ is strictly smaller than $\max\{g_1(\mathsf{A}), g_3(\mathsf{A})\}$.

We next look at $g_3(\mathsf{A})$ when $\mathsf{A} \to \infty$. Note that

$$\lim_{\mathsf{A}\to\infty} \frac{1 - e^{-\frac{1}{\mathsf{A}}}}{\frac{1}{\mathsf{A}}} = 1, \tag{A.197}$$

therefore

$$\lim_{\mathsf{A}\to\infty} g_3(\mathsf{A}) = -\inf_{\mathbf{p}\colon \frac{\lambda(\mathbf{p})}{n_{\mathrm{R}}}>\frac{1}{2}} \mathsf{D}(\mathbf{p}\|\mathbf{q}) \tag{A.198}$$

$$= -\inf_{\mathbf{p}\colon \alpha-\sum_{\mathcal{I}\in\mathcal{U}} p_{\mathcal{I}} s_{\mathcal{I}} \geq \frac{n_{\mathrm{R}}}{2}} \mathsf{D}(\mathbf{p}\|\mathbf{q}) \tag{A.199}$$

$$= -\inf_{\mathbf{p}\colon \alpha-\sum_{\mathcal{I}\in\mathcal{U}} p_{\mathcal{I}} s_{\mathcal{I}} = \frac{n_{\mathrm{R}}}{2}} \mathsf{D}(\mathbf{p}\|\mathbf{q}), \tag{A.200}$$

where the last equality holds because given $\alpha < \alpha_{\mathrm{th}}$, an optimal $\mathbf{p}$ will meet the constraint with equality.

It remains to investigate the behavior of $g_1(\mathsf{A})$ when $\mathsf{A} \to \infty$. To this end, we define

$$\tilde{g}_1(\mathsf{A},\mathbf{p}) \triangleq -\mathsf{D}(\mathbf{p}\|\mathbf{q}) + n_{\mathrm{R}} \log\left(1 + \frac{\mu^*(\mathbf{p})}{1-e^{-\mu^*(\mathbf{p})}} \cdot \frac{\sqrt{2\pi e}\sigma_{\max}}{\mathsf{A}}\right) + n_{\mathrm{R}}\left(1 - \log\left(\frac{\mu^*(\mathbf{p})}{1-e^{-\mu^*(\mathbf{p})}}\right) - \frac{\mu^*(\mathbf{p})\, e^{-\mu^*(\mathbf{p})}}{1-e^{-\mu^*(\mathbf{p})}}\right), \tag{A.201}$$

and note that, for any fixed $\mathbf{p}$,

$$\Delta(\mathsf{A},\mathbf{p}) \triangleq \tilde{g}_1(\mathsf{A},\mathbf{p}) - \lim_{\mathsf{A}\to\infty} \tilde{g}_1(\mathsf{A},\mathbf{p}) = \log\left(1 + \frac{\mu^*(\mathbf{p})}{1-e^{-\mu^*(\mathbf{p})}} \cdot \frac{\sqrt{2\pi e}\sigma_{\max}}{\mathsf{A}}\right). \tag{A.202}$$

Since, when $\mathsf{A} \to \infty$,

$$|\Delta(\mathsf{A},\mathbf{p})| \leq \log\left(1 + \left|\frac{1}{1-e^{-\mathsf{A}^{1-\zeta}}} \cdot \frac{\sqrt{2\pi e}\sigma_{\max}}{\mathsf{A}^{\zeta}}\right|\right) \to \log(1) = 0, \tag{A.203}$$

we see that $\tilde{g}_1(\mathsf{A},\mathbf{p})$ converges uniformly over $\mathbf{p}$ as $\mathsf{A} \to \infty$, and therefore we are allowed to interchange limit and supremum:

$$\lim_{\mathsf{A}\to\infty} g_1(\mathsf{A})$$

$$= \lim_{\mathsf{A}\to\infty} \sup_{\mathbf{p}\colon \frac{\lambda(\mathbf{p})}{n_{\mathrm{R}}} \in \left(\mathsf{A}^{\zeta-1}, \frac{1}{2}\right)} \tilde{g}_1(\mathsf{A},\mathbf{p}) \tag{A.204}$$

$$= \sup_{\mathbf{p}\colon \frac{\lambda(\mathbf{p})}{n_{\mathrm{R}}} \in \left(0, \frac{1}{2}\right)} \lim_{\mathsf{A}\to\infty} \tilde{g}_1(\mathsf{A},\mathbf{p}) \tag{A.205}$$

$$= \sup_{\mathbf{p}\colon \frac{\lambda(\mathbf{p})}{n_{\mathrm{R}}} \in \left(0, \frac{1}{2}\right)} \left\{ n_{\mathrm{R}}\left(1 - \log\frac{\mu^*(\mathbf{p})}{1-e^{-\mu^*(\mathbf{p})}} - \frac{\mu^*(\mathbf{p})\, e^{-\mu^*(\mathbf{p})}}{1-e^{-\mu^*(\mathbf{p})}}\right) - \mathsf{D}(\mathbf{p}\|\mathbf{q}) \right\} \tag{A.206}$$

$$= \sup_{\mathbf{p}\colon \lambda(\mathbf{p}) \in \left(\max\{0, \frac{n_{\mathrm{R}}}{2}+\alpha-\alpha_{\mathrm{th}}\}, \min\{\frac{n_{\mathrm{R}}}{2}, \alpha\}\right)} \left\{ n_{\mathrm{R}}\left(1 - \log\frac{\mu^*(\mathbf{p})}{1-e^{-\mu^*(\mathbf{p})}} - \frac{\mu^*(\mathbf{p})\, e^{-\mu^*(\mathbf{p})}}{1-e^{-\mu^*(\mathbf{p})}}\right) - \mathsf{D}(\mathbf{p}\|\mathbf{q}) \right\} \tag{A.207}$$

$$= \nu. \tag{A.208}$$

Here, in (A.207) we are allowed to restrict the supremum[1] to $\lambda(\mathbf{p}) \in (\frac{n_{\mathrm{R}}}{2}+\alpha-\alpha_{\mathrm{th}}, \alpha)$ because of (A.173) and because

$$\lambda(\mathbf{q}) \triangleq \alpha - \sum_{\mathcal{I}\in\mathcal{U}} s_{\mathcal{I}} q_{\mathcal{I}} = \alpha - \alpha_{\mathrm{th}} + \frac{n_{\mathrm{R}}}{2} \tag{A.209}$$

and for any $\mathbf{p}$ such that $\lambda(\mathbf{p}) \leq \lambda(\mathbf{q})$ the objective function in (A.206) is smaller than for $\mathbf{p} = \mathbf{q}$. In fact, $-\mathsf{D}(\mathbf{p}\|\mathbf{q})$ is clearly maximized for $\mathbf{p} = \mathbf{q}$ and

$$\mu^*(\mathbf{p}) \mapsto n_{\mathrm{R}}\left(1 - \log\frac{\mu^*(\mathbf{p})}{1-e^{-\mu^*(\mathbf{p})}} - \frac{\mu^*(\mathbf{p})\, e^{-\mu^*(\mathbf{p})}}{1-e^{-\mu^*(\mathbf{p})}}\right) \tag{A.210}$$

is decreasing in $\mu^*(\mathbf{p})$, which is a decreasing function of $\lambda(\mathbf{p})$; see (A.175). Finally, (A.208) follows from the definition of ν in (6.23).

It is straightforward to see that ν is larger than the RHS of (A.200). Therefore,

$$\lim_{\mathsf{A}\to\infty} \max\{g_1(\mathsf{A}), g_2(\mathsf{A}), g_3(\mathsf{A})\} = \nu. \tag{A.211}$$

Combining (A.179) with (A.183), (A.185), and (A.211) proves the theorem.

The theorem is proven by normalizing $\bar{\mathbf{X}}$ by A, which results in a factor A^2, and by then letting A go to zero.

Proof of Theorem 32

From [61, Corollary 2], it is known that the capacity is lower-bounded as

$$\mathsf{C}_{\mathsf{H}}(\mathsf{A}, \alpha\mathsf{A}) \geq \frac{1}{2}\max_{P_{\bar{\mathbf{x}}}} \mathrm{tr}\big(\mathsf{K}_{\bar{\mathbf{X}}\bar{\mathbf{X}}}\big) + o\bigg(\max_{P_{\bar{\mathbf{x}}}} \mathrm{tr}\big(\mathsf{K}_{\bar{\mathbf{X}}\bar{\mathbf{X}}}\big)\bigg). \tag{A.212}$$

For an upper bound, we use that

$$\log(1+\xi) \leq \xi, \quad \xi > 0, \tag{A.213}$$

and obtain from Theorem 30 that

$$\mathsf{C}_{\mathsf{H}}(\mathsf{A}, \alpha\mathsf{A}) \leq \frac{1}{2}\max_{P_{\bar{\mathbf{x}}}} \mathrm{tr}\big(\mathsf{K}_{\bar{\mathbf{X}}\bar{\mathbf{X}}}\big). \tag{A.214}$$

A.6 Proofs of Chapter 7

A.6.1 A Proof of Theorem 37

We first lower-bound the mutual information $\mathrm{I}(\mathbf{X}; \mathbf{Y}|\mathbb{H} = \mathsf{H})$ for a given channel realization H by using the independence between $\mathbb{H}$ and $\mathbf{Z}$ and invoking the EPI:

$$\mathrm{I}(\mathbf{X}; \mathbb{H}\mathbf{X} + \mathbf{Z}|\mathbb{H} = \mathsf{H}) = \mathsf{h}(\mathbb{H}\mathbf{X} + \mathbf{Z}|\mathbb{H} = \mathsf{H}) - \mathsf{h}(\mathbf{Z}) \tag{A.215}$$

[1] Notice that because of the supremum and continuity, we can restrict to the open interval instead of the closed interval.

$$\geq \frac{1}{2}\log_2\left(e^{2\,\mathsf{h}(\mathbb{H}\mathbf{X}|\mathbb{H}=\mathsf{H})} + e^{2\,\mathsf{h}(\mathbf{Z})}\right) - \mathsf{h}(\mathbf{Z}) \tag{A.216}$$

$$= \frac{1}{2}\log_2\left(1 + \frac{e^{2\,\mathsf{h}(\mathbb{H}\mathbf{X}|\mathbb{H}=\mathsf{H})}}{(2\pi e)^{n_{\mathrm{R}}}}\right) \tag{A.217}$$

$$= \frac{1}{2}\log_2\left(1 + \frac{e^{2\,\mathsf{h}(\mathsf{H}\mathbf{X})}}{(2\pi e)^{n_{\mathrm{R}}}}\right), \tag{A.218}$$

where the last equality holds because without CSI at the transmitter, the input vector $\mathbf{X}$ is independent of the channel matrix $\mathbb{H}$.

Fix some $\lambda \in (0, \frac{n_{\mathrm{R}}}{2})$ and let the n_{R}-dimensional random vector $\mathbf{V}$ be exponentially distributed with density

$$f(\mathbf{v}) = \frac{1}{\mathsf{A}^{n_{\mathrm{R}}}}\left(\frac{\mu}{1-e^{-\mu}}\right)^{n_{\mathrm{R}}} e^{-\frac{\mu\|\mathbf{v}\|_1}{\mathsf{A}}}, \quad \mathbf{v} \in [0,\mathsf{A}]^{n_{\mathrm{R}}}, \tag{A.219}$$

where μ denotes the unique solution to (6.24). Choose then some matrix G with nonnegative entries, with $\mathrm{rank}(\mathsf{G}) = n_{\mathrm{R}}$, with $\|\mathsf{G}\|_1 \leq \alpha/\lambda$, and with row vectors satisfying $\|\mathbf{g}_i\|_1 \leq 1$, $\forall\, i \in \{1,\ldots,n_{\mathrm{T}}\}$, and define $P_{\mathbf{X}}$ as the distribution of the vector

$$\mathbf{X} = \mathsf{G}\mathbf{V}. \tag{A.220}$$

It can be directly verified that this choice of $P_{\mathbf{X}}$ satisfies the power constraints (7.5) and puts nonzero density only on nonnegative inputs.

Then for a given realization of the channel matrix $\mathbb{H} = \mathsf{H}$, it implies the following density on the channel image vector $\bar{\mathbf{X}} = \mathsf{H}\mathbf{X}$:

$$f_{\mathsf{H}\mathbf{X}}(\bar{\mathbf{x}}) = \frac{1}{\mathsf{A}^{n_{\mathrm{R}}}|\det \mathsf{H}\mathsf{G}|}\cdot\left(\frac{\mu}{1-e^{-\mu}}\right)^{n_{\mathrm{R}}} e^{\frac{-\mu\|(\mathsf{H}\mathsf{G})^{-1}\bar{\mathbf{x}}\|_1}{\mathsf{A}}}. \tag{A.221}$$

The differential entropy $\mathsf{h}(\mathsf{H}\mathbf{X})$ thus evaluates to:

$$\mathsf{h}(\mathsf{H}\mathbf{X}) = n_{\mathrm{R}}\log_2(\mathsf{A}\cdot|\det \mathsf{H}\mathsf{G}|) + n_{\mathrm{R}}\left(1 - \log_2\frac{\mu}{1-e^{-\mu}} - \frac{\mu e^{-\mu}}{1-e^{-\mu}}\right). \tag{A.222}$$

Combining this with (A.218), taking expectation over $\mathbb{H}$, and maximizing over the free parameters concludes the proof.

A.6.2 A Proof of Theorem 40

If $\alpha \geq \alpha_{\mathrm{th}}(\mathsf{H})$, we choose $P_{\mathbf{X}}$ so that $\bar{\mathbf{X}}$ is uniform over $\mathcal{R}(\mathsf{H})$. This is obtained by defining a random variable over $\mathcal{U}$ with probability mass function (PMF) $\mathbf{q}$ and conditional on $\tilde{U} = \mathcal{I}$, choose $\mathbf{X}$ according to the minimum-energy signaling in (3.28) and so that $\bar{\mathbf{X}}$ is uniform over the shifted parallelepiped $\mathbf{v}_{\mathcal{I}} + \mathcal{D}_{\mathcal{I}}$.

If $\alpha < \alpha_{\mathrm{th}}(\mathsf{H})$, we fix a parameter

$$\lambda \in \left(\max\left\{0, \frac{n_{\mathrm{R}}}{2} + \alpha - \alpha_{\mathrm{th}}(\mathsf{H})\right\}, \min\left\{\frac{n_{\mathrm{R}}}{2}, \alpha\right\}\right) \tag{A.223}$$

and a PMF $\mathbf{p} = (p_{\mathcal{I}} \colon \mathcal{I} \in \mathcal{U})$ over the set $\mathcal{U}$ so that

$$\sum_{\mathcal{I} \in \mathcal{U}} p_{\mathcal{I}} s_{\mathcal{I}} = \alpha - \lambda. \tag{A.224}$$

Let then $\tilde{U}$ be a random variable over $\mathcal{U}$ with PMF $\mathbf{p}$, and conditional on $\tilde{U} = \mathcal{I}$, choose $\mathbf{X}$ according to the minimum-energy signaling in (3.28) and so that $\bar{\mathbf{X}}$ follows an n_{R}-dimensional truncated exponential distribution over the shifted parallelepiped $\mathbf{v}_{\mathcal{I}} + \mathcal{D}_{\mathcal{I}}$. Specifically, given $\mathbb{H} = \mathsf{H}$ and $\tilde{U} = \mathcal{I}$, the inputs $\{X_i \colon i \in \mathcal{I}^{\mathrm{c}}\}$ are deterministically set to

$$X_i = \mathsf{A} \cdot g_{\mathcal{I},i}, \quad i \in \mathcal{I}^{\mathrm{c}}, \tag{A.225}$$

where $g_{\mathcal{I},i}$ is defined in (3.23) or Algorithm 4, and the remaining inputs $\{X_i \colon i \in \mathcal{I}\}$ are chosen as the truncated exponential distribution,

$$f_{X_i|\tilde{U}=\mathcal{I}}(x_i) = \frac{\mu}{1 - e^{-\mu}} e^{-\frac{\mu x_i}{\mathsf{A}}}, \quad \forall i \in \mathcal{I}. \tag{A.226}$$

Then at the receiver side, the image vector $\bar{\mathbf{X}} = \mathsf{H}\mathbf{X}$ is of conditional density

$$f_{\bar{\mathbf{X}}|\tilde{U}=\mathcal{I}}(\bar{\mathbf{x}}) = \frac{1}{\mathsf{A}^{n_{\mathrm{R}}} |\det \mathsf{H}_{\mathcal{I}}|} \cdot \left(\frac{\mu}{1 - e^{-\mu}} \right)^{n_{\mathrm{R}}} e^{\frac{-\mu \|\mathsf{H}_{\mathcal{I}}^{-1}(\bar{\mathbf{x}} - \mathbf{v}_{\mathcal{I}})\|_1}{\mathsf{A}}}. \tag{A.227}$$

Consider first the case $\alpha \geq \alpha_{\mathrm{th}}(\mathsf{H})$. With the proposed choice ($\bar{\mathbf{X}}$ uniform over $\mathcal{R}(\mathsf{H})$), for each realization $\mathbb{H} = \mathsf{H}$, the conditional differential entropy is

$$\mathsf{h}(\bar{\mathbf{X}} | \mathbb{H} = \mathsf{H}) = \log_2(\mathsf{A}^{n_{\mathrm{R}}} \cdot \mathsf{V}_{\mathsf{H}}). \tag{A.228}$$

Combining this with (A.217) yields the desired result.

Consider now the case $\alpha < \alpha_{\mathrm{th}}(\mathsf{H})$. We define U to be a discrete random variable that is obtained by applying a function on $\bar{\mathbf{X}}$ in a way to satisfy:

$$\big(U = \mathcal{I}\big) \impliedby \big(\bar{\mathbf{X}} \in (\mathbf{v}_{\mathcal{I}} + \mathcal{D}_{\mathcal{I}})\big). \tag{A.229}$$

We then start from (A.217) and decompose the conditional differential entropy $\mathsf{h}(\bar{\mathbf{X}} | \mathbb{H} = \mathsf{H})$ as

$$\begin{aligned} \mathsf{h}(\bar{\mathbf{X}} | \mathbb{H} = \mathsf{H}) &= \mathsf{I}(\bar{\mathbf{X}}; U | \mathbb{H} = \mathsf{H}) + \mathsf{h}(\bar{\mathbf{X}} | U, \mathbb{H} = \mathsf{H}) && \text{(A.230)} \\ &= \mathsf{H}(U | \mathbb{H} = \mathsf{H}) + \mathsf{h}(\bar{\mathbf{X}} | U, \mathbb{H} = \mathsf{H}) && \text{(A.231)} \end{aligned}$$

where we used that U is a function of $\bar{\mathbf{X}}$. Notice that we do not specify the value of U when $\bar{\mathbf{X}}$ lies on the border of a parallelepiped $\mathbf{v}_{\mathcal{I}} + \mathcal{D}_{\mathcal{I}}$. However, the way we picked $\bar{\mathbf{X}}$ this event happens with probability 0 and does not influence the entropies. Moreover, with probability 1, $U = \tilde{U}$ and these two random variables thus have same (conditional) entropies. By the choice of the PMF $\mathbf{p}$ in (A.224) and the exponential distribution in (A.227), we then have:

$$\begin{aligned} \mathsf{h}(\bar{\mathbf{X}} | \mathbb{H} = \mathsf{H}) &= \mathsf{H}(\tilde{U} | \mathbb{H} = \mathsf{H}) + \mathsf{h}(\bar{\mathbf{X}} | \tilde{U}, \mathbb{H} = \mathsf{H})) && \text{(A.232)} \\ &= \mathsf{H}(\mathbf{p}) + \log_2 |\det \mathsf{H}_{\mathcal{I}}| + n_{\mathrm{R}} \log_2 \mathsf{A} \end{aligned}$$

$$+ n_{\mathrm{R}}\left(1 - \log_2 \frac{\mu}{1-e^{-\mu}} - \frac{\mu\, e^{-\mu}}{1-e^{-\mu}}\right) \tag{A.233}$$

$$= -\mathsf{D}(\mathbf{p}\|\mathbf{q}) + \log_2 \mathsf{V}_{\mathsf{H}} + n_{\mathrm{R}} \log_2 \mathsf{A} + n_{\mathrm{R}}\left(1 - \log_2 \frac{\mu}{1-e^{-\mu}} - \frac{\mu\, e^{-\mu}}{1-e^{-\mu}}\right). \tag{A.234}$$

The result now follows from substituting (A.234) into (A.217), then maximizing over the free parameters λ and $\mathbf{p}$, and taking expectation over $\mathbb{H}$.

A.6.3 A Proof of Theorem 41

For each realization H of $\mathbb{H}$, let $\bar{\mathbf{X}}^\star$ be the capacity-achieving input, and let $U^\star$ be defined by $\bar{\mathbf{X}}^\star$ as in (A.229). Then, the capacity can be upper-bounded as follows:

$$\mathsf{C}_{\mathsf{H}} = \mathrm{I}(\bar{\mathbf{X}}^\star; \mathbf{Y}^\star | \mathbb{H} = \mathsf{H}) \tag{A.235}$$

$$= \mathrm{I}(\bar{\mathbf{X}}^\star; \bar{\mathbf{X}}^\star + \mathbf{Z} | \mathbb{H} = \mathsf{H}) \tag{A.236}$$

$$\leq \mathrm{I}(\bar{\mathbf{X}}^\star; \bar{\mathbf{X}}^\star + \mathbf{Z}, U^\star | \mathbb{H} = \mathsf{H}) \tag{A.237}$$

$$= \mathsf{H}(U^\star | \mathbb{H} = \mathsf{H}) + \mathrm{I}(\bar{\mathbf{X}}^\star; \bar{\mathbf{X}}^\star + \mathbf{Z} | U^\star, \mathbb{H} = \mathsf{H}). \tag{A.238}$$

Moreover, for each size-n_{R} subset $\mathcal{I} \in \mathcal{U}$,

$$\mathrm{I}(\bar{\mathbf{X}}^\star; \bar{\mathbf{X}}^\star + \mathbf{Z} | U^\star = \mathcal{I}, \mathbb{H} = \mathsf{H})$$

$$= \mathrm{I}\big(\bar{\mathbf{X}}^\star - \mathbf{v}_{\mathcal{I}}; (\bar{\mathbf{X}}^\star - \mathbf{v}_{\mathcal{I}}) + \mathbf{Z} \big| U^\star = \mathcal{I}, \mathbb{H} = \mathsf{H}\big) \tag{A.239}$$

$$= \mathrm{I}\big(\mathsf{H}_{\mathcal{I}}^{-1}(\bar{\mathbf{X}}^\star - \mathbf{v}_{\mathcal{I}}); \mathsf{H}_{\mathcal{I}}^{-1}(\bar{\mathbf{X}}^\star - \mathbf{v}_{\mathcal{I}}) + \mathsf{H}_{\mathcal{I}}^{-1}\mathbf{Z} \big| U^\star = \mathcal{I}, \mathbb{H} = \mathsf{H}\big) \tag{A.240}$$

$$= \mathrm{I}(\bar{\mathbf{X}}^\star_{\mathcal{I}}; \bar{\mathbf{X}}^\star_{\mathcal{I}} + \mathbf{Z}_{\mathcal{I}} | U^\star = \mathcal{I}, \mathbb{H} = \mathsf{H}), \tag{A.241}$$

where we defined

$$\mathbf{Z}_{\mathcal{I}} \triangleq \mathsf{H}_{\mathcal{I}}^{-1}\mathbf{Z}, \tag{A.242}$$

$$\bar{\mathbf{X}}^\star_{\mathcal{I}} \triangleq \mathsf{H}_{\mathcal{I}}^{-1}(\bar{\mathbf{X}}^\star - \mathbf{v}_{\mathcal{I}}). \tag{A.243}$$

To further bound the term in (A.241), we then use the duality-based upper-bounding technique with a product output distribution

$$R_{\mathcal{I}}(\mathbf{y}_{\mathcal{I}}) = \prod_{\ell=1}^{n_{\mathrm{R}}} R_{\mathcal{I},\ell}(y_{\mathcal{I},\ell}). \tag{A.244}$$

Denoting by $W_{\mathcal{I}}(\cdot|\bar{\mathbf{X}}^\star_{\mathcal{I}})$ the transition law of the channel $\bar{\mathbf{X}}^\star_{\mathcal{I}} \mapsto \mathbf{Y}_{\mathcal{I}} \triangleq (\bar{\mathbf{X}}^\star_{\mathcal{I}} + \mathbf{Z}_{\mathcal{I}})$ and by $W_{\mathcal{I},\ell}(\cdot|\bar{X}^\star_{\mathcal{I},\ell})$ the marginal transition law for its ℓ-th component, we have:

$$\mathrm{I}(\bar{\mathbf{X}}^\star_{\mathcal{I}}; \bar{\mathbf{X}}^\star_{\mathcal{I}} + \mathbf{Z}_{\mathcal{I}} | U^\star = \mathcal{I}, \mathbb{H} = \mathsf{H})$$

$$\leq \mathsf{E}_{\bar{\mathbf{X}}^\star_{\mathcal{I}}|U^\star=\mathcal{I}}\big[\mathsf{D}\big(W_{\mathcal{I}}(\cdot|\bar{\mathbf{X}}^\star_{\mathcal{I}})\big\|R_{\mathcal{I}}(\cdot)\big)\big] \tag{A.245}$$

$$\leq -\mathsf{h}\big(\bar{\mathbf{X}}^\star_{\mathcal{I}} + \mathbf{Z}_{\mathcal{I}}\big|\bar{\mathbf{X}}^\star_{\mathcal{I}}, U^\star = \mathcal{I}, \mathbb{H} = \mathsf{H}\big) - \mathsf{E}_{\bar{\mathbf{X}}^\star_{\mathcal{I}}|U^\star=\mathcal{I}}\left[\sum_{\ell=1}^{n_{\mathrm{R}}} \mathsf{E}_{W_{\mathcal{I}}(\mathbf{Y}_{\mathcal{I}}|\bar{\mathbf{X}}^\star_{\mathcal{I}})}[\log R_{\mathcal{I},\ell}(Y_{\mathcal{I},\ell})]\right] \tag{A.246}$$

$$= -\frac{n_{\mathrm{R}}}{2}\log 2\pi e + \log|\det \mathsf{H}_{\mathcal{I}}| - \sum_{\ell=1}^{n_{\mathrm{R}}} \mathsf{E}_{Q_{\bar{X}^\star_{\mathcal{I},\ell}|U^\star=\mathcal{I}}}\Big[\mathsf{E}_{W_{\mathcal{I},\ell}(Y_{\mathcal{I},\ell}|\bar{X}^\star_{\mathcal{I},\ell})}[\log R_{\mathcal{I},\ell}(Y_{\mathcal{I},\ell})]\Big], \tag{A.247}$$

where the last equality holds because

$$\mathsf{h}(\bar{\mathbf{X}}^\star_{\mathcal{I}} + \mathbf{Z}_{\mathcal{I}}|\bar{\mathbf{X}}^\star_{\mathcal{I}}, U^\star = \mathcal{I}, \mathbb{H} = \mathsf{H}) = \mathsf{h}(\mathbf{Z}_{\mathcal{I}}) = \frac{1}{2}\log\big((2\pi e)^{n_{\mathrm{R}}}\det \mathsf{H}_{\mathcal{I}}^{-1}\mathsf{H}_{\mathcal{I}}^{-\mathsf{T}}\big). \tag{A.248}$$

For the realization H satisfying $\alpha \geq \alpha_{\mathrm{th}}(\mathsf{H})$, we choose the auxillary distribution $R_{\mathcal{I},\ell}(\cdot)$ as

$$R_{\mathcal{I},\ell}(y) = \begin{cases} \frac{1}{\mathsf{A}+\sqrt{2\pi e}\sigma_{\mathcal{I},\ell}}\, e^{-\frac{y^2}{2\sigma_{\mathcal{I},\ell}}} & \text{if } y < 0, \\ \frac{1}{\mathsf{A}+\sqrt{2\pi e}\sigma_{\mathcal{I},\ell}} & \text{if } y \in [0,\mathsf{A}], \\ \frac{1}{\mathsf{A}+\sqrt{2\pi e}\sigma_{\mathcal{I},\ell}}\, e^{-\frac{(y-\mathsf{A})^2}{2\sigma_{\mathcal{I},\ell}}} & \text{if } y > \mathsf{A}, \end{cases} \tag{A.249}$$

which yields, irrespectively of the value of $\bar{x}^\star_{\mathcal{I},\ell}$:

$$-\mathsf{E}_{W_{\mathcal{I},\ell}(Y_{\mathcal{I},\ell}|\bar{x}^\star_{\mathcal{I},\ell})}[\log R_{\mathcal{I},\ell}(Y_{\mathcal{I},\ell})] \leq \log\big(\mathsf{A} + \sqrt{2\pi e}\sigma_{\mathcal{I},\ell}\big). \tag{A.250}$$

Combining (A.250) with (A.247) ,and (A.241), $\mathsf{C}_{\mathsf{H},1}$ can be derived.

When $\alpha \geq \alpha_{\mathrm{th}}(\mathsf{H})$, we choose $R_{\mathcal{I},\ell}(\cdot)$ as

$$R_{\mathcal{I},\ell}(y) = \begin{cases} \frac{\mu\sqrt{e}}{\mathsf{A}(1-e^{-\mu})+\mu\sqrt{2\pi e}\sigma_{\mathcal{I},\ell}}\, e^{-\frac{y^2}{2\sigma^2_{\mathcal{I},\ell}}} & \text{if } y < 0, \\ \frac{\mu}{\mathsf{A}(1-e^{-\mu})+\mu\sqrt{2\pi e}\sigma_{\mathcal{I},\ell}}\, e^{-\frac{\mu y}{\mathsf{A}}} & \text{if } y \in [0,\mathsf{A}], \\ \frac{\mu\sqrt{e}}{\mathsf{A}(1-e^{-\mu})+\mu\sqrt{2\pi e}\sigma_{\mathcal{I},\ell}}\, e^{-\frac{(y-\mathsf{A})^2}{2\sigma^2_{\mathcal{I},\ell}}} & \text{if } y > \mathsf{A}. \end{cases} \tag{A.251}$$

Following the same steps as in the proof of [62, Appendix B], we obtain:

$$\begin{aligned} &-\mathsf{E}_{W_{\mathcal{I},\ell}(Y_{\mathcal{I},\ell}|\bar{x}^\star_{\mathcal{I},\ell})}[\log R_{\mathcal{I},\ell}(Y_{\mathcal{I},\ell})] \\ &\quad\leq \log\left(\sqrt{2\pi e}\sigma_{\mathcal{I},\ell} + \mathsf{A}\frac{1-e^{-\mu}}{\mu}\right) + \frac{\mu\sigma_{\mathcal{I},\ell}}{\mathsf{A}\sqrt{2\pi}}\left(1 - e^{-\frac{\mathsf{A}^2}{2\sigma^2_{\mathcal{I},\ell}}}\right) + \frac{\mu}{\mathsf{A}}\bar{x}^\star_{\mathcal{I},\ell}. \end{aligned} \tag{A.252}$$

$\mathsf{C}_{\mathsf{H},2}$ can then be derived by combining (A.252) with (A.238), (A.241), and (A.247), and by noting that

$$\frac{\mu}{\mathsf{A}}\,\mathsf{E}_{Q_{U^\star}}\left[\sum_{\ell=1}^{n_{\mathrm{R}}} \mathsf{E}_{Q_{\bar{X}^\star_{U,\ell}|U^\star}}\left[\bar{X}^\star_{U^\star,\ell}\right]\right] = \frac{\mu}{\mathsf{A}}\,\mathsf{E}_{Q_{U^\star}}\left[\left\|\mathsf{H}_{U^\star}^{-1}\big(\mathsf{E}\left[\bar{\mathbf{X}}^\star\,\middle|\,U^\star\right] - \mathbf{v}_{U^\star}\big)\right\|_1\right] \tag{A.253}$$

$$\leq \mu\big(\alpha - \mathsf{E}_{Q_{U^\star}}[s_{U^\star}]\big), \tag{A.254}$$

where (A.254) follows from (A.243), and (A.254) from the average-power constraint.

Taking expectation over $\mathbb{H}$ concludes the proof.

A.6.4 A Proof of Theorem 42

When the realization H satisfying $\alpha \geq \alpha_{\mathrm{th}}(\mathsf{H})$, the proof is straightforward from (7.29) and (7.33).

For the realization H satisfying $\alpha < \alpha_{\mathrm{th}}(\mathsf{H})$, the fact that the left-hand side of (7.34) cannot be smaller than its right-hand side follows directly from (7.29). To show the reverse direction, we rely on (6.27). By following the same arguments as in the proof of Theorem 31 when $\alpha < \alpha_{\mathrm{th}}$, we can obtain:

$$\mathsf{C}_{\mathsf{H},2} - n_{\mathrm{R}} \log \mathsf{A} \leq \sup_{\mathbf{p}} \left\{ \frac{1}{2} \log \left(\frac{\mathsf{V}_{\mathsf{H}}^2}{(2\pi e)^{n_{\mathrm{R}}}} \right) - \mathsf{D}(\mathbf{p} \| \mathbf{q}) + n_{\mathrm{R}} \left(1 - \log \frac{\mu^*}{1 - e^{-\mu^*}} - \frac{\mu^* \, e^{-\mu^*}}{1 - e^{-\mu^*}} \right) \right\} + o(\mathsf{A}). \quad \text{(A.255)}$$

The proof is concluded by letting $\mathsf{A} \to \infty$, and taking expectation over $\mathbb{H}$.

A.6.5 A Proof of Theorem 44

For each realization $\mathcal{F} = \mathrm{f}$, pick an arbitrary positive number $\lambda \in (0, \frac{n_{\mathrm{R}}}{2})$ and let μ denote the solution to (6.24) for the picked value of λ. Then for this λ, pick an arbitrary PMF $\mathbf{p}$ over $\mathcal{U}$ satisfying (7.47), and let $\tilde{U} \sim \mathbf{p}$. Similarly to before, given that $\mathcal{F} = \mathrm{f}$ and $\tilde{U} = \mathcal{I}$, we deterministically set

$$X_i = a_{\mathcal{I},i}(\mathsf{H}), \quad i \in \mathcal{I}^{\mathrm{c}}, \quad \text{(A.256)}$$

and choose the remaining inputs $\{X_i \colon i \in \mathcal{I}\}$ according to the distribution:

$$f_{X_i|\tilde{U}=\mathcal{I}}(x_i) = \frac{\mu}{1 - e^{-\mu}} e^{-\frac{\mu x_i}{\mathsf{A}}}, \quad \forall i \in \mathcal{I}. \quad \text{(A.257)}$$

Then, with $\bar{\mathbf{X}} = \mathsf{H}\mathbf{X}$, we obtain

$$\mathsf{h}(\bar{\mathbf{X}} | \mathbb{H} = \mathsf{H}) = -\mathsf{D}(\mathbf{p} \| \mathbf{q}) + \log \mathsf{V}_{\mathsf{H}} + n_{\mathrm{R}} \log \mathsf{A} + n_{\mathrm{R}} \left(1 - \log \frac{\mu}{1 - e^{-\mu}} - \frac{\mu \, e^{-\mu}}{1 - e^{-\mu}} \right). \quad \text{(A.258)}$$

Substituting (A.258) into (A.218), and taking expectation over $\mathbb{H}$, the proof is concluded.

Bibliography

[1] Mohammad Ali Khalighi and Murat Uysal, "Survey on free space optical communication: A communication theory perspective," *IEEE Comm. Surveys & Tutorials*, vol. 16, no. 4, pp. 2231–2258, fourth quarter 2014.

[2] Murat Uysal and Hatef Nouri, "Optical wireless communications – an emerging technology," in *Proc. IEEE Int. Conf. Transp. Optical Netw.*, Graz, Austria, Jul. 6–10, 2014, pp. 1–7.

[3] Steve Hranilovic, *Wireless Optical Communication Systems.* New York, NY, USA: Springer Verlag, 2005.

[4] Terence H. Chan, Steve Hranilovic, and Frank R. Kschischang, "Capacity-achieving probability measure for conditionally Gaussian channels with bounded inputs," *IEEE Trans. Inf. Theory*, vol. 51, no. 6, pp. 2073–2088, Jun. 2005.

[5] Shlomo Shamai (Shitz), "Capacity of a pulse amplitude modulated direct detection photon channel," in *Proc. IEE*, vol. 137, pt. I (Communications, Speech and Vision), no. 6, Dec. 1990, pp. 424–430.

[6] David Brady and Sergio Verdú, "The asymptotic capacity of the direct detection photon channel with a bandwidth constraint," in *Proc. 28th Allerton Conf. Commun., Control Comput.*, Monticello, IL, USA, Oct. 3–5, 1990, pp. 691–700.

[7] Amos Lapidoth and Stefan M. Moser, "The asymptotic capacity of the discrete-time Poisson channel," in *Proc. Winter School Cod. and Inf. Theory*, Monte Verità, Ascona, Switzerland, Feb. 24–27, 2003.

[8] Yurii M. Kabanov, "The capacity of a channel of the Poisson type," *Theory of Probability and Its Appl.*, vol. 23, pp. 143–147, 1978.

[9] Mark H. A. Davis, "Capacity and cutoff rate for Poisson-type channels," *IEEE Trans. Inf. Theory*, vol. 26, no. 6, pp. 710–715, Nov. 1980.

[10] Aaron D. Wyner, "Capacity and error exponent for the direct detection photon channel — part I," *IEEE Trans. Inf. Theory*, vol. 34, no. 6, pp. 1449–1461, Nov. 1988.

[11] Michael R. Frey, "Information capacity of the Poisson channel," *IEEE Trans. Inf. Theory*, vol. 37, no. 2, pp. 244–256, Mar. 1991.

[12] Amos Lapidoth and Shlomo Shamai (Shitz), "The Poisson multiple-access channel," *IEEE Trans. Inf. Theory*, vol. 44, no. 2, pp. 488–501, Mar. 1998.

[13] Stefan M. Moser, "Capacity results of an optical intensity channel with input-dependent Gaussian noise," 2011, to app. in *IEEE Trans. Inf. Theory*.

[14] Joel G. Smith, "The information capacity of amplitude- and variance-constrained scalar Gaussian channels," *Inf. Contr.*, vol. 18, no. 3, pp. 203–219, Apr. 1971.

[15] Michèle A. Wigger, "Bounds on the capacity of free-space optical intensity channels," Master's thesis, Signal and Inf. Proc. Lab., ETH Zürich, Switzerland, Mar. 2003.

[16] Amos Lapidoth, Stefan M. Moser, and Michèle A. Wigger, "On the capacity of free-space optical intensity channels," *IEEE Trans. Inf. Theory*, vol. 55, no. 10, pp. 4449–4461, Oct. 2009.

[17] Andrew L. McKellips, "Simple tight bounds on capacity for the peak-limited discrete-time channel," in *Proc. IEEE Int. Symp. Inf. Theory*, Chicago, IL, USA, Jun. 27 – Jul. 2, 2004, p. 348.

[18] Ahmed A. Farid and Steve Hranilovic, "Channel capacity and non-uniform signalling for free-space optical intensity channels," *IEEE J. Select. Areas Commun.*, vol. 27, no. 9, pp. 1553–1563, Dec. 2009.

[19] Ahmed A. Farid and Steve Hranilovic, "Capacity bounds for wireless optical intensity channels with Gaussian noise," *IEEE Trans. Inf. Theory*, vol. 56, no. 12, pp. 6066–6077, Dec. 2010.

[20] Andrew Thangaraj, Gerhard Kramer, and Georg Böcherer, "Capacity bounds for discrete-time, amplitude-constrained, additive white Gaussian noise channels," *IEEE Trans. Inf. Theory*, vol. 63, no. 7, pp. 4172–4182, Jul. 2017.

[21] Borzoo Rassouli and Bruno Clerckx, "An upper bound for the capacity of amplitude-constrained scalar AWGN channel," *IEEE Commun. Lett.*, vol. 20, no. 10, pp. 1924–1926, Oct. 2016.

[22] Stefan M. Moser, Ligong Wang, and Michèle Wigger, "Asymptotic high-SNR capacity of MISO optical intensity channels," in *Proc. IEEE Inf. Theory Workshop*, Kaohsiung, Taiwan, Nov. 6–10, 2017, pp. 86–90.

[23] Stefan M. Moser, Ligong Wang, and Michèle Wigger, "Capacity results on multiple-input single-output wireless optical channels," *IEEE Trans. Inf. Theory*, vol. 64, no. 11, pp. 6954–6966, Nov. 2018.

[24] Stefan M. Moser, Michail Mylonakis, Ligong Wang, and Michèle Wigger, "Asymptotic capacity results for MIMO wireless optical communication," in *Proc. IEEE Int. Symp. Inf. Theory*, Aachen, Germany, Jun. 25–30, 2017, pp. 536–540.

[25] Alex Dytso, Mario Goldenbaum, Shlomo Shamai, and H. Vincent Poor, "Upper and lower bounds on the capacity of amplitude-constrained MIMO channels," in *Proc. IEEE Global Commun. Conf.*, Singapore, Dec. 4–8, 2017, pp. 1–6.

[26] Anas Chaaban, Zouheir Rezki, and Mohamed-Slim Alouini, "MIMO intensity-modulation channels: Capacity bounds and high SNR characterization," in *Proc. IEEE Int. Conf. Commun.*, Paris, France, May 21–25, 2017, pp. 1–6.

[27] Anas Chaaban, Zouheir Rezki, and Mohamed-Slim Alouini, "Capacity bounds and high-SNR capacity of MIMO intensity-modulation optical channels," *IEEE Trans. Wireless Commun.*, vol. 17, no. 5, pp. 3003–3017, May 2018.

[28] Anas Chaaban, Zouheir Rezki, and Mohamed-Slim Alouini, "Low-SNR asymptotic capacity of MIMO optical intensity channels with peak and average constraints," *IEEE Trans. Commun.*, vol. 66, no. 10, pp. 4694–4705, Oct. 2018.

[29] Zixiong Wang, Wen-De Zhong, Songnian Fu, and Chinlon Lin, "Performance comparison of different modulation formats over free-space optical (FSO) turbulence links with space diversity reception technique," *IEEE Photonics J.*, vol. 1, no. 6, pp. 277–285, Dec. 2009.

[30] Ertugrul Başar, Erdal Panayirci, Murat Uysal, and Harald Haas, "Generalized LED index modulation optical OFDM for MIMO visible light communications systems," in *Proc. IEEE Int. Conf. Commun.*, Kuala Lumpur, Malaysia, May 23–27, 2016, pp. 1–5.

[31] Anil Yesilkaya, Ertugrul Basar, Farshad Miramirkhani, Erdal Panayirci, Murat Uysal, and Harald Haas, "Optical MIMO-OFDM with generalized LED index modulation," *IEEE Trans. Commun.*, vol. 65, no. 8, pp. 3429–3441, Aug. 2017.

[32] Shane M. Haas, Jeffrey H. Shapiro, and Vahid Tarokh, "Space-time codes for wireless optical communications," *EURASIP J. App. Sig. Proc.*, no. 3, pp. 211–220, 2002.

[33] Ehsan Bayaki and Robert Schober, "On space–time coding for free–space optical systems," *IEEE Trans. Commun.*, vol. 58, no. 1, pp. 58–62, Jan. 2010.

[34] Xuegui Song and Julian Cheng, "Subcarrier intensity modulated MIMO optical communications in atmospheric turbulence," *IEEE/OSA J. of Optical Comm. & Networking*, vol. 5, no. 9, pp. 1001–1009, Sept. 2013.

[35] Jaime Anguita, Ivan Djordjevic, Mark Neifeld, and Bane Vasic, "Shannon capacities and error-correction codes for optical atmospheric turbulent channels," *J. Opt. Netw.*, vol. 4, no. 9, pp. 586–601, 2005.

[36] Hector E Nistazakis, Evangelia A Karagianni, Andreas D Tsigopoulos, Michael E Fafalios, and George S Tombras, "Average capacity of optical wireless communication systems over atmospheric turbulence channels," *J. Lightw. Technol.*, vol. 27, no. 8, pp. 974–979, 2009.

[37] Mohammad Ali Khalighi, Kosai Raoof, and Geneviève Jourdain, "Capacity of wireless communication systems employing antenna arrays, a tutorial study," *Wireless Pers. Commun.*, vol. 23, no. 3, pp. 321–352, 2002.

[38] İ. Emre Telatar, "Capacity of multi-antenna Gaussian channels," AT&T Bell Laboratories, Tech. Rep., 1995.

[39] Jack Winters, "On the capacity of radio communication systems with diversity in a rayleigh fading environment," *IEEE J. Select. Areas Commun.*, vol. 5, no. 5, pp. 871–878, Jun. 1987.

[40] Gerard J. Foschini, "Layered space-time architecture for wireless communication in fading environments when using multi-element antennas," *Bell Syst. Tech. J.*, pp. 41–59, 1996.

[41] Andrea Goldsmith, Syed Ali Jafar, Nihar Jindal, and Sriram Vishwanath, "Capacity limits of MIMO channels," *IEEE J. Select. Areas Commun.*, vol. 21, no. 5, pp. 684–702, Jun. 2003.

[42] David J Love, Robert W Heath, and Thomas Strohmer, "Grassmannian beamforming for multiple-input multiple-output wireless systems," in *Proc. IEEE Int. Conf. Commun.*, Anchorage, AK, USA, May 11–15, 2003, pp. 2618–2622.

[43] Syed Ali Jafar, Sriram Vishwanath, and Andrea Goldsmith, "Channel capacity and beamforming for multiple transmit and receive antennas with covariance feedback," in *Proc. IEEE Int. Conf. Commun.*, Helsinki, Finland, Jun. 11–14, 2001, pp. 2266–2270.

[44] Krishna Kiran Mukkavilli, Ashutosh Sabharwal, Elza Erkip, and Behnaam Aazhang, "On beamforming with finite rate feedback in multiple-antenna systems," *IEEE Trans. Inf. Theory*, vol. 49, no. 10, pp. 2562–2579, Oct. 2003.

[45] Eugene Visotsky and Upamanyu Madhow, "Space-time transmit precoding with imperfect feedback," *IEEE Trans. Inf. Theory*, vol. 47, no. 6, pp. 2632–2639, 2001.

[46] David James Love and Robert W Heath, "Limited feedback unitary precoding for spatial multiplexing systems," *IEEE Trans. Inf. Theory*, vol. 51, no. 8, pp. 2967–2976, Aug. 2005.

[47] Claude E. Shannon, "A mathematical theory of communication," *Bell Syst. Tech. J.*, vol. 27, pp. 379–423 and 623–656, Jul. and Oct. 1948.

[48] R. L. Dobrušin, "General formulation of Shannon's main theorem in information theory," in *Proc. Amer. Math. Soc. Transl.*, ser. 2, 1963, vol. 33, pp. 323–438.

[49] Sergio Verdú and Te Sun Han, "A general formula for channel capacity," *IEEE Trans. Inf. Theory*, vol. 40, no. 4, pp. 1147–1157, Jul. 1994.

[50] Igor Vajda, *Theory of Statistical Inference and Information*. Dordrecht, The Netherlands: Kluwer Academic Publishers, 1989.

[51] Stefan M. Moser, "Duality-based bounds on channel capacity," Ph.D. dissertation, ETH Zürich, Oct. 2004, Diss. ETH No. 15769. Available: http://moser-isi.ethz.ch/publications.html

[52] Longguang Li, Stefan Moser, Ligong Wang, and Michèle Wigger, "On the capacity of MIMO optical wireless channels," in *Proc. IEEE Inf. Theory Workshop*, Guangzhou, China, Nov. 25–29, 2018, pp. 1–5.

[53] Longguang Li, Stefan Moser, Ligong Wang, and Michèle Wigger, "On the capacity of MIMO optical wireless channels," Feb. 2019, subm. to *IEEE Trans. Inf. Theory*.

[54] Thomas M. Cover and Joy A. Thomas, *Elements of Information Theory*, 2nd ed. New York, NY, USA: Wiley, 2006.

[55] Yihong Wu and Sergio Verdú, "The impact of constellation cardinality on gaussian channel capacity," in *Proc. 48th Allerton Conf. Commun., Control Comput.*, Monticello, IL, USA, Sept. 29– Oct. 1, 2010.

[56] Ram Zamir and Meir Feder, "On the volume of the Minkowski sum of line sets and the Entropy-Power Inequality," *IEEE Trans. Inf. Theory*, vol. 44, no. 7, pp. 3039–3043, Nov. 1998.

[57] Geoffrey C. Shephard, "Combinatorial properties of associated zonotopes," *Canad. J. Math.*, vol. 26, no. 2, pp. 302–321, Feb. 1974.

[58] Amos Lapidoth and Stefan M. Moser, "Capacity bounds via duality with applications to multiple-antenna systems on flat fading channels," *IEEE Trans. Inf. Theory*, vol. 49, no. 10, pp. 2426–2467, Oct. 2003.

[59] Stefan M. Moser, *Information Theory (Lecture Notes)*, 6th ed. Signal and Inf. Proc. Lab., ETH Zürich, Switzerland, and Inst. Commun. Eng., Nat. Chiao Tung Univ., Hsinchu, Taiwan, 2018. Available: http://moser-isi.ethz.ch/scripts.html

[60] Vyacheslav V. Prelov and Edward C. van der Meulen, "An asymptotic expression for the information and capacity of a multidimensional channel with weak input signals," *IEEE Trans. Inf. Theory*, vol. 39, no. 5, pp. 1728–1735, Sept. 1993.

[61] Vyacheslav V. Prelov and Sergio Verdú, "Second-order asymptotics of mutual information," *IEEE Trans. Inf. Theory*, vol. 50, no. 8, pp. 1567–1580, Aug. 2004.

[62] Longguang Li, Stefan M. Moser, Ligong Wang, and Michèle Wigger, "The MISO free-space optical channel at low and moderate SNR," in *Proc. Annu. Conf. Inf. Sci. Syst.*, Princeton, NJ, USA, Mar. 21–23, 2018, pp. 1–6.

Université Paris-Saclay
Espace Technologique / Immeuble Discovery
Route de l'Orme aux Merisiers RD 128 / 91190 Saint-Aubin, France